Modeling the Interactions between Host Dynamics and Epidemics of Foliar Diseases in Three Plant Pathosystems

Von der Naturwissenschaftlichen Fakultät

der Gottfried Wilhelm Leibniz Universität Hannover

zur Erlangung des Grades

Doktor der Gartenbauwissenschaften

Dr. rer. hort.

genehmigte Dissertation

von

Master of Science John Koech Chelal

Geboren am 29. März 1984 in Keiyo, Kenia

2014

Referent: Prof. Dr. Bernhard Hau

Korreferent: Prof. Dr. Hartmut Stützel

Tag der Promotion: 28.02.2014

… dedicated to my wife Lilian

In love and gratitude…

ABSTRACT

In glasshouse experiments on tomato plants artificially inoculated with powdery mildew, actual disease severity increased progressively to a maximum that ranged from 0.53 to 0.83 (proportion). One fungicide spray reduced the maximum severity of powdery mildew significantly by two to fourfold. Despite adjustments for defoliation, there were instances when the actual severity on a whole plant basis declined between successive assessments. The powdery mildew epidemic did not affect the final amount of the cumulative leaf area formed. However, the actual leaf area of inoculated plants was reduced significantly due to accelerated shriveling and defoliation of diseased leaves. Disease-induced defoliation accounted for up to 63.1% loss in leaf area of diseased plants. Similarly, the duration of healthy leaf area and yield of tomato plants was significantly reduced by the powdery mildew epidemics.

With this background information, the subsequent studies focused on developing models that couple the growth dynamics of the host with the development of the disease in order to describe the dynamic interaction between the host and the disease under a constant or variable disease rate as influenced by temperature and relative humidity. Powdery mildew (*Oidium neolycopersici*) and early blight (*Alternaria solani*) on tomato as well as rust (*Uromyces appendiculatus*) on common bean were used as model pathosystems. The models were formulated as a set of differential equations for the rate of change in the amount of healthy, diseased and defoliated leaf area of a diseased plant relative to a healthy crop. Model parameters were estimated through fitting the model to experimental data obtained from glasshouse and controlled climate chamber experiments.

Generally, simulations of the disease progress and of the different leaf areas, i.e. healthy, diseased and defoliated area were considerably consistent with experimental observations ($R^2 > 0.97$). Specifically for powdery mildew, a host growth rate r_H of 0.112 to 0.123 day^{-1}, defoliation rate r_D of 0.050 to 0.083 day^{-1} and disease rate r_Y of 0.128 to 0.130 day^{-1} were estimated in two experiments while the rates in the other experiment clearly differed. Except

for slight deviations, there were no considerable differences between progress curves of either host or disease dynamics under a constant or variable disease rate. Moreover, the models showed that the contribution of defoliated healthy area to total plant defoliation is insignificant.

From the early blight model, it was demonstrated that the diseased leaf area can increase up to 58% of the actual leaf area just within the early cycle of the epidemic (9 days after inoculation). Defoliation rates were 2.5 times higher in older plants (late inoculated) compared to the younger (early inoculated) plants. Similarly, the disease rate r_Y was three-folds higher in the late inoculations (0.380 and 0.305 per day) when compared to the early inoculations (0.151 and 0.095 per day).

Simulations from the bean rust model showed that in the presence of disease, the total host area production is significantly reduced and levels off at proportions ranging from 0.5901 to 0.7668 of the maximum host area. Leaf defoliation rate is enhanced by more than 7 times in a diseased plant compared to the disease-free situation. The model also established that production of new healthy tissue is proportional to the healthy area, not the actual host area.

Given the good fit of models to the observations coupled with the biological realism of estimated parameter values, the models can be considered as satisfactorily describing the dynamic interaction between the disease epidemic and host growth of the three foliar plant pathosystems studied in this dissertation.

Additional key words: Defoliation, biotrophic, necrotrophic, senescence, *Solanum lycopersicum*, *Phaseolus vulgaris*

ZUSAMMENFASSUNG

In Gewächshausversuchen wurden Tomatenpflanzen künstlich mit Mehltau inokuliert, wobei die Befallsstärke (als Proportion) Höchstwerte von 0,53 bis 0,83 erreichte. Eine Fungizidbehandlung reduzierte die maximale Befallsstärke des Mehltaus deutlich um das zwei bis vierfache. Trotz Berücksichtung der Entlaubung der Pflanzen gab es Fälle, in denen die tatsächlich ermittelte Befallsstärke der gesamten Pflanze zwischen aufeinander folgenden Beobachtungen zurückging. Die Mehltau-Epidemie hatte keine Auswirkungen auf die gebildete Gesamtblattfläche. Die tatsächliche Blattfläche von inokulierten Pflanzen wurde jedoch signifikant durch beschleunigte Schrumpfung und Entlaubung von kranken Blättern reduziert. Krankheitsinduzierte Entlaubung verursachte bis zu 63,1% Verlust an Blattfläche bei erkrankten Pflanzen. Die Dauer der gesunden Blattfläche und Ertrag der Tomatenpflanzen wurden durch die Mehltau-Epidemie deutlich reduziert.

Diese Hintergrundinformationen nutzend, konzentrierte sich die folgende Entwicklung der Modelle auf die Verbindung der Wachstumsdynamik des Wirts mit der Entwicklung der Krankheit mit dem Ziel, die dynamische Interaktion zwischen dem Wirt und der Krankheit zu beschreiben, wobei eine konstanten oder variable von der Temperatur und relativen Luftfeuchtigkeit beeinflusste Krankheitsrate verwendet wurde. Echter Mehltau (*Oidium neolycopersici*) und die Dürrfleckenkrankheit (*Alternaria solani*) an Tomate sowie Rost (*Uromyces appendiculatus*) an Bohne wurden als Modellpathosysteme verwendet. Die Modelle wurden als Differentialgleichungen für die gesunde, kranke und entblätterte Blattfläche einer erkrankten Pflanze im Vergleich zu einer gesunden Pflanze formuliert. Die Modellparameter wurden durch Anpassung des Modells an experimentelle Daten von Experimenten im Gewächshaus und Klimakammer geschätzt.

Allgemein waren die Simulationen des Krankheitsverlaufs und der drei verschiedenen Blattflächen, d.h. gesund, krank und entlaubt, im Einklang mit experimentellen Beobachtungen ($R^2 > 0,97$). Für Echten Mehltau wurden Werte für die Wachstumsrate des

Zusammenfassung

Wirtes r_H von 0,112 bis 0,123 d^{-1}, die Entlaubungsrate r_D von 0,050–0,083 d^{-1} und die Krankheitsrate r_Y von 0,128–0,130 d^{-1} in zwei Experimenten ermittelt, während sich die Raten in dem anderen Experiment deutlich unterschieden. Bis auf geringfügige Abweichungen gab es keine erheblichen Unterschiede zwischen den Verlaufskurven der Wirts- und der Krankheitsdynamik bei konstanter bzw. variabler Krankheitsrate. Darüber hinaus folgt aus den Modellen, dass der Beitrag der gesunden Blattfläche zur Gesamtfläche der Entlaubung unbedeutend war.

Das Modell der Dürrfleckenkrankheit zeigte, dass sich der Anteil der erkrankten Blattfläche an der tatsächlichen Blattfläche bereits in der frühen Phase der Epidemie (9 Tage nach der Inokulation) auf bis zu 58% erhöhte. Die Entlaubungsraten waren 2,5-mal höher bei älteren Pflanzen (spät-inokuliert) im Vergleich zu den jüngeren (früh-inokulierten) Pflanzen. Auch die Krankheitsrate r_Y war bei den späten Inokulationen (0.380 und 0.305 d^{-1}) dreimal höher als bei den frühen Inokulationen (0.151 und 0.095 d^{-1}).

Simulationen des Bohnenrostmodells zeigten, dass in Gegenwart der Krankheit die Gesamtproduktion der Blattfläche signifikant reduziert wird und sich bei einem Anteil von 0,5901 bis 0,7668 der maximalen Wirtsblattfläche einpendelt. Die Entlaubungsrate der erkrankten Pflanzen ist um das 7-fache erhöht im Vergleich zu der krankheitsfreien Situation. Das Modell zeigt auch, dass die Produktion von neuem gesundem Gewebe proportional zur gesunden Flächen, aber nicht zur tatsächlichen Wirtsfläche ist.

Aufgrund der sehr gute Datenanpassung und der biologischen Relevanz der geschätzten Parameterwerte liefern die Modelle eine befriedigende Beschreibung der dynamischen Wechselwirkungen zwischen der Epidemie und dem Wirtswachstum in allen drei Pathosystemen, die in dieser Dissertation betrachtet wurden.

Weitere Begriffe: Entlaubung, biotroph, nectotroph, Seneszenz, *Solanum lycopersicum*, *Phaseolus vulgaris*

TABLE OF CONTENTS

GENERAL INTRODUCTION

Plant diseases cause serious losses in yield of many food crops globally. It is estimated that at least 10–16% of the global food production is lost due to plant diseases annually (Strange and Scott, 2005; De Wolf and Isard, 2007; Chakraborty and Newton, 2011). Consequently, more than 11% of the global population are faced with a serious food shortage while about 19% live on less than $1 a day (Strange and Scott, 2005). These facts draw attention to the neccesity of developing and implementing adequate, economically feasibly and environmentally acceptable control strategies to supress plant disease epidemics and thus avert potential crop losses (Campbell and Madden, 1990; Van Maanen and Xu, 2003; De Wolf and Isard, 2007).

A significant progress has been made over the last century in the management of plant diseases. For instance, the development of crop cultivars that are resistant to disease and the integrated use of chemical, biological as well as cultural control methods have had a major impact on agricultural productivity (Madden et al., 2007). This success is in part attributed to an increased understanding of how diseases develop in host plant populations and how various biotic and abiotic factors influence their epidemic development (Xu, 2006). It follows that as more information about each of the major and sub-components of an epidemic are known, the better it is to describe the epidemic and predict its direction and severity at a given time or space (Agrios, 2005).

The interactions of the components of a plant disease epidemic, i.e. host plant, pathogen, and environment, have been often viewed as a disease triangle (Campbell and Madden, 1990; Agrios, 2005; Pangga et al., 2011). Thus, a disease is capable of developing and progressing only if a virulent pathogen and a susceptible host plant are present under favorable environmental conditions. Since the activities of humans may also have considerable influence on disease epidemics, Zadoks and Schein (1979) and Kranz (2003), among others,

have included human interferences on plants, pathogens and the environment as a component of a plant disease epidemic.

It is widely acknowledged that diseases interfere with the different physiological functions of the host plant and their growth but they do so in processes that are often dynamic and complex (Bailey and Gilligan, 2004; Agrios, 2005). Based on the type of damage they cause on crop growth and yield, pests in general and plant diseases in specific can be classified into seven categories: tissue consumers, leaf senescence accelerators, stand reducers, light stealers, photosynthetic rate reducers, assimilate sappers, and turgor reducers (Boote et al., 1983). Two general categories can be drawn from this classification: either effects on radiation interception or on radiation-use efficiency (Johnson, 1987).

Plant pathogenic fungi are also often broadly divided into biotrophic and necrotrophic fungi based on their modes of nutrition (Lopes, 1999; Laluk and Mengiste, 2010). Biotrophic pathogens, such as the rust and powdery mildew fungi, are parasites that feed on living host tissue, and therefore do not kill their host plants immediately (Glazebrook, 2005). Thus, a highly specialized as well as structurally and biochemically complex relationship exists between biotrophic pathogens and their host (Laluk and Mengiste, 2010). Through these means, the biotrophic pathogens are able to penetrate the host, evade detection or suppress immune responses while, simultaneously, diverting the plants' nutrients using specialized feeding structures such as haustoria to further their own growth at the expense of plant growth (Schulze-Lefert and Panstruga, 2003; Oliver and Ipcho, 2004; Laluk and Mengiste, 2010; Talbot, 2010) Generally, biotrophic pathogens do not produce toxins and only secrete limited amounts of lytic enzymes in exceptional cases (Oliver and Ipcho, 2004).

In contrast, necrotrophic pathogens, such as the blight and rotting fungi, are facultative saprophytes that actively destroy host tissue using various phytotoxins, cell wall degrading enzymes and other depolymerising enzymes that are secreted both prior to and during colonization (Lopes, 1999; Stone, 2001; Oliver and Ipcho, 2004; Agrios, 2005). These

destructive pathogenesis mechanisms often result in extensive necrotic lesions which are photosynthetically unuseful and culminate in plant death and decay (Alfano and Collmer, 1996). Necrotic lesions induced by some necrotrophic fungi pathogens not only hinder photosynthesis in the necrotic spots, but also interfere with photosynthesis of those leaves lower in the canopy by intercepting light before it reaches them. For instance, Boote et al. (1983) demonstrated for *Cercospora spp.* on peanut (*Arachis hypogae* L.) that photosynthesis of diseased plant canopies was reduced not only by loss of leaves which abscised as a result of infection, but also because diseased leaves that remained on the plants were less efficient in fixing CO_2.

Although extensive studies have been dedicated towards understanding pathogen dynamics and the effects which diseases have on their host, there has also been a renewed and greater interest than just a few decades ago to integrate host dynamics in the analyses and description of the dynamics of disease epidemics (Campbell and Madden, 1990, Kranz, 2003; Madden et al., 2007; Pangga et al., 2011). This arises from the knowledge that changes in the size and characteristics of a host that occur during their growth and development influence epidemic progression by either increasing the amount of susceptible leaf tissue (Ferrandino, 2008) or decreasing the disease severity through growth flushes of the host and defoliation of already diseased area (Hau, 1990). Moreover, changes in the size, density and architecture of the canopy modify the prevailing canopy microclimate which in turn influences disease progression (Aust and Hoyningen-Huene, 1986). Leaf wetness, temperature, wind, and radiation are important microclimatic components that influence plant disease epidemics (Pangga et al., 2011).

Host plant resistance is also an important factor that influences the rate of epidemic development. There are various types and levels of host plant resistance that may vary from small, where the rate of disease increase is slowed but only slightly, to large where

incomplete pathogenesis occurs and pathogen reproduction is slowed to a greater extent (Van Maanen and Xu, 2003; Deadman, 2006).

The dynamic interaction of the components of an epidemic and their changes over time due to the external variables influencing them can be quantitatively analyzed through modeling (Campbell and Madden, 1990; Rossi et al., 2010). By definition, a plant disease model is a simplified conceptual representation of the interactions between a pathogen/disease, a host plant, and the environment that determine whether and how an epidemic develops over time and space (Rossi et al., 2010; Medina-Ruíz et al., 2011). In epidemiology, models are an essential tool in understanding, describing, predicting, and comparing epidemics or their components. For example, disease forecasts provide information that enable growers to make timely and tactical disease management decisions (van Maanen and Xu, 2003; Madden et al., 2007).

Some of the earliest works in modeling epidemics of plant diseases were done by van der Plank (1963). Subsequently, growth curve analysis, empirical models, analytical, and simulation models, among others, have been employed in modeling disease development of many pathosystems (Campbell and Madden, 1990; Hau, 1990; van Maanen and Xu, 2003; Xu, 2006; De Wolf and Isard 2007; Madden et al., 2007; Pangga et al., 2011). However, based on the aforementioned reasons, it is apparent that modeling studies that account for the synchronous interaction of the host and disease under given conditions of the environment would offer a better description of the variability in epidemic behavior and the capacity of host dynamics to modify epidemic progress (Kranz, 2003; Calonnec et al., 2008) than studies that only focus on pathogen development (Van Maanen and Xu, 2003).

Specific research topics are the epidemiological consequences of a changing host area either through growth flushes of the host or loss of the diseased area through leaf abscission (Hau, 1990). Certainly, there may be instances when it is not critical to correct for host growth in epidemic models, for instance in the case of systemic diseases where host growth does not

essentially influence disease progress (van der Plank, 1963; Madden et al., 2007) or in epidemics such potato late blight (*Phytophthora infestans*) that increase rapidly over a short period of time (Fry et al., 1983) thus there are only slight changes in the host area. In these instances, the basic assumption of the availability of a constant host area that can be diseased would be sufficient.

However, for many pathosystems such as coffee rust (Kushallappa and Ludwig, 1982), barley powdery mildew (Hau, 1990), and Alternaria blight of pigeon pea (Singh et al., 1986), host growth occurs during the course of an epidemic and these changes in host area may influence the rate at which the disease increases and the shape of the epidemic curve (Berger and Jones, 1985; Campbell and Madden, 1990). Thus, erroneous conclusions about the nature of the observed disease progress may be drawn if host growth is disregarded in the analysis of epidemics. This limitation can be overcome by adopting methods of correcting for host growth when calculating the apparent infection rate, such as proposed by van der Plank (1963) and Kushalappa and Ludwig (1982).

The other important feature in modeling host-disease interactions is the loss of the diseased area through leaf defoliation. However, this aspect is often left unquantified or ignored in many modeling studies. To our knowledge, Waggoner (1986), Jeger (1986) and Madden et al. (2007) have made significant contributions towards incorporating defoliation in plant disease models. However, a key limitation of their models is that the total amount of leaf area formed as well as the total defoliated leaf area increase over time without bound.

One of the primary reasons for modeling disease epidemics and their interaction with host dynamics arises from our desire to compare epidemics (Campbell, 1998). Comparative epidemiology is regarded as an important research tool in which studies across plant disease epidemics are conducted (Kranz, 2003). The aim is to evaluate the differences and similarities between diseases and their hosts, or their relevant attributes and parameters. For example, the influence of environmental factors and human interferences on epidemics may be compared

across different climatic conditions or agricultural practices either within the same disease-host combination or for multiple disease epidemics (Kranz, 2003; Madden et al., 2007). Ultimately, comparative epidemiology is of great importance in developing integrated and sustainable crop protection strategies.

Therefore, in this dissertation, a coordinated research framework that combines theoretical, experimental and modeling approaches is developed using powdery mildew and early blight of tomato and rust of common bean as case studies, in order to examine and compare the dynamics of a disease epidemic and host growth interacting together.

The cultivated tomato is one of the most popular vegetables globally and is grown either in outdoor fields or in greenhouses (Jones et al., 1991; Arie et al., 2007). Its wide spread use can be attributed to its versatility and adaptability in fresh and processed forms. Besides constituting a rich source of vitamins A and C (Wener, 2000), tomatoes are known to be rich in lycopene, a powerful antioxidant important in the prevention of many forms of cancer. The abundance and diversity of diseases that limit tomato production in many parts of the world emphasizes its importance as a favorable model for studying plant-pathogen interactions (Arie et al., 2007). Among the diseases of tomato, powdery mildew and early blight are some of the most economically significant.

Powdery mildew (caused by the biotrophic pathogen *Oidium neolycopersici* Kiss.) is an important disease of tomato worldwide. It poses a significant threat to glasshouse-grown tomatoes and is also gaining importance on field-grown tomato crops. Typical symptoms are powdery white lesions mainly on the tomato leaf surface though symptoms can also be observed on the petioles and calyx. Severely diseased leaves turn chlorotic and drop prematurely such that the disease results in considerable defoliation and a significant reduction in fruit size and quality (Whipps et al., 1998; Jones, et al., 2001). Similarly, early blight (caused by the necrotrophic pathogen *Alternaria solani* (Ellis and Martin) Sorauer) is one of the major destructive diseases of tomatoes particularly in tropical and subtropical

countries. It is characterized by leaf blight, stem blight, and apical fruit rot and severe epidemics lead to complete defoliation and loss of the crop (Pandey et al., 2003; Chaerani and Voorrips, 2006).

The common bean (*Phaseolus vulgaris* L.) is one of the most important food legume crops worldwide (Souza et al., 2013). It is consumed throughout the world either as dry seeds or as fresh green pods for their nutritional content (Michaels, 2005). In 2011 approximately 30 million hectares of the dry bean cultivars were grown and consumed in about 120 countries of the world (Souza et al., 2013). However, in spite of its popularity, bean production has been limited by an extensive list of widely distributed diseases with a potential to cause huge crop losses (Michaels, 2005; Souza et al., 2013). Amongst them is bean rust, caused by the biotrophic fungus *Uromyces appendiculatus* (Pers.: Pers.) Unger, which is one of the most widespread diseases of common bean (Jesus Junior et al., 2001; Stavely, 2005; Liebenberg and Pretorius, 2010). Typical symptoms are rust-colored pustules developing particularly on leaf surfaces. Larger pustules are usually surrounded by a chlorotic halo and severe epidemics lead to premature senescence, defoliation and significant reduction in yield (Mersha and Hau, 2008; Liebenberg and Pretorius, 2010; Schwartz et al., 2011).

This dissertation dealing with the host-disease interaction in three pathosystems is divided into four chapters.

In chapter 1, quantitative information on the temporal progress of powdery mildew epidemics and its effects on the host dynamics of tomato (*Solanum lycopersicum* L.) are presented. Chapters 2, 3 and 4 of this dissertation focus on developing improved models coupling host growth with temporal disease progress of tomato powdery mildew (chapter 2), tomato early blight (chapter 3), and bean rust (chapter 4) under the assumption of a constant and/or a variable rate of disease progress.

Past efforts in modeling similar epidemics, their application, resemblance, and limitations are evaluated and compared with the improved models developed in the current study. Specifically for early blight, the effects of the time of inoculation and physiological age of the host plant at disease onset on epidemic development are investigated.

The dissertation concludes with a general discussion. Here the main highlights of the adopted modeling approaches and results from the previous chapters are reviewed, and their implications for future studies are discussed. More specifically, comparative analysis of the three studied pathosystems: tomato-powdery mildew, tomato-early blight, and common bean-rust is done to evaluate if there are differences and similarities between these epidemics and the interaction with their hosts. It is hoped that these studies will elaborate on the most important attributes and parameters of these pathosystems.

Chapter 1

Temporal dynamics of powdery mildew and its effects on the host dynamics of tomato

John Chelal and Bernhard Hau*

Leibniz Universität Hannover

Institut für Gartenbauliche Produktionssysteme, Abteilung Phytomedizin

Herrenhäuser Str. 2, D-30419 Hannover, Germany

*Corresponding author: hau@ipp.uni-hannover.de

Manuscript prepared for submission to Phytopathology

ABSTRACT

Controlled glasshouse experiments were conducted to investigate the temporal progress of powdery mildew and its effects on host dynamics of tomato, without and with one fungicide application. Healthy tomato transplants (5 to 6 weeks old) were artificially inoculated with powdery mildew and disease progress as well as host growth were monitored in both fungicide sprayed and unsprayed treatments and compared with non-inoculated plants. Actual disease severity on a plant basis increased progressively in unsprayed plants reaching maximum severity in the proportionate range of 0.53 to 0.83. One fungicide spray significantly reduced the maximum disease severity by 2 to 4 folds. Despite adjustments for defoliation, declines in the proportion of disease severity between successive assessments were evident. Whereas the estimated growth rates of diseased plants were significantly lower than that of healthy plants, no significant differences were observed in the maximum leaf area formed of inoculated and non-inoculated plants. A considerable effect of the powdery mildew epidemics was manifested through hastened shriveling and defoliation of diseased leaves within the tomato canopy. An average of 18 to 29% and 40 to 52% of leaves had abscised from the plant canopy at the last date of assessment in sprayed and non-sprayed plants, respectively. Accordingly, defoliation accounted for 14 to 33.3% and 58.3 to 63.1% losses in leaf area of sprayed and non-sprayed plants, respectively. Duration of healthy leaf area and yield of inoculated plants was also significantly reduced by powdery mildew epidemics.

Additional key words: Disease epidemics, defoliation, yield, *Solanum lycopersicum*, *Oidium neolycopersici*

INTRODUCTION

A pathosystem consists of a host plant and a pathogen under prevailing environmental conditions. Determining the role that a specific pathogen plays in limiting yield necessitates quantitative knowledge of the interaction between host and pathogen as well as of the influence of biotic and abiotic factors on the host-pathogen interaction itself (Rouse, 1988).

Under favorable conditions for infection and disease development, pathogens constrain the development of host plants in various ways, for instance by leaf tissue destruction, reduction of the photosynthetic rate, altering dry matter partitioning as well as accelerating dry matter loss through premature leaf senescence and defoliation (Charles-Edwards, 1982; Boote et al., 1983; Garry et al., 1998; Béasse et al., 2000; Robert et al., 2004; Agrios, 2005). Conversely, during their growth and development, host plants integrate all external factors from the environment and cultural practices, which in turn affect their interaction with pathogens through varying levels of susceptibility (Kranz, 1977). The nature and levels of intrinsic host resistance and age-related resistance associated with specific host tissues is also a critical factor in determining epidemic development (Van Maanen and Xu, 2003; Mersha and Hau, 2011).

Quantitative description of the temporal disease progress on its host is an important step in elucidating the epidemiology of any plant disease (Ojiambo and Scherm, 2005). Here the pathosystem tomato – powdery mildew will be investigated.

Powdery mildew of tomato (*Solanum lycopersicum* L.), caused by *Oidium neolycopersici* Kiss., is a disease of worldwide occurrence in glasshouse-grown tomatoes but is also of increasing importance on field-grown tomato crops (Jones et al., 2001). Typical symptoms include powdery white lesions on leaf blades but the fungus can as well infect petioles and the calyx. Heavily mildewed leaves become chlorotic and prematurely senescent so that the disease results in considerable defoliation (Mieslerová et al., 2004).

Except very few reports (Correll et al., 1988; Jacob et al., 2008), little research has been undertaken to quantify the temporal dynamics of tomato powdery mildew and its effects on the host's growth dynamics. Key information on the timing and magnitude of premature defoliation and how it relates to disease progress would help fill critical knowledge gaps and act as a basis for sustainable management of this foliar disease.

Therefore, the objectives of this study were to: (i) characterize the temporal progress of powdery mildew on tomato, (ii) analyze the impact of powdery mildew on host growth parameters of tomato, (iii) quantify the dynamics of disease-induced defoliation (timing and magnitude) and its relationship to disease progress, and (iv) quantify the effect of powdery mildew epidemics on yield of tomato.

MATERIALS AND METHODS

Experimental set-up. Two controlled glasshouse experiments were conducted at the Institut für Gartenbauliche Produktionssysteme (Abteilung Phytomedizin) of Leibniz Universität Hannover. Tomato plants of susceptible cultivar Hildares F1 were used in all experiments. These experiments were laid out in a split plot design where inoculation with *O. neolycopersici* was considered as the main factor (I = inoculated; NI = non-inoculated) and the two treatments, i.e. fungicide sprayed (F) and unsprayed, as subfactors. Each treatment consisted of 15 replications (experiment A) and 11 replications (experiment B) whereby a single vigorously grown tomato plant was considered as the experimental unit following the single-plant approach of Kranz and Jörg (1989).

Production and management of experimental plants. Tomato cv. Hildares F1 seedlings were raised in a nursery for an average of three weeks. Each seedling was then transplanted into a 10-litre capacity (Ø 30 cm x 19.8 cm high) perforated plastic pot filled with the substrate Frühstorfer Erde (Industrie-Erden Werk, Germany). Neudorff's organic fertilizer Azet [®] (7-3-10 N, P_2O_5, and K_2O, respectively) was incorporated at transplanting at the rate of

50 g per plant. The transplants were raised in a glasshouse compartment where all crop managements practices were observed with day and night temperatures of 22 ± 3 °C and 19 ± 3 °C, respectively, and a photoperiod of 13 h. Biological control agents *Amblyseius cucumeris* and *Steinernema feltiae* were used against western flower thrips and fungus gnats, respectively.

Establishment of a relationship between leaf length and leaf area of tomato. A sample of 250 compound leaves derived from nine weeks old tomato plants cultivar Hildares F1 grown under similar conditions as the experimental plants was selected and the respective leaf length *LL* (cm) of each compound leaf was measured using a metric ruler. The corresponding leaf area *LA* (cm²) was determined from a leaf area meter (Model LI – COR LI–3100, Lincoln, NE, USA). The two-parametric power function $LA = a\,LL^{\,b}$ was established to describe the relationship between leaf length and leaf area of individual leaves. The regression coefficients *a* and *b* were determined through non-linear regression analysis using the statistical analysis software SigmaPlot11.0 (San Jose, CA, USA). Consequently, owing to its simplicity and ease of measurement, the power function, *LA = 0.016 LL$^{2.09}$* (*n = 250*; *R² = 0.85*) was used in subsequent experiments to determine non-destructively the area of each leaf from its length measurement.

Pathogen isolate and its maintenance. Following the procedure of Kiss et al. (2001), conidia of *O. neolycopersici* on freshly sporulating leaves of naturally infected tomato plants at the department of Phytomedizin were dusted onto leaves of healthy two months old tomato plants. The inoculated plants were grown in a glasshouse at temperatures of 22 ± 3 °C and 70 ± 15% relative humidity under natural light supplemented with artificial light to provide a photoperiod of 16 h.

O. neolycopersici **inoculation.** Healthy tomato transplants (5-6 weeks old) with an average of 7 leaves per plant were placed in an inoculation chamber, then an additionally

heavily diseased tomato plant was put in the middle at a raised position (~ 40 cm) above the rest of the plants to form the inoculum source. A ceiling fan was then used to disperse the conidia randomly on the healthy plants. Six hours after inoculation, the plants were transferred to a glasshouse compartment where germination and infectivity of the conidia were maximized by creating optimal favorability at temperatures of 22 ± 3 ℃ and relative humidity of 70 ± 15%. Natural light was supplemented with artificial light to provide a photoperiod of 16 hrs. Non-inoculated treatments (NI) were raised in a separate glasshouse cubicle, with strict separation to curb any possible inadvertent spread of inoculum.

In the fungicide sprayed treatment (F), plants received a single application of Bayfidan[®] 250 EC (Triadimenol 250 g L^{-1}) at the rate of 400 mL ha^{-1}. Fungicide application was carried out 10 days after inoculation (DAI) in experiment A but 20 DAI in experiment B to enable full establishment of the powdery mildew epidemic at the time of spraying. On average, 12 and 15 leaves per plant were present at the time of fungicide application in experiment A and B, respectively.

Host growth, disease severity and yield assessment. Just a day before inoculation, the length of each leaf of the experimental plants was measured using a metric ruler. Plant height (*PH*) was measured from the base of the stem to the tip of the youngest leaf. Successive measurements of leaf lengths and plant height were done every 5–7 days. Accordingly, leaf area (*LA*) was computed using the fitted power function as described above. Similar measurements were conducted on plants of the non-inoculated treatments.

Starting at the first appearance of disease symptoms, disease was assessed on a leaf basis at 3- to 4-day intervals over a period of 8 weeks. To mitigate subjective errors, disease assessments were solely conducted by the researcher. Disease severity of each leaf (y_i) was visually estimated as the proportion of the leaf surface covered by powdery mildew symptoms in comparison to the total leaf area. Only the fully unfolded leaves (5 to 7 leaflets) were considered for disease evaluation. In experiment B, fruits were harvested at the mature green

stage during the last two weeks of the experimental period and their respective weights (g) were determined using a weighing balance. Total yield on a plant basis was thus determined as the sum of two harvests.

Derived variables. The sum of areas of individual leaves available on a plant at any time (t) was determined and termed as actual leaf area per plant (HA). Diseased leaf area of individual leaves (Y_i) was computed as the product of estimated disease severity (y_i) in proportion with the corresponding leaf area (LA_i). Accordingly, diseased leaf area on a plant basis (Y) was calculated as the sum of the respective Y_i of individual leaves present at each assessment time (t_j). Healthy leaf area (in cm^2) per plant (H) is then computed as: $H = HA - Y$. Once a leaf defoliated, the maximum leaf area recorded prior to defoliation was noted. For each consecutive assessment time, the sum of areas of all leaves that had defoliated from the whole plant was termed as the cumulative defoliated leaf area (D). The cumulative total leaf area per plant (HT) was thus calculated as the sum of HA and D.

Disease severity on a plant basis (y) was computed as: $y = Y/(H+Y)$. Once a leaf defoliated, the value of the latest estimated severity was assigned and this was assumed to be constant throughout the rest of the experiment duration. Accordingly, disease severity adjusted for defoliation on a plant basis was computed and is herein referred to as adjusted disease severity.

Data analysis. The three-parametric logistic (Eqn. 1) and the Gompertz growth functions (Eqn. 2) were fitted to the data of host growth dynamics expressed in terms of cumulative total leaf area of a plant (HT) over time t:

$$HT(t) = H_{max} / \left[1 + \left(H_{max} / H_0 - 1 \right) \cdot \exp\left(-r_{HL} \cdot t \right) \right] \tag{1}$$

$$HT(t) = H_{max} \cdot \exp\left[\ln\left(H_0 / H_{max} \right) \cdot \exp\left(-r_{HG} \cdot t \right) \right] \tag{2}$$

The parameters H_0 and H_{max} are the initial and maximum plant size in terms of cm² leaf area, respectively, while r_{HL} and r_{HG} refer to the rate of host growth (day^{-1}) for the logistic and

Gompertz function, respectively. Equations 1 and 2 were also fitted to the host growth dynamics expressed in plant height (cm).

Due to the inverse correlation between the parameters H_0 and r_H, a direct comparison of the rate parameter between pairs of treatments, for instance I and NI, was not possible. To solve this problem, an identical H_0 value calculated as the average of H_0 values of the individual treatments (I and NI) was used in regression analyses of cumulative total leaf area and plant height according to the logistic function. A similar procedure was done for the Gompertz function.

To compare epidemics, the area under disease progress curve (*AUDPC*, proportion-days) was estimated using the trapezoidal integration method of Campbell and Madden (1990):

$$AUDPC = \sum_{j=1}^{m-1} \left(\frac{\left(y(t_j) + y(t_{j+1}) \right)}{2} \cdot \left(t_{j+1} - t_j \right) \right) \qquad (3)$$

Where y represents the disease severity (proportion) on a whole plant basis, m is the number of assessments and $(t_{j+1} - t_j)$ is the time interval between two consecutive assessments. Similarly, the healthy leaf area duration (*HLAD*, cm^2 - days) was computed as:

$$HLAD = \sum_{j=1}^{m-1} \left(\frac{\left(H(t_j) + H(t_{j+1}) \right)}{2} \right) \cdot \left(t_{j+1} - t_j \right) \qquad (4)$$

Where H is the healthy leaf area on a whole plant basis.

The non-linear relation between yield (g plant^{-1}) and *HLAD* was described by a monomolecular function using the combined data of NI, I + F and I treatment:

$$yield(HLAD) = yield_{max} \cdot \left[1 - \exp\left(- r_M \cdot [HLAD - HLAD_{min}] \right) \right] \qquad (5)$$

The parameter $yield_{max}$ is the maximum yield possible, $HLAD_{min}$ the minimum *HLAD* needed to produce any yield.

All regression analysis of host dynamics and disease epidemics parameters were performed using SigmaPlot11.0 (San Jose, CA, USA).

RESULTS

Powdery mildew epidemics. Initial symptoms of powdery mildew on artificially inoculated plants were generally observed 6 days after inoculation. In spite of a few instances when the disease severity between successive assessments declined, the actual disease severity on a plant basis (y) increased progressively in treatments without fungicide spray (I) reaching an average maximum severity of 0.83 (proportion) in experiment A (Fig. 1, left).
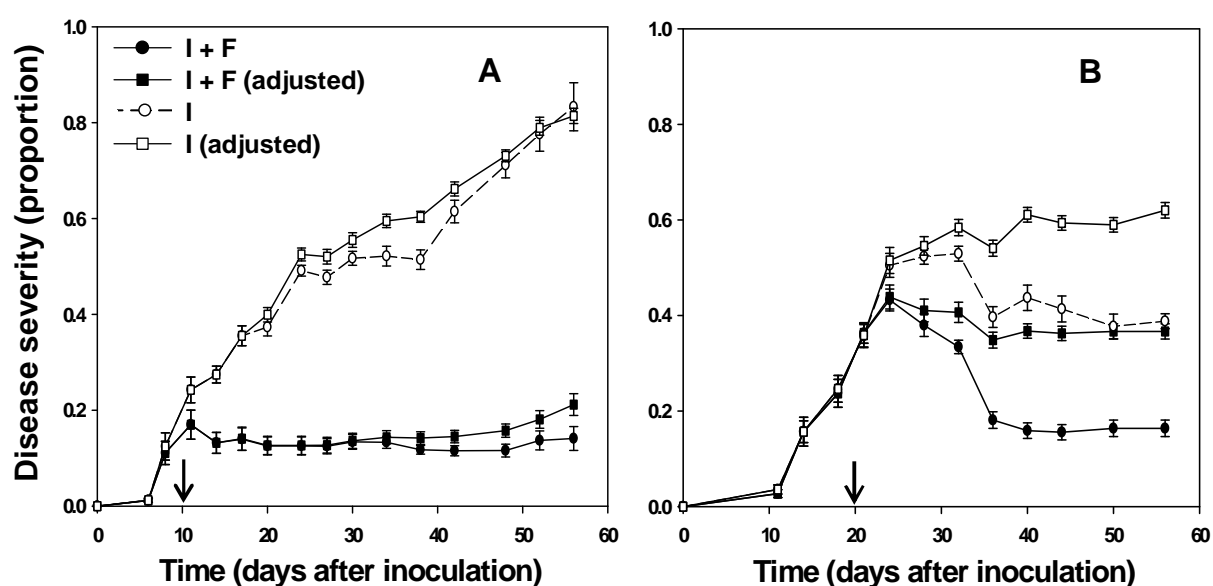
Fig. 1. Progress curves of powdery mildew (*Oidium neolycopersici*) epidemics on tomato in experiments A and B. Circles (● and ○) show progress of actual disease severity (± SE) in proportion per plant of inoculated treatments with (I + F) and without (I) fungicide spray. Squares (■ and □) show the corresponding disease progress curves adjusted for defoliation, i.e. once a leaf defoliated, the value of the latest estimated severity was assigned and this was assumed to be constant throughout the rest of the experiment duration. Arrows show the timing of fungicide application.

However, in experiment B an average maximum severity of 0.53 (proportion) was subsequently followed by a gradual decline in the proportion of disease severity due to defoliation of severely diseased leaves in the last half of the disease assessment period (Fig. 1, right). The more conducive conditions for infection and sporulation resulted in higher disease levels in experiment A (Fig. 1, left) than in B (Fig. 1, right).

The disease progress curves adjusted for defoliation showed also an increasing trend in disease severity reaching maximum proportions of 0.81 (experiment A) and 0.62 (experiment B). Despite adjustments for defoliation, declines in the proportion of disease severity between successive assessments were still evident in the progress curves of the sprayed (I + F) and non-sprayed (I) treatments in experiment B (Fig. 1, right).

Fungicide application significantly reduced the severity of powdery mildew epidemics as depicted by a comparison of progress curves of inoculated treatments with and without fungicide application (I and I + F, with and without adjustment). Accordingly, the final adjusted disease severity of the treatment with fungicide application I + F was 4-fold (experiment A) and 2-fold (experiment B) reduced compared to treatment I. These reductions also highlight the magnitude to which early fungicide spraying (10 DAI, experiment A) and late spraying (20 DAI, experiment B) influenced progress of powdery mildew epidemics.

Computation of the area under disease progress curves (*AUDPC*, proportion-days) on a whole plant basis further affirmed the significant differences in the powdery mildew epidemics between inoculated treatments with and without fungicide application (Table 1). The early fungicide spray (on day 10) in experiment A resulted in a much higher difference in AUDPC between treatments I and I + F than in experiment B with a spray on day 20.

TABLE 1. Area under disease progress curve (*AUDPC*, proportion- days) of tomato plants inoculated with powdery mildew (*Oidium neolycopersici*) considering fungicide sprayed (I + F) versus unsprayed (I) treatments during experiments A and B.

Experiment	Treatments	AUDPC (proportion- days)[x]
A	I	$26.26 \pm 0.61a$[y]
	I + F	$7.20 \pm 0.83b$
B	I	$17.59 \pm 0.62a$
	I + F	$15.44 \pm 0.83b$

[x] AUDPC values were computed for disease progress curves adjusted for defoliation.

[y] Treatment means designated with same letters within the columns of experiment A and B are not statistically different according to Tukey's test at $p < 0.05$.

On a leaf basis, analysis of the final disease severity of a leaf relative to its position in the canopy shows that 85% and 57% of leaves in plants inoculated without fungicide spray (I) of experiment A and B, respectively, had a final disease severity > 0.5 (proportion). Generally, leaves in the lower and intermediate positions of plants inoculated but unsprayed were more severely infected with powdery mildew than those in the upper positions (Fig. 2). Notably, leaves in canopy positions ≥ 13 (experiment A) and ≥ 17 (experiment B) of I + F treatments either remained disease free or had a final $y < 0.05$ (proportion). The mean disease severity (in proportion) of leaves prior to defoliation in the treatment I was 0.79 (± 0.018) in experiment A and 0.78 (± 0.021) in experiment B.
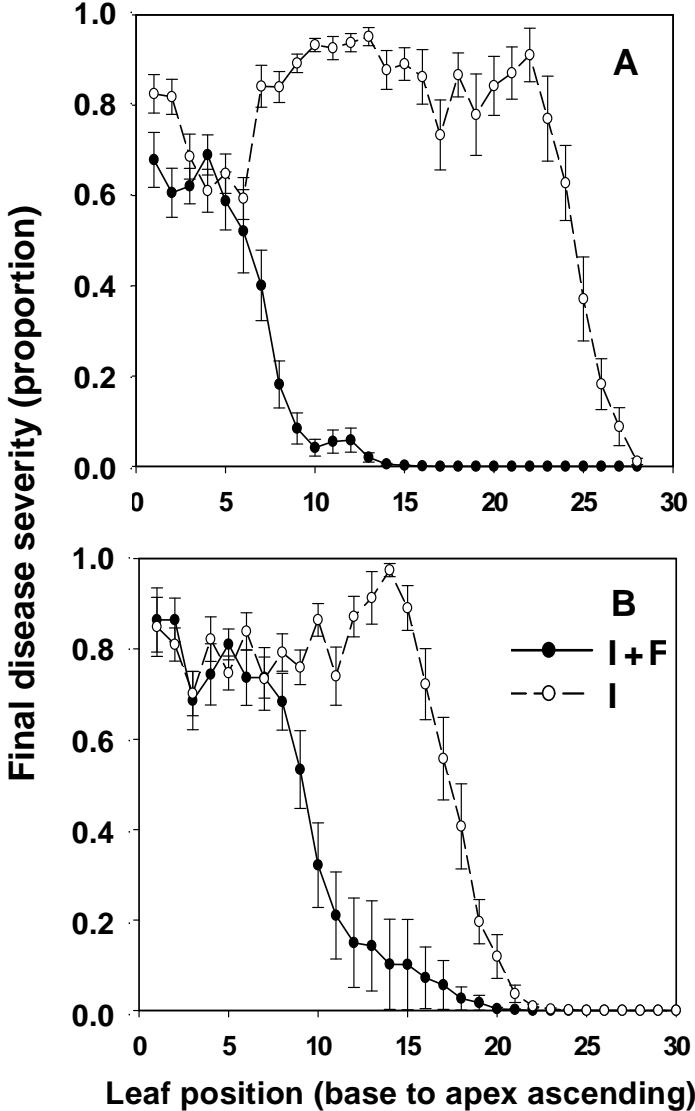
Fig. 2. Final disease severity (i.e. disease severity at the last assessment date or prior to defoliation for those leaves that abscised prematurely) for individual leaf positions from base to apex ascending following artificial inoculation of tomato plants with powdery mildew (*Oidium neolycopersici*) in experiments A and B.

Host dynamics of tomato under the influence of powdery mildew epidemics

Disease effects on total and actual leaf area formed. Non-inoculated treatments (NI) consistently maintained higher levels of host growth in terms of cumulative total leaf area formed (*HT*) on a plant basis when compared with treatments inoculated with powdery mildew (I and I + F) throughout the observation period of experiments A and B (Fig. 3). Comparison of NI and I treatments at each assessment date showed that the cumulative total leaf area formed was only significantly different between 18 to 36 DAI and 18 to 44 DAI in experiments A and B, respectively (Fig. 3).
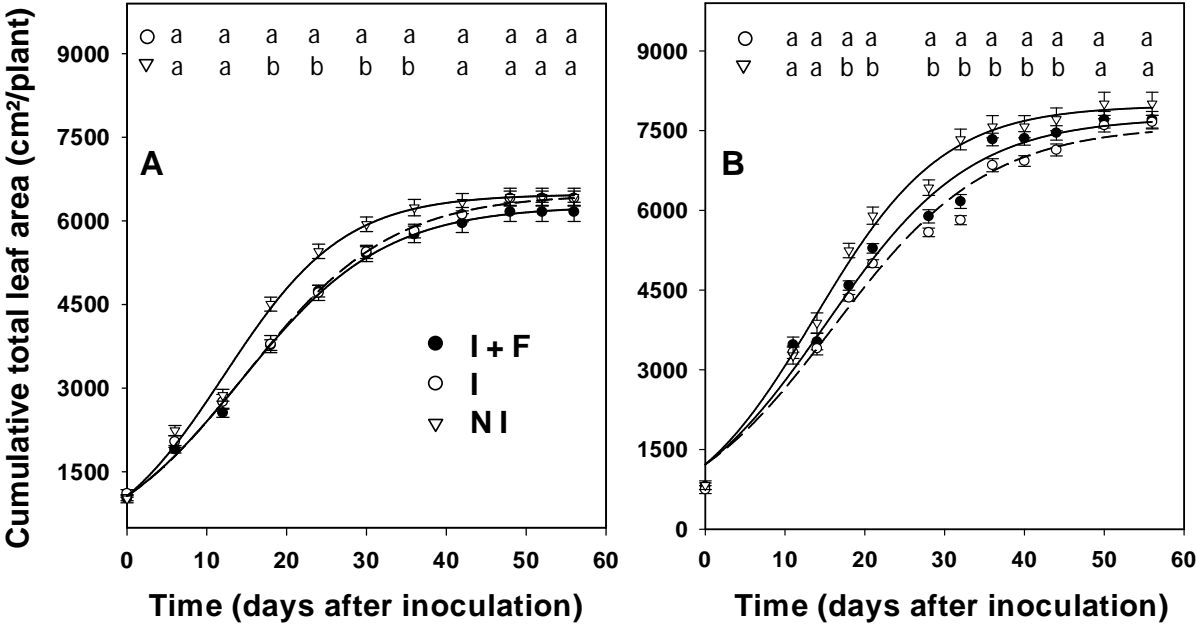
Fig. 3. Logistic growth function fitted to the host dynamics of tomato expressed in terms of cumulative total leaf area, *HT* (cm²/plant) with and without powdery mildew (*Oidium neolycopersici*) inoculation (I and NI) and fungicide application (I + F) during experiments A and B. A constant value of the initial leaf area H_0 which was calculated as the average of H_0 values of the individual treatments was used in the regression analyses. Same letters indicate that values were not statistically different at $p < 0.05$ in pairwise comparison of I and NI.

The progress curves of the cumulative total leaf area (cm²/plant) were well described by the logistic (Eqn. 1) and Gompertz (Eqn. 2) growth functions with high values of coefficient of determination ($R^2 > 0.98$) in both experiments. The coefficient of determination (R^2) values indicated that the logistic function gave a better fit in experiment A while the Gompertz function was superior in experiment B (Table 2).

In experiment A, the progress curve of HT of the non-inoculated treatment with fungicide application (NI + F) was largely identical to that of treatment NI (without fungicide spray) and is therefore not shown in Fig. 3. The similarity of both curves was further reflected in the non-significant differences of the estimated maximum host size (H_{max}) of these two treatments. In addition, the values of the host growth rate r_H (for the logistic and the Gompertz function) of these two treatments did not significantly differ (Table 2) implying that there was no significant fungicidal side effect on host growth. The NI + F treatment was thus omitted in the subsequent experiment B.

Pairwise comparisons of the H_{max} estimates of non-inoculated and inoculated treatments without and with one fungicide application showed no statistically significant differences (Table 2). This was already expected as the pairwise comparisons of the total leaf area of the treatments I and NI in Fig. 3 did not show significant differences at the last 4 (experiment A) and 2 (experiment B) assessment dates. Thus it can be concluded that the cumulative total leaf area formed by the tomato plant by the end of the assessment period was not substantially affected by the artificial inoculation with powdery mildew.

Assuming an identical initial host size (H_0), the estimated growth rate (r_{HL} or r_{HG}) of diseased plants with and without fungicide application were significantly lower compared to healthy plants in both experiments (Table 2). This difference was more apparent when I and NI treatments are compared. However, the rate of growth of fungicide sprayed plants (I + F) did not differ significantly from the non-sprayed plants (I) plants.

TABLE 2. Estimated parameter values (± standard errors) and coefficients of determination (R^2) of the logistic and Gompertz functions fitted to the cumulative total leaf area (cm² plant[-1]) of tomato with and without powdery mildew (*Oidium neolycopersici*) inoculation and fungicide spray during experiments A and B. To enable a comparison of treatments, the values of H_0 were fixed at the mean value estimated separately for the treatments within each experiment.

| Experiment | Trt.[x] | Logistic function | | | | Gompertz function | | | |
| | | Estimated parameter values | | | | Estimated parameter values | | | |
		R^2	H_{max}	H_0	r_{HL}	R^2	H_{max}	H_0	r_{HG}
A	I	0.998	6482.3a[y] (59.47)[z]	1064.0	0.109b[y] (0.003)	0.996	6739.1a[y] (100.9)	895.0	0.072b[y] (0.003)
	I + F	0.998	6267.1a (47.5)	1064.0	0.111b (0.002)	0.995	6497.7a (112.5)	895.0	0.074b (0.003)
	NI	0.994	6490.5a (79.2)	1064.0	0.132a (0.004)	0.989	6653.8a (136.4)	895.0	0.088a (0.005)
	NI + F	0.995	6478.1a (72.4)	1064.0	0.133a (0.004)	0.990	6631.8a (121.5)	895.0	0.090a (0.005)
B	I	0.978	7596.5a (215.5)	1219.0	0.103b (0.005)	0.987	7932.3a (214.2)	902.0	0.069b (0.004)
	I + F	0.981	7747.7a (188.1)	1219.0	0.111b (0.005)	0.987	8053.7a (199.6)	902.0	0.074b (0.004)
	NI	0.991	7974.0a (116.1)	1219.0	0.125a (0.004)	0.993	8250.3a (128.3)	902.0	0.084a (0.003)

[x] Treatments: I = inoculated, I + F = inoculated with fungicide spray, NI = non-inoculated, NI + F = non-inoculated with fungicide spray.

[y] Values of H_{max}, r_{HL} and r_{HG} designated with same letters within the columns of experiment A and B are not statistically different according to Tukey's test at $p < 0.05$ in pairwise comparisons of I and NI, I + F and NI + F, NI and NI + F.

[z] Standard errors of the estimates are given in parentheses

A considerable effect of powdery mildew epidemics on host dynamics was particularly discernible from a comparison of actual leaf area per plant (*HA*) of inoculated and non-inoculated treatments (Fig. 4). Progress curves of *HA* of treatments without powdery mildew inoculation clearly differed from their inoculated counterparts in both experiments. Hastened

shriveling and defoliation of affected leaves as a result of the powdery mildew epidemics significantly reduced the actual leaf area of inoculated plants. Significant gains in actual leaf area were observed in I + F treatments when compared with I treatments because of an impeded disease progress and thus reducing losses through disease-induced defoliation (Fig. 4).
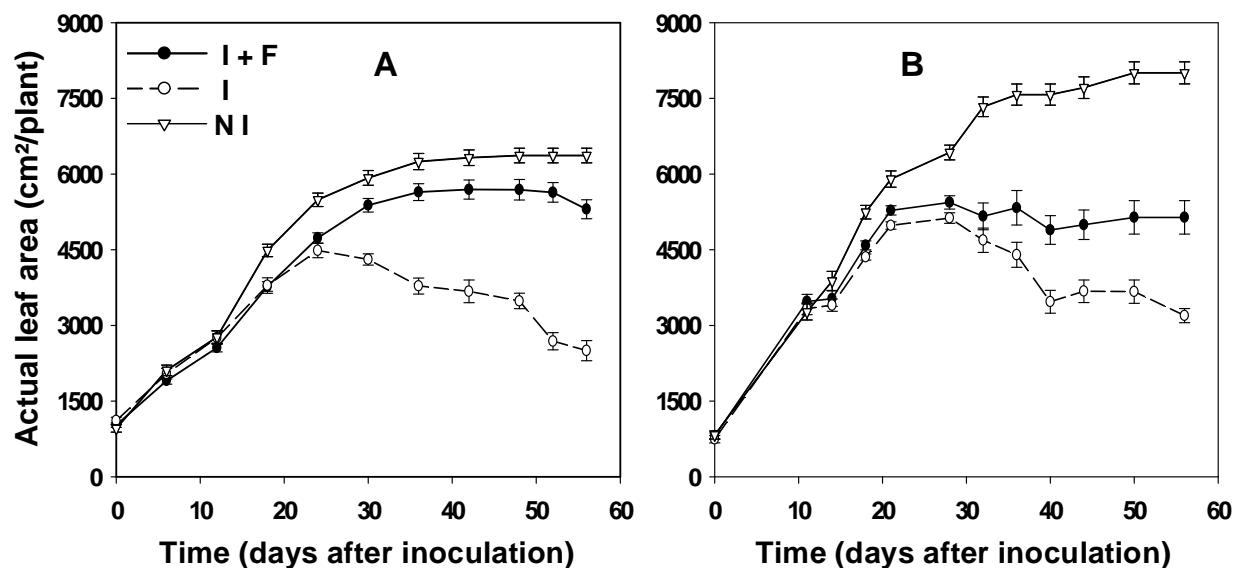
Fig. 4. Progress curves of actual leaf area per plant (*HA*) of tomato under the influence of powdery mildew (*Oidium neolycopersici*) epidemics with (I + F) and without (I) fungicide application compared to the non-inoculated (NI) treatment during experiments A and B.

Disease effects on leaf defoliation. Loss of leaf area through natural senescence was not observed in the non-inoculated (NI) treatments throughout the duration of experiments. After inoculation, however, a significant effect of the powdery mildew epidemics on the host was manifested through a hastened and severe defoliation of diseased leaves within the tomato canopy. Defoliation of affected leaves commenced around 20 days after inoculation with the mature fully expanded leaves of the lower plant canopy layers. On a whole plant basis, disease-induced defoliation started when disease severity had reached the threshold y_{DT} of

0.34 (± 0.01). After this trigger, defoliation proceeded upwards resulting in a progressive increase in the proportion of abscised leaves on a plant basis (Fig. 5a and b). An average of 52% and 18% of leaves had abscised from the tomato plant canopy at the last date of assessment during experiment A in I and I + F treatments, respectively (Fig. 5a). In experiment B, an average of 40% and 29% of leaves abscised in I and I+ F treatments, respectively (Fig. 5b).

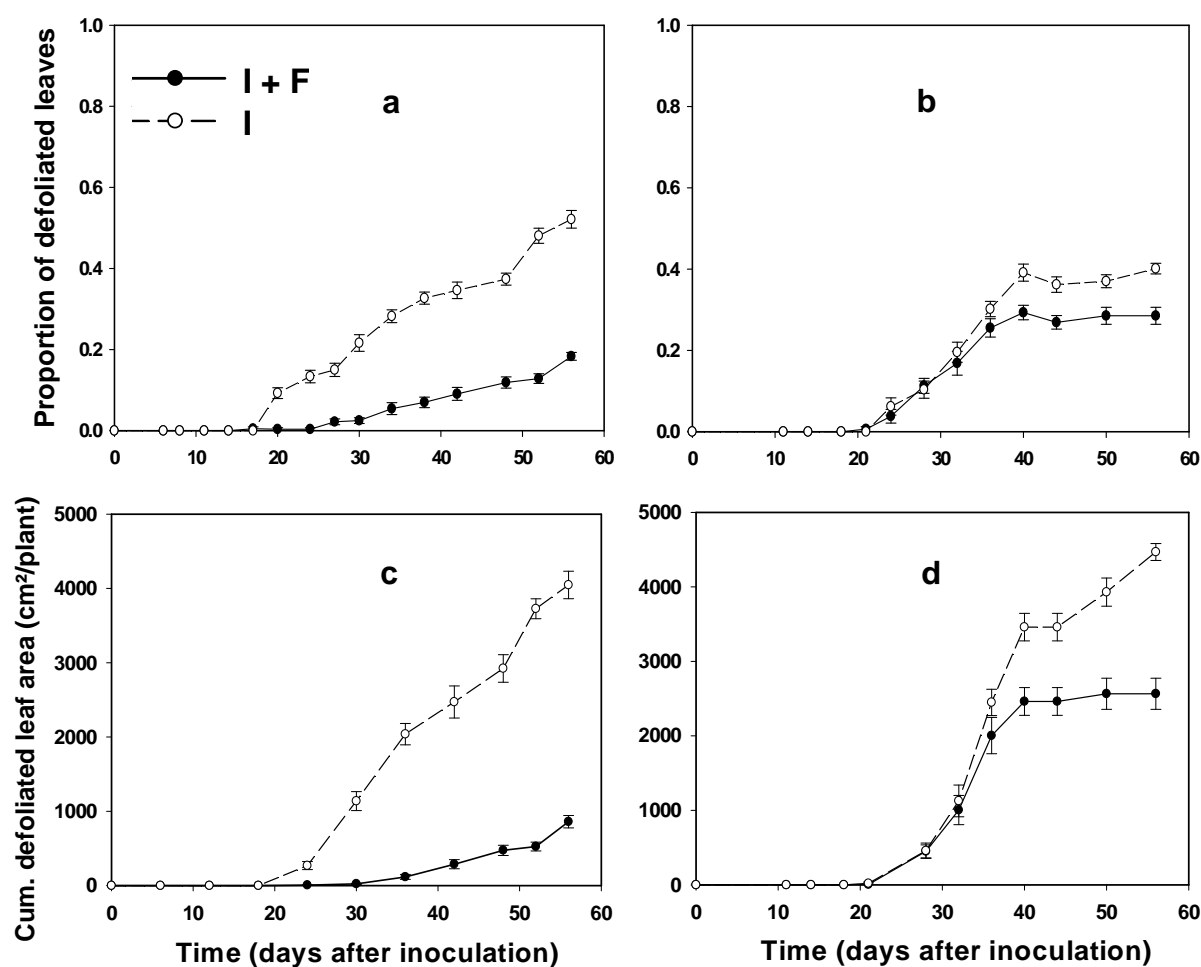**Fig. 5.** Progress curves of the proportion of defoliated leaves (a and b) and the cumulative defoliated leaf area (D, cm² plant⁻¹) (c and d) under the influence of powdery mildew (*Oidium neolycopersici*) epidemics with (I + F) and without (I) fungicide application during experiments A (left) and B (right). On average, a total of 28 and 30 leaves per plant were formed in experiments A and B, respectively.

Accordingly, when the cumulative defoliated leaf area (D, cm² plant^{-1}) is considered in relation to the cumulative total leaf area per plant (HT) at the last date of assessment, defoliation accounted for 63.1% and 58.3% losses in leaf area of I treatments in experiments A and B, respectively, whereas 14% and 33.3% losses in leaf area were observed for I + F treatments in experiments A and B, respectively (Fig. 5c and d).

Disease effects on plant height. The observed progress curves of plant height (cm) clearly differed between I and NI treatments (Fig. 6). Interestingly, powdery mildew epidemics in both experiments enhanced growth of host plants with regard to plant height. This phenomenon was further evident in inoculated treatments with fungicide spray.

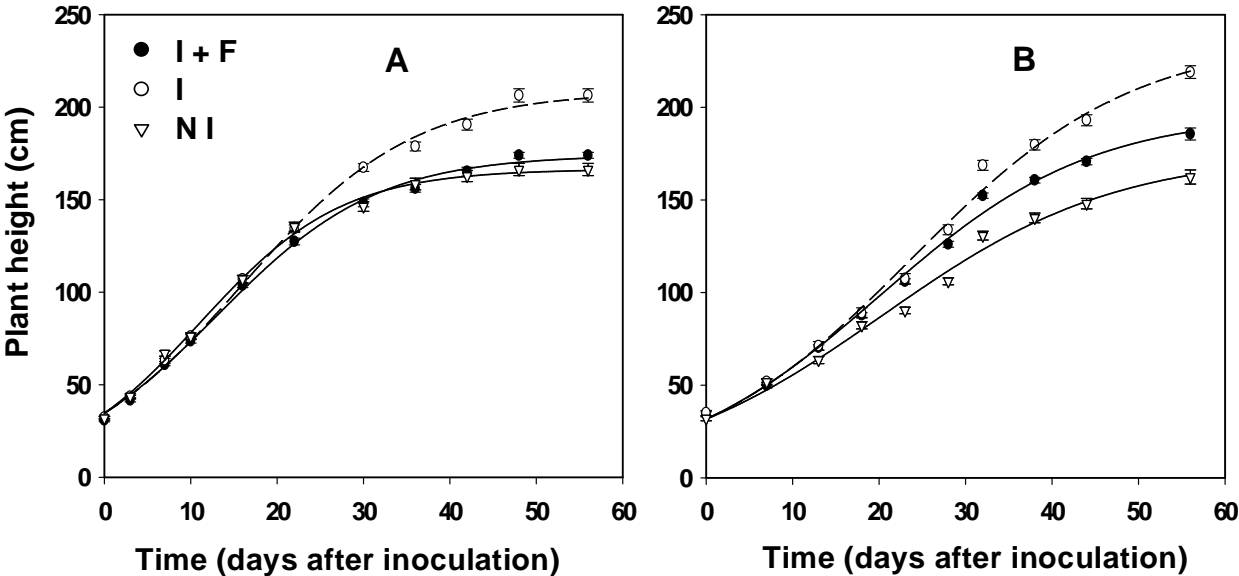**Fig. 6.** Logistic growth function fitted to the host dynamics of tomato expressed in terms of plant height (cm) with and without powdery mildew (*Oidium neolycopersici*) inoculation (I and NI) and fungicide application (I + F) during experiments A and B. A constant value of the initial plant height H_0 which was calculated as the average of H_0 values of the individual treatments was used in the regression analyses.

The dynamics of plant height were well described by the logistic (Eqn. 1) and Gompertz (Eqn. 2) growth functions with high values of coefficient of determination ($R^2 > 0.98$) in both experiments (Fig. 6). In contrast to the dynamics of cumulative total leaf area (Table 2), the coefficient of determination (R^2) values indicated that the Gompertz function gave a better fit to the dynamics of plant height in experiment A while the logistic function was preferable in experiment B (Table 3).

TABLE 3. Estimated parameter values (± standard errors) and coefficients of determination (R^2) of the logistic and Gompertz functions fitted to plant height (cm) of tomato with and without powdery mildew (*Oidium neolycopersici*) inoculation and fungicide spray during experiments A and B. To enable a comparison of treatments, the values of H_0 were fixed at the mean value estimated separately for the treatments within each experiment.

Experiment	Trt.[x]	Logistic function				Gompertz function			
		Estimated parameter values				Estimated parameter values			
		R^2	H_{max}	H_0	r_{HL}	R^2	H_{max}	H_0	r_{HG}
A	I	0.998	208.56 a[y] (2.65)[z]	34.6	0.1008 c[y] (0.003)	0.999	221.06a[y] (2.77)	30.2	0.0637c[y] (0.002)
	I + F	0.998	174.15 b (1.88)	34.6	0.1074 b (0.003)	0.999	181.01b (1.52)	30.2	0.0722b (0.001)
	NI	0.997	166.45 c (1.61)	34.6	0.1214 a (0.003)	0.997	170.98c (1.98)	30.2	0.0839a (0.003)
B	I	0.992	237.12 a (8.18)	31.7	0.0785 ab (0.003)	0.987	277.53a (20.21)	28.4	0.0420b (0.003)
	I + F	0.995	196.64 b (4.69)	31.7	0.0821 a (0.003)	0.989	218.27b (10.94)	28.4	0.0481a (0.003)
	NI	0.991	175.06 c (5.92)	31.7	0.0742 b (0.003)	0.988	194.05c (11.36)	28.4	0.0444ab (0.004)

[x] Treatments: I = inoculated, I + F = inoculated with fungicide spray, NI = non-inoculated.

[y] Values of H_{max} and r_{HL} designated with same letters within the columns of experiment A and B are not statistically different according to Tukey's test at $p < 0.05$ in pairwise comparisons of I, I + F, and NI.

[z] Standard errors of the estimates are given in parentheses

The H_{max} estimates of plant height significantly differed across all treatments in both experiments (Table 3) with highest values always in treatment I and lowest values in treatment NI. The difference in H_{max} between the treatments I + F and NI was particularly higher in experiment B than in A. Assuming an identical initial host size (H_0), the estimated values of the rate parameter for host growth, r_{HL} and r_{HG}, differed significantly across all treatments of experiment A. Healthy plants in treatment NI had the highest growth rates, while diseased plants in treatment I the lowest (Table 3). In experiment B, however, the I + F plants showed a significantly higher r_{HL} value compared to NI plants (logistic function) and I plants (Gompertz function).

Effects on healthy leaf area duration and yield. The disease-induced defoliation also significantly reduced the duration of healthy leaf area ($HLAD$, cm²-days). In experiment A, a significantly higher healthy leaf area duration of 273672.7 ($\pm$ 7208.8) (cm²-days) was calculated for NI plants than for I + F (212951.8 $\pm$ 6833.9) and I plants (101104.9 $\pm$ 3272.5), respectively. Similarly for experiment B, $HLAD$ (cm²-days) values were 324768.2 ($\pm$ 6293.0), 193216.3 ($\pm$ 6533.4) and 133065.2 ($\pm$ 2759.1) for NI, I + F and I plants, respectively. Obviously, the reduction in $HLAD$ was predominantly pronounced in comparisons between I and NI treatments. Moreover, fungicide application remarkably prolonged the duration of healthy leaf area when compared to the non-sprayed treatments.

Yield (g plant^{-1}) of tomato plants (only determined in experiment B) was significantly reduced when inoculated with powdery mildew. The yield loss was 22% when the yield of NI plants (503.7 $\pm$ 15.7 g plant^{-1}) was compared with that of the I plants (392.5 $\pm$ 15.1). The control of powdery mildew by one fungicide spray at 20 DAI completely eliminated the negative disease effect on yield, because the plants in treatment I + F produced the same yield (503.3 $\pm$ 17.6) like those in treatment NI.

The relationship between *HLAD* (cm²-days) and yield (g plant[-1]) of the 34 tomato plants of all treatments (NI, I and I + F) in experiment B is shown in Fig. 7. The non-linear relationship was fairly described by the monomolecular function (Eqn. 5): yield = 516.93 [1- exp(-0.0000239 [*HLAD*-71167.89])] with R^2 = 0.4358. According to this function, at least a *HLAD* of 71167.89 cm²-days was needed to produce any yield. Thereafter yield increased with increasing *HLAD* initially linearly, but later asymptotically to a maximum yield of 517 g. Thus further increments in *HLAD* beyond roughly 2×10^5 cm²-days do not result in more yield.
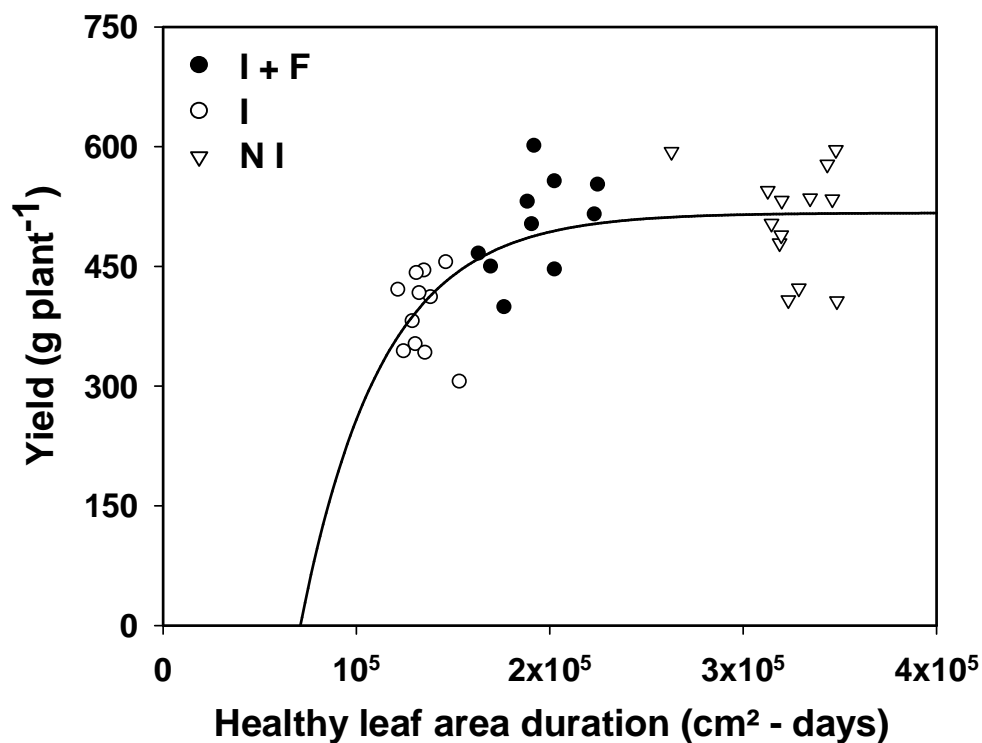
Fig. 7. Relationship between healthy leaf area duration *HLAD (cm²- days)* and fruit yield (g plant[-1]) of 34 tomato plants grown under the influence of powdery mildew (*Oidium neolycopersici*) epidemics with (I + F) and without (I) fungicide application compared to non-inoculated (NI) plants in experiment B. The line is the fitted monomolecular function, yield = 516.93 [1- exp(-0.0000239 [*HLAD*-71167.89])] with R^2 = 0.4358.

DISCUSSION

The effects of the powdery mildew fungus (*O. neolycopersici*) on the host dynamics of tomato mainly revolve around its effects on the main photosynthetic organ, the leaves. Leaf area (cm²) measured non-destructively was thus the main parameter quantified to monitor the host growth dynamics of tomato.

Following artificial inoculation with powdery mildew, disease severity on a plant basis progressed increasingly in non-sprayed plants with secondary infections on newly emerged leaves due to the polycyclic nature of the disease. In terms of the actual disease severity, maximum proportions of 0.83 and 0.53 were recorded in experiments A and B, respectively. These results corroborated with the findings of Jacob et al. (2008) who reported more than 0.6 proportion disease severity from experiments carried out under greenhouse conditions 44 days after inoculation.

Declines in the proportion of actual disease severity on a whole plant basis between successive assessments were evident during the observational period of both experiments. Generally, a decline in disease severity can be caused by the production of new healthy leaves or by the defoliation of severely diseased leaves. In our experiments, the decrease of the severity is primarily attributed to the defoliation of diseased leaves within the plant canopy. The defoliation necessitated adjustments in computing disease severity, an approach also taken by Ojiambo and Scherm (2005) to correct for leaf abscission in the Septoria leaf spot-blueberry pathosystem. However, despite making these adjustments for defoliation, declines in the proportion of disease severity between successive assessments were still evident especially in experiment B. This observation is beside the fact that the total amount of diseased leaf area (in cm²) actually increased (data not shown). A possible explanation for this is that the leaf area of the tomato plant grew with a higher rate than the disease was

progressing, i.e. proportion of diseased leaf tissue thus '*diluting*' the proportion of disease severity (Nelson and Campbell, 1993).

This phenomenon of declining disease severity due to the intermittent addition and removal of host tissue through host growth and defoliation, respectively, has been highlighted among others by Campbell and Madden (1990), Hau (1990) and Xu (2006). Examples of pathosystems that show this pattern of behavior include coffee rust (Kushalappa and Ludwig, 1982), bean rust (Mersha and Hau, 2008), leaf spot on white clover (Nelson and Campbell, 1993) and Alfalfa spot (Thal and Campbell, 1988).

Owing to the non-monotonic nature of the observed disease progress curves, the application of the commonly used growth functions (Gompertz and logistic) in the analysis of disease progress curves was deemed inappropriate. The basic assumption of the presence of a constant host area that can be diseased is inherent in these growth models and lack of consideration of it could lead to erroneous conclusions about the nature of the disease progress or a failure to capture the essential characteristics of the observed temporal pattern (Campbell and Madden, 1990).

When the cumulative total leaf area of non-inoculated and inoculated (without fungicide spray) plants are compared at each assessment date, the later assessments ($t > 36$ and $t > 44$ DAI in experiment A and B, respectively) showed no significant differences. Powdery mildew therefore did not change the final amount of the cumulative total leaf area. This is in contrast to what has been observed in other pathosystems for instance, late leafspot (*Cercosporidium personatum*) on peanut (*Arachis hypogaea*) (Aquino et al., 1992), *Mycosphaerella* blight (*Mycosphaerella pinodes*) on pea (*Pisum sativum*) (Béasse et al., 2000) and bean rust (*Uromyces appendiculatus*) on common bean (*Phaseolus vulgaris*) (Mersha and Hau, 2008), whereby epidemics significantly reduced crop growth at the later stages.

The host dynamics, either given as cumulative total leaf area or as plant height, were well described by the logistic and the Gompertz function ($R^2 > 0.98$), but there was no general trend that one of both functions was superior to the other in describing the dynamics. With respect to the cumulative total leaf area, powdery mildew significantly lowered the growth rate r_H of diseased plants when compared to healthy plants. However, estimates of maximum host size (H_{max}) of non-inoculated and inoculated plants with or without fungicide application showed no statistically significant differences implying that the cumulative total leaf area formed was not considerably reduced by the powdery mildew epidemics as already concluded from the pairwise comparisons of the cumulative total leaf area at the last assessments. Several explanations for this observation exist.

Firstly, the general agreement is that within a tomato canopy, the lower leaves not only have reduced photosynthetic efficiency but contribute little to net canopy photosynthesis (Xu et al., 1997; Adams et al., 2002; Valdes et al., 2010). According to Acock et al. (1978), the upper most layer of a tomato plant canopy which accounts for 23% of the total leaf area is the main receptor of light and assimilates 66% of the net CO_2 fixed by the canopy. In the current study, powdery mildew disease on tomato was confined mainly to the middle and lower stratum of the canopy while defoliation of diseased leaves began from the lower plant layers and proceeded upwards. Therefore it can be inferred that, despite a reduction in the net canopy photosynthesis through loss of photosynthesizing tissue, the extent to which this occurred was not significant enough to cause a negative effect on formation of leaves.

Secondly, powdery mildew fungi are typically obligate fungal pathogens that form haustoria only in the epidermal cells. The pathway of carbon flow is primarily from the source (chloroplasts in the mesophyll) to the sink (epidermal cells which lack chloroplasts) then into a secondary sink, fungus via haustoria in epidermal cells (Whipps et al., 1998; Mieslerová et al., 2004; Agrios, 2005). Leaves infected by powdery mildew fungi show a progressive loss in the overall photosynthetic activity although this is usually noticeable only in the later stages

of infection when premature senescence of the leaves commence (Lucas, 1998; Prokopová et al., 2010).

With respect to plant height and contrary to expected, powdery mildew epidemics notably enhanced growth of host plants as is evident when progress curves of inoculated and non-inoculated treatments are compared. The exact mechanism behind this stimulatory effect is not clear and needs to be further investigated.

Whereas leaf abscission due to natural senescence was not observed on non-inoculated plants throughout the duration of the experiments, disease-induced defoliation accounted for 63.1% and 58.3% losses in leaf area of inoculated plants in experiments A and B, respectively. Correll et al. (1988) reported defoliation in the range of 30 to 40% in unsprayed tomato fields affected by *Leveillula taurica*, another causal agent of powdery mildew disease on tomato.

The final disease severity assessed on individual leaves before they abscised was quite high, 0.79 in experiment A and 0.78 in experiment B, both values from the I treatments. These disease levels are much higher than those in the study of Kranz (1977) of five different pathosystems, where the frequency of the highest class (0.3711 to 1 proportion disease severity) never reached 10%. Specifically for powdery mildew on barley, Kranz (1977) reported only a frequency of 6.3% in this highest disease class.

The integral variables healthy leaf area duration and healthy leaf area absorption have been used extensively in the analysis of host, disease and yield relationships (Waggoner and Berger, 1987; Bergamin Filho et al., 1997). The non-linear nature of the relationship between yield and *HLAD* described in this paper collaborates with that reported by Waggoner and Berger (1987) and Aquino et al. (1992) for the peanut - *Cercosporidium personatum* pathosystem. In these papers, the relationship was described by Gompertz functions, which would predict yield even when *HLAD* was very low. We decided to use a monomolecular function which allows estimating the minimum *HLAD* needed to produce any yield.

Yield loss attributable to *O. neolycopersici* has not been reported in earlier studies. In the present study, a significant 22% reduction in fruit yield due to the powdery mildew epidemic was apparent. However, fungicide application significantly mitigated this effect. Whereas fruits may not be directly affected, premature defoliation of diseased leaves may lead to a reduction in fruit size and nutritional quality resulting in diminished yields (Whipps et al., 1998; Mieslerová et al., 2004). Declining photosynthetic area of plants through leaf tissue destruction and defoliation results in reduced photosynthetic output which often translates to reduced yield (Agrios, 2005). Additionally, the fact that powdery mildew epidemics cause considerable defoliation may in turn predispose the fruits to damage such as sun burning and insect damage especially in field-grown tomato crops (Correll et al., 1988).

The timing of any fungicide application is critical towards achieving maximum effectiveness in disease control as well as avoiding wastage of fungicides. In the current study, application of the fungicide 10 days after inoculation (DAI) led to a proportionately 4-fold reduction in final severity of powdery mildew epidemics in comparison to a 2-fold reduction achieved when the fungicide is applied 20 DAI. Adequate knowledge of the disease epidemiology and proper diagnostic procedures are thus important aspects that should to be taken into consideration if significant disease control through fungicide use is to be achieved (Cook and Yarham, 1998).

LITERATURE CITED

Acock, B., Charles-Edwards, D. A., Fitter, D. J., Hand, D. W., Ludwig, L. J., Wilson, J. W., and Withers, A. C. 1978. The contribution of leaves from different levels within a tomato crop to canopy net photosynthesis: An experimental examination of two canopy models. J. Exp. Bot. 29:815-827.

Adams, S. R., Woodward, G. C., and Valdés, V. M. 2002. The effects of leaf removal and modifying temperature set-points with solar radiation on tomato yields. J. Hort. Sci. Biotechnol. 77:733-738.

Agrios, G. N. 2005. Plant Pathology, 5th ed. Elsevier Academic Press, San Diego, CA.

Aquino, V. M., Shokes, F. M., Berger, R. D., Gorbet, D. W., and Kucharek, T. A. 1992. Relationships among late leafspot, healthy leaf area duration, canopy reflectance, and pod yield of peanut. Phytopathology 82:546-552.

Béasse, C., Ney, B., and Tivoli, B. 2000. A simple model of pea (*Pisum sativum*) growth affected by *Mycosphaerella pinodes*. Plant Pathol. 49:187-200

Bergamin Filho, A. B., Carneiro, S. M. T. P. G., Godoy, C. V., Amorim, L., Berger, R. D., and Hau, B. 1997. Angular leaf spot of *Phaseolus* beans: Relationships between disease, healthy leaf area and yield. Phytopathology 87:506-515.

Boote, K. J., Jones, J. W., Mishoe, J. W., and Berger, R. D. 1983. Coupling pests to crop growth simulators to predict yield reductions. Phytopathology 73:1581-87.

Campbell, C. L., and Madden, L. V. 1990. Introduction to Plant Disease Epidemiology. Wiley, New York.

Charles-Edwards, D. A. 1982. Physiological Determinants of Crop Growth. Academic Press, London, U.K.

Cook R. J., and Yarham D. J. 1998. Epidemiology in sustainable systems. Pages 260-77 in: The Epidemiology of Plant Diseases. D. G. Jones, ed. Kluwer Academic Publishers, Dordrecht, The Netherlands.

Correll, J. C., Gordon, T. R., and Elliott, V. J. 1988. Powdery mildew of tomato: The effect of planting date and Triadimefon on disease onset, progress, incidence, and severity. Phytopathology 78:512-519.

Garry, G., Jeuffroy, M. H., Ney, B. and Tivoli, B. 1998. Effects of Ascochyta blight (*Mycosphaerella pinodes*) on the photosynthesizing leaf area and the photosynthetic efficiency of the green leaf area of dried-pea (*Pisum sativum*). Plant Pathol. 47: 473-479.

Hau, B. 1990. Analytic models of plant disease in a changing environment. Ann. Rev. Phytopathol. 28: 221-245.

Jacob, D., David, R. D., Sztjenberg, A., and Elad, Y. 2008. Conditions for development of powdery mildew of tomato caused by *Oidium neolycopersici*. Phytopathology 98:270-281.

Jones, H., Whipps, J. M., and Gurr, S. J. 2001. The tomato powdery mildew fungus *Oidium neolycopersici*. Mol. Plant Pathol. 2:303-309.

Kiss, L., Cook, R. T. A., Saenz, G. S., Cunnington, J. H., Pascoe, I., Bardin, M., Nicot, P. C., Takamatsu, S., Sato, Y., and Rossman, A. Y. 2001. Identification of two powdery mildew fungi, *Oidium neolycopersici* sp. nov. and *O. lycopersici,* infecting tomato in different parts of the world. Mycol. Res. 105: 684-697.

Kranz, J. 1977. A study on maximum severity in plant diseases. Pages 169-173 in: Travaux dédiés à G. Viennot-Bourgin. Société Francaise de Phytopathologie, Paris.

Kranz, J. 2003. Comparative Epidemiology of Plant Diseases. Springer-Verlag, Berlin-Heidelberg, Germany.

Kranz, J., and Jörg, E. 1989. The synecological approach in plant disease epidemiology. Rev. Trop. Plant Pathol. 6:27-38.

Kushalappa, A. C., and Ludwig, A. 1982. Calculation of apparent infection rate in plant diseases: development of a method to correct for host growth. Phytopathology 72:1373-1377.

Lucas, J. A. 1998. Plant Pathology and Plant Pathogens. Blackwell Science, Bristol.

Mersha, Z., and Hau, B. 2011. Reciprocal effects of host and disease dynamics in the bean rust pathosystems. J. Plant Dis. Protec. 118:54-62.

Mersha Z., and Hau, B. 2008. Effect of bean rust (*Uromyces appendiculatus*) epidemics of host dynamics of common bean (*Phaseolus vulgaris*). Plant Pathol. 57:674-686.

Mieslerová, B., Lebeda, A., and Kennedy, R. 2004. Variation in *Oidium neolycopersici* development on host and non-host plant species and their tissue defense responses. Ann. Appl. Biol. 144:237-248.

Nelson, S. C., and Campbell, C. L. 1993. Disease progress, defoliation and spatial pattern in a multiple-pathogen disease complex on white clover. Phytopathology 83:419-429.

Ojiambo, P. S., and Scherm, H. 2005. Temporal progress of Septoria leaf spot on rabbiteye blueberry (*Vaccinium ashei*). Plant Dis. 89:1090-1096.

Prokopová, J., Mieslerová, B., Hlaváčková, V., Hlavinka, J., Lebeda, A., Nauš, J., and Špundová, M. 2010. Changes in photosynthesis of *Lycopersicon spp.* plants induced by tomato powdery mildew infection in combination with heat shock pre-treatment. Physiol. Mol. Plant Pathol. 74:205-213.

Robert, C., Bancal, M. O., Nicolas, P., Lannou, C., Ney, B. 2004. Analysis and modelling of effects of leaf rust and *Septoria tritici* blotch on wheat growth. J. Exp. Bot. 55:1079-1094.

Rouse, D. I. 1988. Use of crop growth-models to predict the effects of disease. Ann. Rev. Phytopathol. 26:183-201.

Thal, W. M., and Campbell, C. L. 1988. Analysis of progress of alfalfa leaf spot epidemics. Phytopathology 78:389-395.

Valdes, V. M., Woodward, G. C., and Adams, S. R. 2010. The effects of long-day lighting and removal of young leaves on tomato yield. J. Hort. Sci. Biotechnol. 85:119-124.

Van Maanen, A., and Xu, M. 2003. Modelling plant disease epidemics. Eur. J. Plant Pathol. 109:669-682.

Waggoner, P. E., and Berger, R. D. 1987. Defoliation, disease, and growth. Phytopathology 77:393-98

Whipps, J. M., Budge, S. P., and Fenlon, J. S. 1998. Characteristics and host range of tomato powdery mildew. Plant Pathol. 47:36-48.

Xu, H. L., Gauthier, L., Desjardins, Y., and Gosselin, A. 1997. Photosynthesis in leaves, fruits, stem and petioles of greenhouse-grown tomato plants. Photosynthetica 33:113-123.

Xu, X. 2006. Modelling and interpreting disease progress in time. Pages 215-238 in: The Epidemiology of Plant Diseases, 2nd ed. B. M. Cooke, D. Gareth Jones, and B. Kaye, eds. Springer, Dordrecht, The Netherlands.

Chapter 2

Modeling the interaction between powdery mildew epidemics and host dynamics of tomato

John Chelal and Bernhard Hau*

Leibniz Universität Hannover

Institut für Gartenbauliche Produktionssysteme, Abteilung Phytomedizin

Herrenhäuser Str. 2, D-30419 Hannover, Germany

*Corresponding author: hau@ipp.uni-hannover.de

ABSTRACT

A model simulating the progress of powdery mildew coupled to the growth dynamics of tomato is developed. The model is formulated as a set of differential equations for the rate of change in the amount of healthy, diseased and defoliated leaf area of a diseased plant relative to that of a healthy crop. The main assumption of the model is that the total host area formed is limited and identical in the disease and non-disease situation. Host and disease parameters were estimated through fitting the model to experimental data obtained from glasshouse experiments. Model outputs of powdery mildew severity and tomato leaf area showed a good fit to observed data with $R^2 > 0.97$. In the two experiments with a bigger pot size, the estimated rates for host growth (r_H: 0.112 and 0.123 day^{-1}), defoliation (r_D: 0.050 to 0.083 day^{-1}) and disease (r_Y: 0.128 to 0.130 day^{-1}) were very similar while the rates in the other experiment clearly differed. The simulated effect of the disease on the host growth rate was not uniform, predicting in only one experiment that powdery mildew epidemics significantly lowered the growth rate r_H of diseased plants when compared to the healthy plants. The model showed that defoliation of healthy area does not contribute significantly to total defoliated area. Except for slight deviations, there were no significant differences between progress curves of either host or disease dynamics under a constant or variable disease rate influenced by temperature and relative humidity. Since there was a reasonably good fit between model outputs and experimental data, the model can be considered to satisfactorily describe the interaction between powdery mildew epidemics and growth dynamics of tomato.

Additional key words: Host-disease interaction, defoliation, *Oidium neolycopersici*, *Solanum lycopersicum*.

INTRODUCTION

Powdery mildew of tomato (*Solanum lycopersicum* L.), caused by *Oidium neolycopersici* Kiss., is a disease of worldwide occurrence in glasshouse-grown tomatoes but is also of increasing importance on field-grown tomato crops (Whipps et al., 1998; Jones et al., 2001). Characteristic symptoms include powdery white lesions on the adaxial leaf surface but lesions may also be observed on petioles and the calyx. Infected leaves show a gradual decline in the overall photosynthetic activity although this is usually noticeable only in the later stages of infection (Lucas, 1998, Prokopová et al., 2010). Severely mildewed leaves become chlorotic and prematurely senescent such that the disease results in considerable defoliation and a marked reduction in fruit size and quality (Jones et al., 2001, Mieslerová et al., 2004).

Though tomato powdery mildew poses such significant threat to tomato production, little research has been dedicated towards modeling the synchronous interaction between the disease and its host plant under prevailing environmental conditions. This is of importance since the dominant features of an epidemic such as its overall severity and spatio-temporal dynamics are the result of the dynamic interactions of the host and pathogen systems with the environment as the driving force (Newton et al., 1995; Van Maanen and Xu, 2003).

Environmental variables particularly temperature, relative humidity and leaf wetness influence the rate of progress of different stages of the disease cycle ranging from germination to dissemination of spores (Agrios, 2005; Jacob et al., 2008). Likewise, during their growth and development, host plants undergo changes in their susceptibility to disease development (Kranz, 2003). Such changes in the susceptibility of the host relate not only to the amount of host tissue available for infection but also to the nature and levels of intrinsic host resistance and age-related resistance that is associated with specific host tissues (Hau, 1990; Van Maanen and Xu, 2003; Mersha and Hau, 2011).

Furthermore, disease-induced defoliation of leaves which is predominantly a key feature of powdery mildew epidemics, has received little attention in modeling and is often left unquantified. So far, only Waggoner (1986) and Jeger (1986) have proposed models to incorporate decrease in the proportion of diseased units of the host due to defoliation.

Given that the dynamics of host growth can be partitioned into healthy and diseased components, the model of the host-disease system proposed by Waggoner (1986) can be written as a pair of differential equations:

$$\frac{dH}{dt} = r_H \cdot (H+Y) \cdot (1-(H+Y)/H_{max}) - r_Y \cdot Y \cdot (1-Y/(H+Y))$$

$$\frac{dY}{dt} = r_Y \cdot Y \cdot (1-Y/(H+Y)) - r_D \cdot Y$$

(1)

In these equations, H is healthy host size in absolute units (for example in cm^2) at any time, Y is the diseased host size, measured in the same absolute units. $H + Y$ is equivalent to the actual host size, r_Y and r_H are rate parameters of disease change and host growth, respectively, H_{max} represents maximum host size. For defoliation it is assumed that only diseased areas are defoliated and that the change is proportional to the diseased area Y with a proportionality factor r_D, so that the dynamics of defoliated area D is given by the differential equation $dD/dt = r_D \cdot Y$. In his original model, Waggoner (1986) replaced r_D by the inverse of t_D, which is the average time from infection to defoliation. On a long run, the differential system asymptotically leads to constant levels of H and Y and thus also for the disease severity $y = Y/(H + Y)$. This steady state means that finally the increase of the host due to growth and the loss due to defoliation is identical. Thus the total amount of leaf area formed as well as the total defoliated leaf area $D(t)$ will increase continuously without bound. However, the majority of seasonal and annual crops have an initial vegetative phase during which leaf area increases rapidly but then gradually levels off at its maximum towards the end of the growing season as carbohydrates are allocated to the storage and reproductive parts of the plant

(Ferrandino, 2008). The assumption of unlimited leaf area production in the disease situation as in Waggoner's model is thus implausible.

In Waggoner's model (equation 1) the increase of the host is driven by the actual host size including the diseased area. However, the disease may negatively affect host growth. This negative effect was included in the model of Jeger (1986) by introducing an additional term $(1 - Y/(H + Y))$ in the differential equation for host growth which can also be applied in equation 1:

$$\frac{dH}{dt} = r_H \cdot (H + Y) \cdot (1 - Y/(H + Y)) \cdot (1 - (H + Y)/H_{max}) - r_Y \cdot Y \cdot (1 - Y/(H + Y))$$

$$= r_H \cdot H \cdot (1 - (H + Y)/H_{max}) - r_Y \cdot Y \cdot (1 - Y/(H + Y)) \tag{2}$$

$$\frac{dY}{dt} = r_Y \cdot Y \cdot (1 - Y/(H + Y)) - r_D \cdot Y$$

The second kind of writing of the differential equation of the healthy area shows that the increase of healthy area is now driven by the healthy area H, and not the actual host area $H + Y$ as in equation 1. In this case, the healthy area H and the diseased area Y show periodic damped oscillations over time leading to dynamic equilibria for H and Y (Jeger, 1986) and thus to a constant disease severity y. However, also in this case, the total leaf area formed and the total defoliated area $D(t)$ increase over time without limitation. Therefore, this approach is also unrealistic particularly for host-disease pathosystems pertaining to seasonal crops such as is the case of tomato and powdery mildew investigated in this paper.

To enable a better description and understanding of powdery mildew epidemics and its interaction with the growth dynamics of tomato, an improved model coupling host growth with temporal disease progress under the assumption of a constant and a variable rate of disease progress was developed.

MATERIALS AND METHODS

Experimentation. Data for disease dynamics and host growth were obtained from three glasshouse experiments conducted at the Institut für Gartenbauliche Produktionssysteme (Abteilung Phytomedizin) of Leibniz Universität Hannover.

Experimental plants. Tomato *cv.* Hildares F1 seedlings were raised in a nursery for an average of three weeks. Each seedling was then transplanted into a 2-litre (experiment A) and 10-litre (experiment B and C) capacity perforated plastic pot filled with the substrate Frühstorfer Erde (Industrie-Erden Werk, Germany). Neudorff's organic fertilizer Azet ® (7-3-10 N, P_2O_5, and K_2O, respectively) was incorporated at transplanting at the rate of 50 g/ plant.

Artificial inoculation. Fully established tomato transplants (5-6 weeks old) with an average of 7 leaves per plant were artificially inoculated in a fan-equipped inoculation chamber by blowing conidia from a heavily diseased plant hence inducing a random distribution of the disease on healthy plants. Inoculated plants were then transferred to a glasshouse compartment, whereas non-inoculated plants were raised in a separate glasshouse cubicle to prevent any unintended spread of inoculum on healthy plants. The single-plant approach of Kranz and Jörg (1989) was adopted in which each treatment, i.e. inoculated with powdery mildew and non-inoculated, comprised 10, 15 and 11 plants in experiment A, B and C, respectively.

Glasshouse conditions. Daily and hourly readings of both temperature and relative humidity were obtained from a centralized data logger located within the glasshouse compartments. Generally, temperature and relative humidity readings were within the range of 19–25°C and 35–67%, respectively. Natural light was supplemented with artificial light to provide a photoperiod of 16 hrs.

Host growth and disease analyses. The length of each leaf of the experimental plants was measured using a metric ruler on a weekly basis. Accordingly, following the approach of

Schwarz and Klaring (2001) and Blanco and Folegatti (2005), leaf areas of experimental plants were determined non-destructively by the power function, $LA=0.016LL^{2.09}$ ($n = 250$; $R^2 = 0.85$) derived from non-linear regression analysis of the relationship between leaf length (*LL*) and leaf area (*LA*) using the statistical analysis software SigmaPlot11.0 (San Jose, CA, USA).

At the onset of powdery mildew symptoms, disease severity of each leaf (fully unfolded with 5 to 7 leaflets) was visually estimated as proportion of powdered leaf surface in comparison with the total leaf area. The actual leaf area per plant at any given time was determined from the sum of areas of individual leaves available on the plant. The diseased leaf area of individual leaves was summed up to obtain the total diseased leaf area on a plant. Diseased leaf area was deducted from the actual leaf area to determine healthy leaf area. Once a leaf defoliated, the maximum leaf area recorded prior to defoliation was noted. Thus, the cumulative defoliated leaf area for each consecutive assessment time was obtained by summing up areas of all leaves that had defoliated from the plant.

Modeling approach

Basic model

This modeling approach incorporates two major components: tomato as the host plant and powdery mildew as the disease. Since the detrimental effects of powdery mildew on tomato mainly revolve around its effects on the main photosynthetic organ, the leaves, leaf area expressed in cm^2 was adopted as the measurement unit for the respective healthy *H*, diseased *Y* and defoliated *D* host tissue. In our model, like in those of Jeger (1986) and Waggoner (1986), the diseased area *Y* is not subdivided into the three categories latent, infectious and post-infectious area like in the models of Madden et al. (2007). The basic model examines the behavior of the tomato-powdery mildew pathosystem under the implicit assumption that the

effects of the variations of environmental factors in the greenhouse can be neglected and therefore constant rates for host and disease dynamics can be supposed. Principal variables and parameters used in the model are listed in Table 1.

TABLE 1. Principal variables and parameters used in the models.

Symbol	Description	Unit
State variables		
H	Healthy leaf area (in the diseased situation)	cm² plant^{-1}
H_{DF}	Healthy leaf area (in the disease-free situation)	cm² plant^{-1}
Y	Diseased leaf area	cm² plant^{-1}
D	Defoliated leaf area	cm² plant^{-1}
Derived variables		
$y = Y/(H + Y)$	Disease severity	proportion
Influencing variables		
T	Temperature	°C
RH	Relative humidity	%
Parameters		
H_0	Initial host size	cm² plant^{-1}
H_{max}	Maximum leaf area	cm² plant^{-1}
Y_0	Initial diseased area	cm² plant^{-1}
r_{LIN}	Linear rate parameter for initial disease increase	cm² day^{-1}
r_Y	Logistic rate parameter for disease increase	day^{-1}
r_{LINmax}	Maximum possible rate (for $IP \leq t < LP + IP$)	day^{-1}
r_{Ymax}	Maximum possible rate (for $t \geq LP + IP$)	day^{-1}
r_H	Logistic rate parameter for host growth	day^{-1}
r_D	Defoliation rate	day^{-1}
r_{DY}	Defoliation rate of diseased area	day^{-1}
r_{DH}	Defoliation rate of healthy area	day^{-1}
f_{red}	Factor of the disease effect on host growth rate	-
Predetermined parameters		
IP	Incubation period (fixed at 6)	days
LP	Latent period (fixed at 7)	days
y_{DT}	Defoliation threshold (fixed at 0.34)	proportion
t_{DT}	Time when y_{DT} is reached for the first time	DAI

Host and disease development. The dynamics of the healthy leaf area (H) in the disease situation is given by the differential equation with initial condition $H(t = 0) = H_0$:

$$\frac{dH}{dt} = r_H \cdot (H + Y) \cdot (1 - (H + Y + D)/H_{max}) - Rate_{HY} \tag{3}$$

The first term on the right hand side describes the increase of the healthy area by newly produced tissue, while the second term reflects the rate at which healthy area becomes diseased. As natural defoliation was not observed in the disease-free situation during the experimental period, no natural defoliation is considered in the disease situation, too. Moreover, it is assumed that healthy area H is not affected by disease induced defoliation. The production of new tissue is essentially proportional to the actual area $H + Y$ and density regulated by the total host area formed $H + Y + D$ (cm^2) which is limited by H_{max} (cm²). Before the disease-induced defoliation starts, i.e. $D = 0$, the production of healthy leaf area is a logistic function with rate r_H and maximum value H_{max}. When leaf area is defoliated, the increase of H differs from a logistic function, but the inclusion of D in the regulation term limits the total production. This is the main difference to the host growth in equations 1 and 2 in which an unlimited production is assumed.

In the absence of the disease, i.e. $Y = 0$ and $D = 0$, the healthy host area is equivalent to the total host area. In order to differentiate the healthy area in the disease-free situation from that with disease, it is marked with an index DF. From equation 3 it follows that the healthy host area H_{DF} will increase logistically starting from $H_{DF}(t = 0) = H_0$ and approaching an asymptotic value H_{max} (cm^2) at a rate r_H (day^{-1}):

$$\frac{dH_{DF}}{dt} = r_H \cdot H_{DF} \cdot (1 - H_{DF}/H_{max}) \tag{3'}$$

When powdery mildew is present, the infection process begins when conidia land on tomato leaves, germinate and subsequently establish infections with the assumption taken that host tissue is continually susceptible to infection irrespective of host age. Powdery white

mildew lesions become visible on the leaf surface within 5 to 7 days (Whipps and Budge, 2000). The dynamics of the diseased area (Y) after artificial inoculation at time $t = 0$ is described by the differential equation:

$$\frac{dY}{dt} = Rate_{HY} - \frac{dD}{dt} \qquad (4)$$

The first term in equation 4 describes the increase of the diseased area Y by new symptoms, while the second term reflects the defoliation due to the disease.

For the $Rate_{HY}$ three time periods are differentiated:

$$Rate_{HY} = \begin{cases} 0 & \text{if } 0 \le t < IP \\ r_{LIN} & \text{if } IP \le t < LP + IP \\ r_Y \cdot Y \cdot (1 - Y/(H+Y)) & \text{if } t \ge LP + IP \end{cases}$$

The first equation is based on the fact that during the incubation period *IP* the symptoms caused by the artificial inoculation at $t = 0$ are not visible. For tomato powdery mildew, *IP* was set to 6 days as it takes an average of 6 days to symptom expression (Whipps and Budge, 2000). In the second equation of $Rate_{HY}$, it is assumed that under the strong inoculum pressure of the inoculation the visible powdery mildew epidemic after the end of the incubation period increases linearly within an early cycle with disease rate r_{LIN} (cm^2 day^{-1}), starting from $Y(t = IP) = Y_0$. The primary disease cycle is assumed to end 13 days after inoculation, i.e. before the symptoms of the second cycle that starts after the latent period *LP* (= 7 days) appear at *LP* + *IP*. Later on ($t \ge LP + IP$), the epidemic follows the ordinary pattern of a polycyclic disease given by a logistic differential equation with a disease rate r_Y (day^{-1}) and variable capacity $H + Y$ (cm^2), the actual leaf area.

For defoliation, the assumption is made that it is only caused by the disease and therefore that the contribution of natural leaf senescence in an infected plant is negligible compared to disease-induced defoliation (Allorent and Savary, 2005). In our experiments, natural defoliation was not observed in the disease-free situation during the experimental period. In

the model, defoliation is triggered once a certain level of disease severity on a whole plant basis is reached. This defoliation threshold for y (y_{DT}) per plant was determined as 0.34 from experimental data. The time when this threshold is reached for the first time is named t_{DT}. After t_{DT}, the rate of defoliated leaf area (D) due to the disease is proportional to diseased leaf area (Y) with proportionality factor r_D such that:

$$\frac{dD}{dt} = \begin{cases} 0 & \text{if } t < t_{DT} \\ r_D \cdot Y & \text{if } t \geq t_{DT} \end{cases} \qquad (5)$$

Modification 1: Negative effect of the disease on host production

In equation 3, the production of new healthy area is essentially proportional to the actual area $H + Y$. As a modification it could be assumed that the production is only proportional to the healthy area H like in Jeger's equation 2 so that equation 3 is replaced by:

$$\frac{dH}{dt} = r_H \cdot H \cdot \left(1 - (H + Y + D)/H_{\max}\right) - Rate_{HY} \qquad (6)$$

Equations 3 and 6 describe two special cases, namely that the diseased area is producing new tissue in the same way as healthy area (equation 3) or not at all (equation 6). One may, however, also assume an intermediate case that the diseased area is contributing to the production but less than the healthy area. This can be derived by the following equation for host growth:

$$\frac{dH}{dt} = \left(r_H \cdot H + r_H \cdot (1 - f_{red}) \cdot Y\right) \cdot \left(1 - (H + Y + D)/H_{\max}\right) - Rate_{HY} \qquad (7)$$

A value of the factor f_{red} between 0 and 1 represents the reducing effect of disease on the host production by new healthy tissue. If $f_{red} = 0.0$, the diseased area Y contributes in the same way to the production of new tissue like the healthy area H and therefore equation 7 is then identical to equation 3. On the other hand, if $f_{red} = 1.0$, the disease has a strong negative effect so that the host production is only proportional to the healthy area H like in equation 6.

Theoretically f_{red} can attain values greater than 1, meaning that the disease is reducing also the production due to the healthy area.

Equation 7 can be re-written as:

$$\frac{dH}{dt} = r_H \cdot \left(1 - f_{red} \cdot Y / (H + Y)\right) \cdot (H + Y) \cdot \left(1 - (H + Y + D)/H_{max}\right) - Rate_{HY} \qquad (8)$$

Compared to equation 3, this equation shows that production of healthy area is proportional to $H + Y$, but the proportionality factor $r_H \cdot (1 - f_{red} \cdot Y/(H + Y))$ is not constant but decreases with increasing disease severity $y = Y/(H + Y)$. For tomato powdery mildew it is known (Chelal and Hau, 2012) that the disease can lower the rate of growth r_H of diseased plants relative to the healthy plants.

Modification 2: Defoliation of healthy leaf area

According to equation 5, it is assumed that only diseased areas are defoliated after the threshold has been reached. In principle, however, defoliation of diseased areas in a leaf could also lead to the removal of healthy areas belonging to the same diseased leaves (Allorent and Savary, 2005). Thus this feature was examined as a modification of the basic model by partitioning total defoliation in such a way that the dynamics of defoliated leaf area (D) was described by the dynamics of change in the defoliated fraction of diseased area and healthy area D_Y and D_H, respectively, such that defoliation $D(t) = D_Y(t) + D_H(t)$. Diseased area Y is defoliated like in equation 5 with a rate r_{DY}:

$$\frac{dD_Y}{dt} = r_{DY} \cdot Y \qquad (9)$$

The defoliation of healthy area it is assumed to be proportional to the healthy area H, but also to the disease severity $y = Y/(H + Y)$ with a rate r_{DH}:

$$\frac{dD_H}{dt} = r_{DH} \cdot \left(Y/(H + Y)\right) \cdot H \qquad (10)$$

Accordingly, the dynamics of healthy leaf area H (equation 3) and diseased area Y (equation 4) are re-written as:

$$\frac{dH}{dt} = r_H \cdot (H + Y) \cdot (1 - (H + Y + D)/H_{max}) - Rate_{HY} - \frac{dD_H}{dt} \tag{11}$$

$$\frac{dY}{dt} = Rate_{HY} - \frac{dD_Y}{dt} \tag{12}$$

Like before, defoliation is triggered in this modification when the disease severity has reached the threshold y_{DT} at time t_{DT}.

Modification 3: Variable rate of disease progress

The basic model was further extended to examine the behavior of the host and disease system under changing environment. Therefore the disease rate r_{LIN} and r_Y in $Rate_{HY}$ (equation 4) were considered to be influenced by temperature and relative humidity, while the effects of changing environment on the host growth parameters r_H and H_{max} in equation 3 were disregarded since that would require input of agronomic-related information in order to describe the effects of external factors on host development (Hau, 1990).

Pathogen development. The epidemics of powdery mildew are largely influenced by the combined effects of temperature (T) and relative humidity (RH) (Whipps and Budge, 2000). Optimum temperatures for powdery mildew development have been reported at 20°C with temperatures below 10°C and above 28°C being detrimental to disease development (Jacob et al., 2008). Optimal relative humidity for development and spread of powdery mildew lies in the range of 60% to 80% (Whipps and Budge, 2000).

To apply the combined effects of temperature and relative humidity on the rate of disease progress, the effects of temperature $r(T)$ and relative humidity $r(RH)$ were combined as a function of environmental conditions assuming that the joint effects are multiplicative, such that: $r(T, RH) = r(T) \cdot r(RH)$. Accordingly, using the daily temperature and relative humidity values recorded during the experimental duration and following the approach of Berger et al.

(1995), a function for the daily environmental favorability was derived from fitting a Beta-Richards' equation to the response surface of temperature and relative humidity in relation to disease efficiency (Fig. 1) whereby, disease efficiency DE ($0.0 \leq DE \leq 1.0$) in relation to T and RH was described as:

$$DE(T,RH) = \begin{cases} 0 & T < T_{min} \\ d \cdot (T - T_{min})^n \cdot (T_{max} - T)^m \cdot (1 - e^{-a \cdot RH})^b & T_{min} \leq T \leq T_{max} \\ 0 & T > T_{max} \end{cases}$$

The following parameter values were estimated from experimental data: $T_{min} = 8\ °C$, $T_{max} = 28\ °C$, $n = 3.6872$, $m = 0.9722$, $a = 0.0981$, $b = 10.423$ and $d = 0.000009153$ whereby T_{min} and T_{max} are cardinal temperatures for disease development.
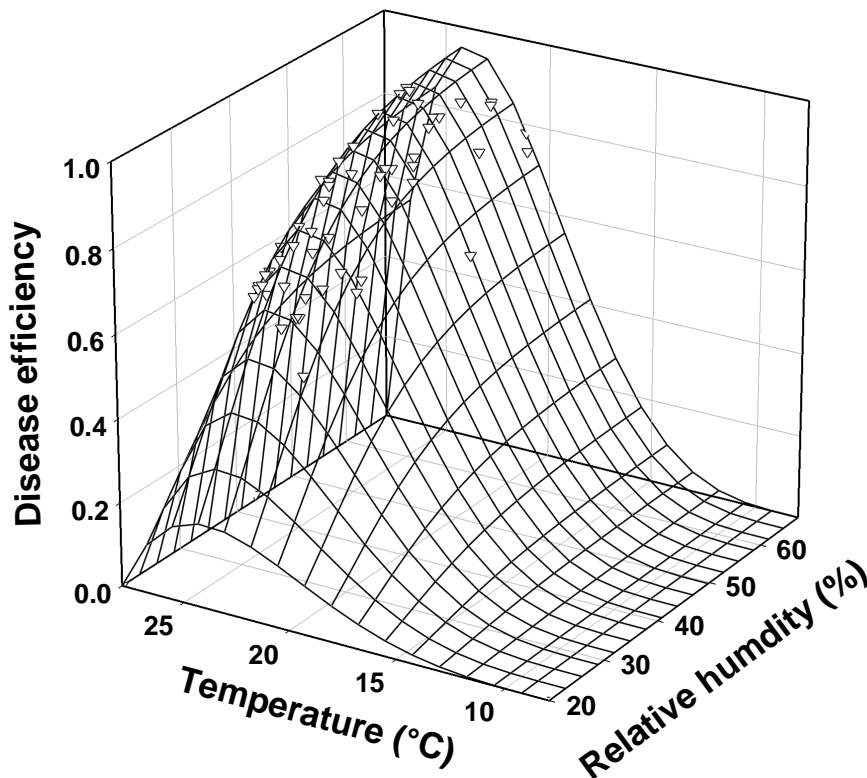

Fig. 1. Disease efficiency (*DE*) of powdery mildew (*Oidium neolycopersici*) on tomato in relation to temperature (*T*) and relative humidity (*RH*) conditions recorded in the glasshouse during experiment B. The response surface was described as: $DE = ([0.000009153(T - 8)^{3.6872}] [(28 - T)^{0.9722}] \{[1 - exp(-0.0981RH)]^{10.423}\})$.

Depending on the observation time, the rate of disease progress on a daily basis was thus computed from the daily disease efficiency value and the maximum possible rate (r_{LINmax} or r_{Ymax}) such that the disease rate r_{LIN} and r_Y in equation 4 is:

$$r_{LIN}(T,RH) = r_{LINmax} \cdot DE(T,RH) \qquad \text{if } IP \leq t < LP + IP$$

$$\tag{13}$$

$$r_Y(T,RH) = r_{Ymax} \cdot DE(T,RH) \qquad \text{if } t \geq LP + IP$$

The two parameters r_{LINmax} and r_{Ymax} were estimated by the optimization procedure.

Model evaluation and statistics. The models were built using ModelMaker version 4.0. (Oxford, UK) using the Runge-Kutta 4th order integration algorithm. Parameters were optimized using the Marquardt method by fitting the differential equations 3, 4 and 5 (basic model), equations 4, 5 and 6 or 7 (modification 1) and equations 9, 10, 11 and 12 (modification 2) to the data of the diseased situation and equation 3' to the data of the disease-free situation. Specifically the host growth rate r_H and the initial and maximum host area, H_0 and H_{max}, were simultaneously estimated in both situations.

The goodness-of-fit statistics were generated by procedures inbuilt in the software package. In particular, the variance ratio or F-Value which takes into account not only the goodness of fit but also the number of parameters in the model was used to verify whether the modifications (with additional parameters) gave a significantly better fit to the data when compared to the basic model. The higher the F-Value the less likely it is that the model explained the variation by chance (ModelMaker 4.0. Oxford, UK).

RESULTS

Basic Model

The model examined the dynamics of the interacting powdery mildew epidemic and the growth of tomato under the assumption of constant rates. Estimates of parameter values and coefficients of determination obtained from model fitting to experimental data are presented in Table 2. Generally, simulations of the different categories of leaf area were consistent with experimental data (Fig. 2). R^2 values of 0.976, 0.992 and 0.974 were computed for experiment A, B and C, respectively, thus giving an indication of a good fit of the model to the observations.

TABLE 2. Estimated parameter values and coefficients of determination (R^2) of the **basic model** (equations 3, 3', 4 and 5) simulating epidemics of powdery mildew (*Oidium neolycopersici*) on tomato and the dynamics of host growth under the assumption of constant rates (see Table 1 for explanation of acronyms).

Experiment	Estimated parameter values								
	H_0	r_H	H_{max}	Y_0	r_{LIN}	r_Y	r_D	F	R^2
A	435.3 (58.2)*	0.177 (0.021)	2186.9 (90.3)	17.99 (21.17)	59.48 (7.05)	0.302 (0.035)	0.335 (0.049)	321.8	0.976
B	1101.6 (87.3)	0.123 (0.007)	6511.7 (96.3)	13.96 (5.44)	144.3 (15.9)	0.130 (0.007)	0.050 (0.002)	964.6	0.992
C	1351.0 (210.4)	0.112 (0.013)	7883.3 (244.6)	2.70 (131.1)	124.1 (33.2)	0.128 (0.010)	0.083 (0.008)	331.4	0.974

*Standard errors of the parameter estimates are given in parentheses

Host growth. The model offered a satisfactory description of the general trend of host dynamics in terms of the healthy, diseased and defoliated leaf areas (Fig. 2). In the disease-free situation, the healthy host H_{DF} increased logistically approaching its asymptote H_{max}. However, in the presence of powdery mildew, a considerable effect of the disease on host growth was particularly discernible from a comparison of the healthy leaf area H relative to H_{DF} (Fig. 2). The increase of Y after the end of the incubation period, initially linearly and later logistically, lowers the growth of the healthy area H. The major changes in the dynamics start after the defoliation threshold $y_{DT} = 0.34$ is reached between 14 and 15 DAI in experiment A, 16 and 17 DAI in experiment B, and 21 and 22 DAI in C. In experiment A (Fig. 2A), the diseased area Y and also the healthy area H decrease continuously after t_{DT}, because the estimated value of r_D is greater than of r_Y (Table 2). In the two other experiments (Fig. 2B and C) with condition $r_Y > r_D$, Y and H increase to a maximum value and decrease thereafter. In all experiments, the defoliated area D increases monotonously although the shape of the curve is rather variable (Fig. 2).

Comparatively, estimates of the maximum amount of leaf area produced H_{max} were three to four-folds higher in experiment B and C, respectively, than in A (Table 2). Primarily, this was related to the size of potting container on which the plants were raised. In experiment A, plants were raised in 2-litre capacity perforated plastic pots, while in experiment B and C pots with a volume of 10 liters were used and thus more substrate was available for plant growth.

The estimated values of the rate parameter for host growth r_H (day^{-1}) were rather similar in experiments B and C (0.123 and 0.112) while that of experiment A was surprisingly high (0.177). The difference was even more pronounced when the values of the defoliation rate r_D (day^{-1}) were considered with a significantly higher estimate in experiment A (0.335) compared to experiments B (0.050) and C (0.083).
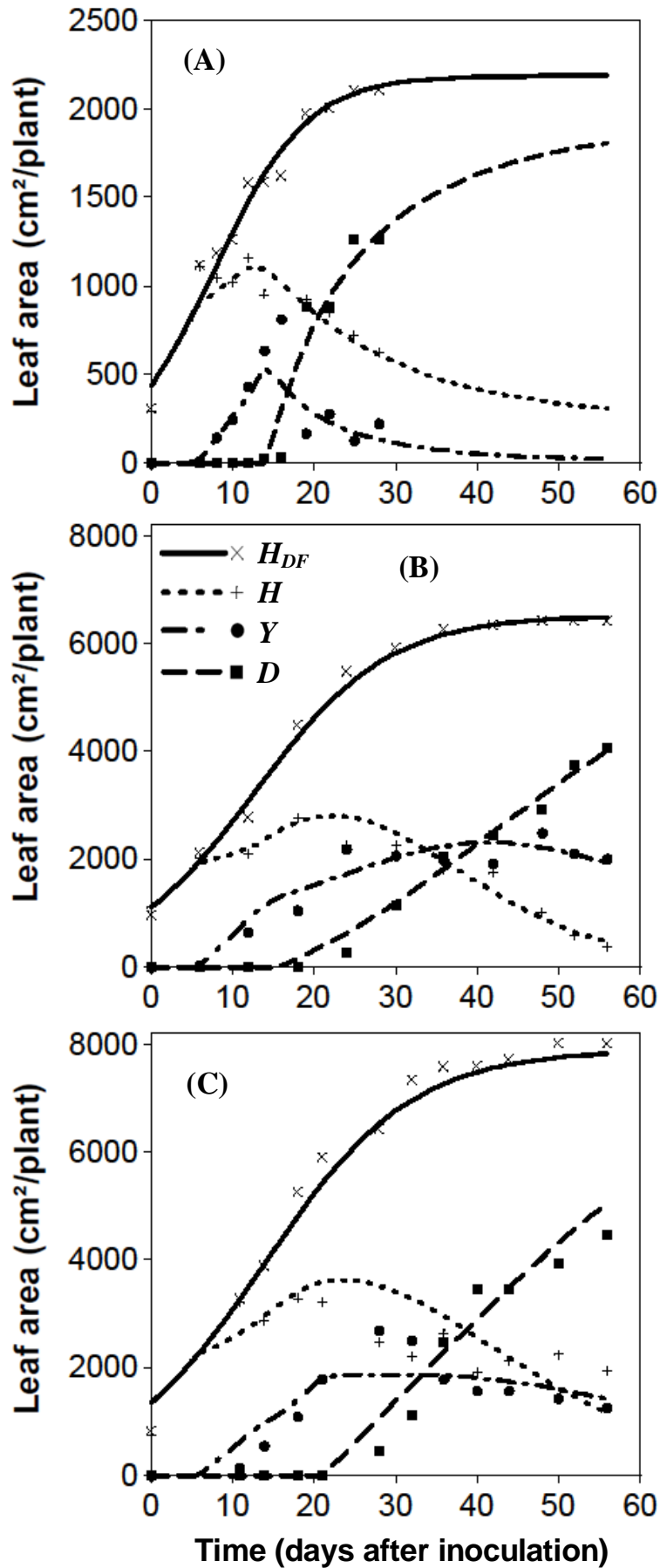
Fig. 2. Progress curves of the healthy leaf area in the disease-free situation (H_{DF}), and of the healthy leaf area (H), diseased leaf area (Y) and defoliated leaf area (D) of tomato as influenced by powdery mildew (*Oidium neolycopersici*) epidemics during experiment A, B, and C, observed (dots) and simulated (lines) with the basic model (equations 3, 3', 4 and 5) under the assumption of constant rates.

Disease progress. Progress curves of powdery mildew severity are illustrated in Fig. 3.
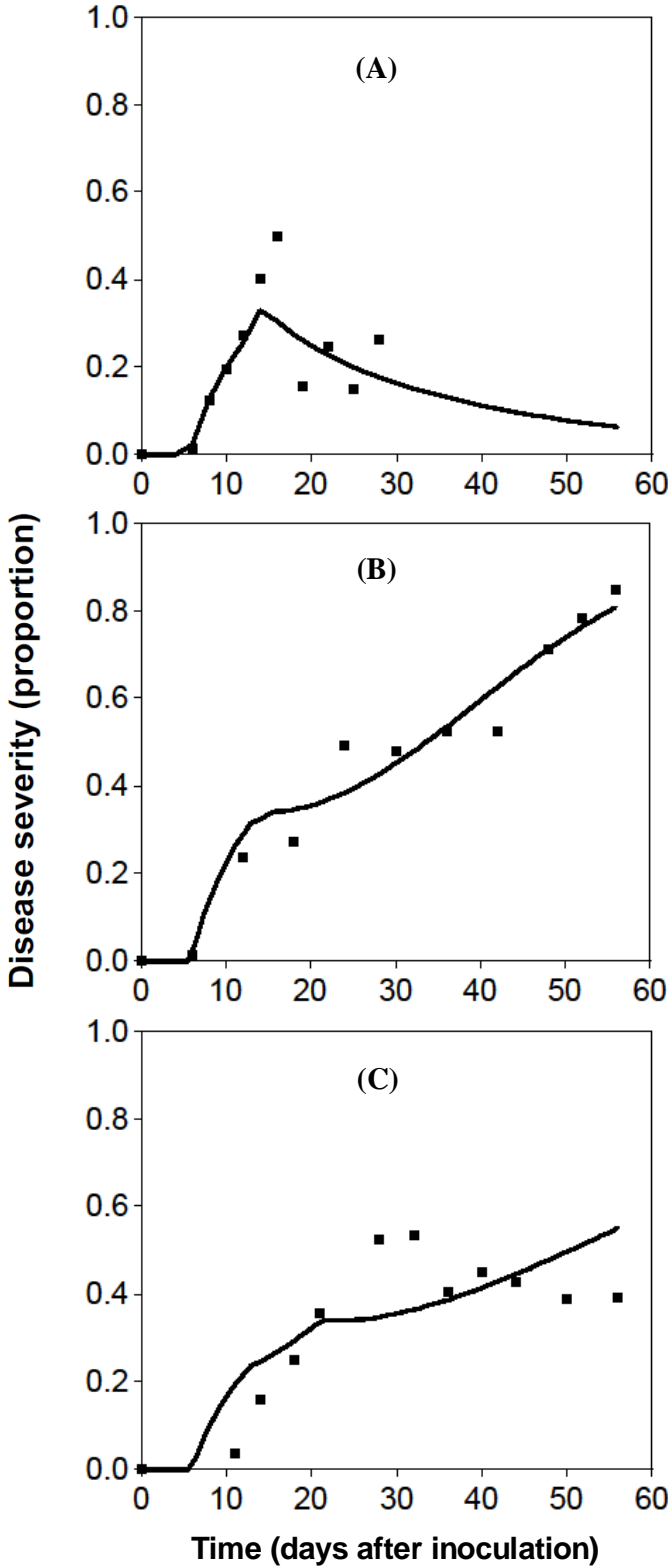
Fig. 3. Progress curves of powdery mildew (*Oidium neolycopersici*) severity on tomato during experiment A, B and C, observed (dots) and simulated (lines) with the basic model (equations 3, 3', 4 and 5) under the assumption of constant rates.

The temporal disease progress was conspicuously similar in all the three experiments during the initial phases of the epidemics before the defoliation threshold 0.34 was reached. Henceforth, the progress curves were distinctly different across the three experiments. In experiment A, the disease progress curve declined continuously after t_{DT}. In experiment B and C (Fig. 3B and C), a progressive increment in the proportion of mildewed leaf area occurred, particularly discernibly in experiment B (Fig. 3B). The simulated disease progress in experiment C also depicts an increasing trend which is contrary to the observed experimental data after 30 DAI (Fig. 3C).

For the initial linear disease rate r_{LIN}, high values of 59.5, 144.3 and 124.1 cm² per day were estimated for experiment A, B and C (Table 2), respectively, due to the strong inoculum pressure within the early cycle of the powdery mildew epidemic ($IP \leq t < LP + IP$). As the size of the plants at the inoculation time was much smaller in experiment A, it is not a surprise that also the rate r_{LIN} was lower compared to the two other experiments. The estimated values of r_Y were nearly identical, 0.130 and 0.128 per day in experiment B and C in comparison to 0.302 per day in experiment A. The initial disease values Y_0 were only in the experiment B significantly different from 0, while in experiment A and C, the initial value could also be chosen as 0.

Modification 1

When in the basic model the equation for the host growth (equation 3) is replaced by equation 6 (assuming that host growth is only proportional to H and not to $H + Y$), the estimated parameter values are not changing dramatically (Table 3). In all experiments, the estimated values for H_0 are lower, those of r_H higher than before. The goodness of fit, expressed in R^2 or the F-value, is slightly lower in the experiments A and B, but higher in experiment C. Due to the small differences in the goodness of fit, the dynamics of the different leaf areas as well as

the disease progress curves are hardly discernible from those in Fig. 2 and 3 and are therefore not shown.

TABLE 3. Estimated parameter values and coefficients of determination (R^2) of the **modified model 1** (equations 4, 5, and 6) simulating epidemics of powdery mildew (*Oidium neolycopersici*) on tomato and the dynamics of host growth under the assumption of constant rates. The hypothesis of the modification is that area covered with powdery mildew does not produce new healthy tissue (eq. 6) (see Table 1 for explanation of acronyms).

Experiment	Estimated parameter values							F	R^2
	H_0	r_H	H_{max}	Y_0	r_{LIN}	r_Y	r_D		
A	430.2 (59.6)*	0.194 (0.023)	2142.0 (80.2)	8.01 (19.57)	56.54 (4.86)	0.300 (0.032)	0.337 (0.050)	318.8	0.976
B	953.7 (87.2)	0.143 (0.009)	6525.7 (97.5)	1.01 (70.45)	114.4 (14.45)	0.134 (0.006)	0.054 (0.003)	893.9	0.991
C	1205.9 (169.3)	0.123 (0.011)	7969.7 (201.3)	1.06 (125.7)	103.1 (36.53)	0.133 (0.010)	0.088 (0.008)	451.4	0.981

*Standard errors of the parameter estimates are given in parentheses

The basic model and the above modification are two special cases in which in equation 7 or 8 f_{red} is chosen as 0 or 1. As expected, allowing a variable factor f_{red} for the reducing effect of disease severity on r_H (equation 7 or 8) improved the goodness of fit further (Table 4). The value of f_{red} estimated for experiment A was 0.331, a value not significantly different from 0, while for experiment B a value of 0.506 was determined which was significantly different from 0. The application of these values led to a slightly better fit to the experimental data of experiments A and B when compared with the basic model, but due to the additional parameter the F-values were lower than those of the basic model. For experiment C, however, the value estimated for f_{red} was 1.166 which is significantly different from 0, but not from 1. The F-value was 387.3 which is lower than 451.4, the value achieved with fixed value $f_{red} = 1$.

The curves describing the dynamics of the different leaf areas and the disease progress curves are very similar to those given in Fig. 2 and 3 and are therefore not displayed.

TABLE 4. Estimated parameter values and coefficients of determination (R^2) of the **modified model 1** (equations 4, 5, and 7 or 8) simulating epidemics of powdery mildew (*Oidium neolycopersici*) on tomato and the dynamics of host growth under the assumption of constant rates. The hypothesis of the modification is that powdery mildew severity negatively affects the host's growth rate (eq. 8) (see Table 1 for explanation of acronyms).

Experiment	Estimated parameter values								F	R^2
	H_0	r_H	f_{red}	H_{max}	Y_0	r_{LIN}	r_Y	r_D		
A	433.1 (61.3)*	0.189 (0.024)	0.331 (0.671)	2136.0 (80.5)	8.23 (17.01)	59.11 (8.07)	0.300 (0.035)	0.337 (0.050)	278.4	0.976
B	1047.5 (80.4)	0.130 (0.008)	0.506 (0.172)	6536.2 (93.3)	22.79 (73.83)	129.0 (16.72)	0.133 (0.008)	0.051 (0.002)	919.6	0.993
C	1179.0 (178.9)	0.127 (0.013)	1.166 (0.263)	7962.4 (196.9)	0.09 (43.82)	104.4 (22.05)	0.131 (0.011)	0.088 (0.008)	387.3	0.981

*Standard errors of the parameter estimates are given in parentheses

Modification 2

In modification 2 it was assumed that defoliation is affecting the diseased (equation 9) as well as the healthy area (equation 10). The parameter r_{DH} (the defoliation rate of healthy area) was estimated as 0.202 ($\pm$0.135), 0.008 ($\pm$0.029) and 0.0000004 ($\pm$0.046) (Table 5) in experiment A, B and C, respectively, but these estimates were not significantly different from 0 at 5% probability. Furthermore, the *F*-values calculated for this modification (293.3, 810.7 and 278.7 for experiments A, B and C) were comparatively lower than those of the basic model (Table 2) in all the three experiments. Consequently, it was concluded that the modification 2 does not give a significantly better fit to the experimental data. Thus it was supposed that defoliation of healthy area D_H does not contribute significantly to total defoliated area D and that only diseased area is defoliated. Due to the fact that the values of r_{DH} are close to 0, the

estimated values of the other parameters and coefficients of determination were largely identical to those of the basic model (Table 2). Consequently, there were practically no visible differences when progress curves of host growth and disease severity simulated using modification 2 (figures not shown) are compared to those of the basic model (Fig. 2 and 3).

TABLE 5. Estimated parameter values and coefficients of determination (R^2) of the **modification 2** (equations 9, 10, 11 and 12) simulating epidemics of powdery mildew (*Oidium neolycopersici*) on tomato and the dynamics of host growth under the assumption of constant rates. The hypothesis of the modification is that defoliation is affecting the diseased (eq. 9) as well as the healthy (eq. 10) area (see Table 1 for explanation of acronyms).

Experiment	Estimated parameter values								F	R^2
	H_0	r_H	H_{max}	Y_0	r_{LIN}	r_Y	r_{DY}	r_{DH}		
A	432.5 (59.2)*	0.191 (0.023)	2102.3 (75.4)	25.54 (18.6)	63.0 (8.4)	0.148 (0.090)	0.293 (0.083)	0.202 (0.135)	293.3	0.978
B	1103.0 (88.8)	0.123 (0.007)	6515.0 (98.0)	16.19 (68.2)	143.6 (10.3)	0.123 (0.027)	0.046 (0.012)	0.008 (0.029)	810.7	0.992
C	1350.9 (220.2)	0.111 (0.013)	7899.5 (250.6)	1.18 (3.83)	123.5 (35.8)	0.128 (0.043)	0.083 (0.024)	0.000004 (0.046)	278.7	0.974

*Standard errors of the parameter estimates are given in parentheses

Modification 3

While the basic model and the two modifications presented so far had constant rates, the disease rates in modification 3 could vary depending on environmental conditions (equation 13). Contrary to expected and except for slight deviations, there were hardly any significant differences between progress curves of host leaf area simulated with a constant or variable disease rate as illustrated for experiment B (Fig. 2B vs. Fig. 4a). Under changing environmental conditions and thereby a variable disease rate r_{LIN} (cm² day^{-1}), and r_Y (day^{-1}), the disease progress curve increased monotonously, but the curve was not smooth (Fig. 4b) when compared to the curve depicting a constant disease rate (Fig. 3B).

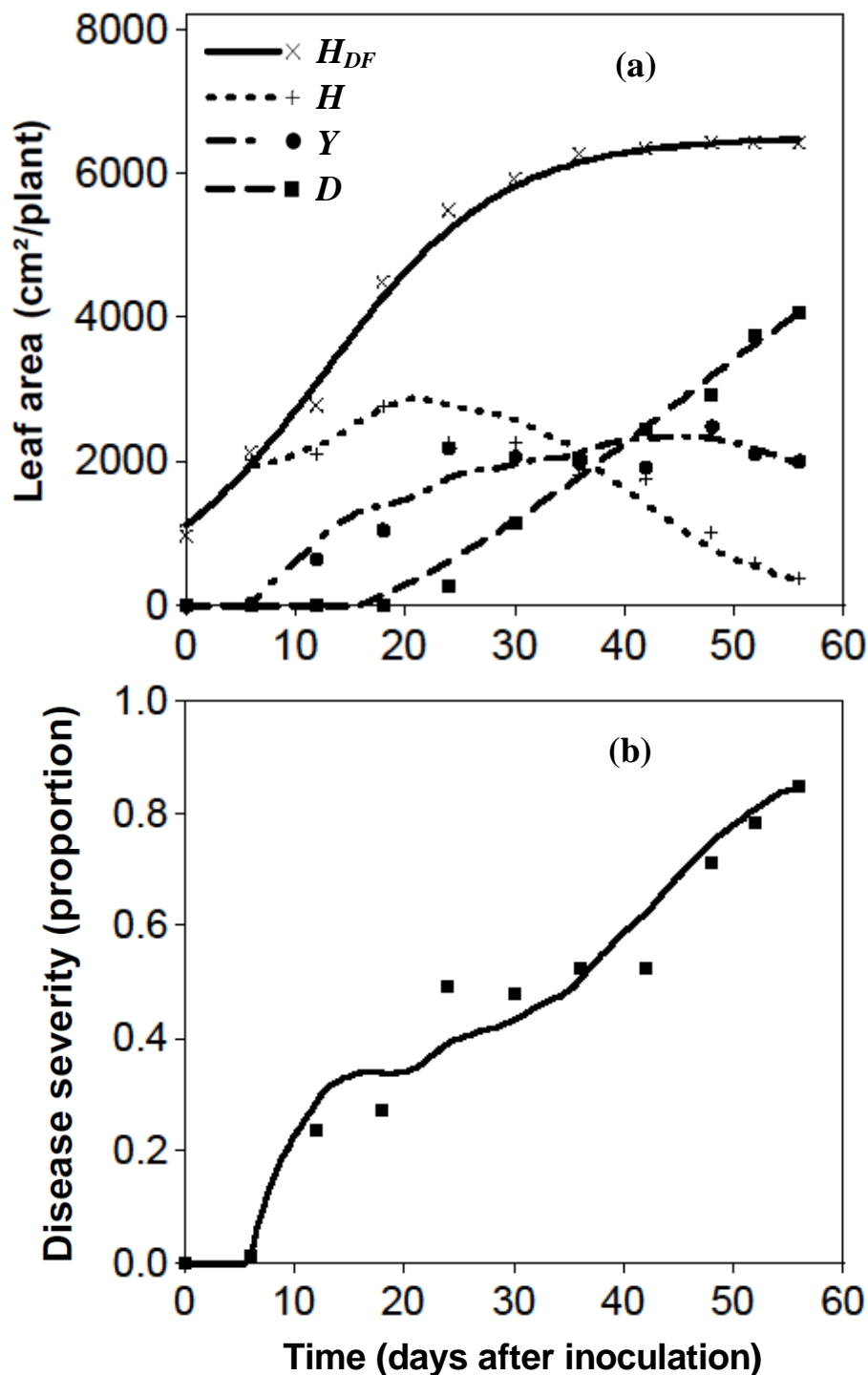**Fig. 4.** Progress curves of a) the healthy leaf area in the disease-free (H_{DF}) and in the diseased situation (H), diseased leaf area (Y) and defoliated leaf area (D) and b) powdery mildew (*Oidium neolycopersici*) severity during experiment B, observed (dots) and simulated (lines) under the assumption of variable disease rates r_{LIN} and r_Y influenced by changing temperature and relative humidity.

The values of the maximum possible rate r_{LINmax} during the early phase of the powdery epidemic ($IP \leq t < LP + IP$) varied between 74.0 (experiment A) and 208.7 cm² day^{-1} (experiment B) (Table 6). Estimates of the maximum possible rate r_{Ymax} during the later phase ($t \geq LP + IP$) were closely identical in experiment B and C (0.181 and 0.163 day^{-1}), but clearly higher in experiment A (0.336 day^{-1}).

TABLE 6. Estimated parameter values and coefficients of determination (R^2) of the **modified model 3** simulating epidemics of powdery mildew (*Oidium neolycopersici*) on tomato and the dynamics of host growth under the assumption of constant rates, except of the disease rates r_{LIN} and r_Y which in this refinement were considered to be influenced by changing temperature and humidity conditions (see Table 1 for explanation of acronyms).

Experiment	Estimated parameter values							F	R^2
	H_0	r_H	H_{max}	Y_0	r_{LINmax}	r_{Ymax}	r_D		
A	441.8 (58.9)*	0.184 (0.022)	2147.6 (80.1)	0.038 (0.368)	74.0 (8.8)	0.336 (0.039)	0.312 (0.045)	332.0	0.976
B	1097.7 (90.0)	0.124 (0.008)	6485.6 (93.6)	1.793 (75.770)	208.7 (24.8)	0.181 (0.006)	0.051 (0.002)	987.7	0.992
C	1318.2 (202.1)	0.115 (0.013)	7859.0 (223.3)	0.023 (1.568)	206.3 (28.2)	0.163 (0.009)	0.080 (0.007)	358.7	0.976

*Standard errors of the parameter estimates are given in parentheses

In terms of the R^2 values, the modified model showed a slightly better fit to experimental data in comparison to the basic model. Furthermore, the F-values of the three experiments (Table 5) calculated for this modification were comparatively higher than those of the basic model (Table 2). Therefore, it was concluded that the modification 3 gives a significantly better fit to the experimental data when compared to the basic model.

DISCUSSION

In this study a simple but comprehensive model was developed that incorporates the dynamics of tomato growth and powdery mildew epidemics interacting together. In the model, leaf area is adopted as a measure of host growth for primarily two reasons: Firstly, *Oidium neolycopersici* is an obligate foliar biotroph implying that the development and sporulation of colonies depends upon the successful initial penetration of the host, continued haustorial formation and active transport of nutrients from the host cytoplasm across the haustorial plasma membranes (Jones et al., 2001). The progress of the powdery mildew fungus thus revolves around the availability and susceptibility of the leaves. Secondly, lowering of the photosynthetic area of host plants through leaf tissue destruction and defoliation consequently leads to a reduced photosynthetic output that often translates to smaller growth and yield of these plants (Agrios, 2005).

The basic model is a system of differential equations describing the change of healthy H, diseased Y and defoliated leaf area D, relative to a healthy crop. Such partitioning of the dynamics of host growth represents more realistically the observed epidemic data than epidemiological studies that focus only on pathogen development on the host (Van Maanen and Xu, 2003; Calonnec et al., 2008). In our model, like in those of Jeger (1986) and Waggoner (1986), the diseased area Y is not subdivided into the three categories latent, infectious and post-infectious area like in the models of Madden et al. (2007). While defoliation is often ignored in models, it is explicitly incorporated in the present model, and its effects on the dynamics of disease epidemics and host growth are examined and quantified.

The model was built upon a set of assumptions for host area and disease dynamics. Like in other models (Jeger, 1986; Waggoner, 1986; Madden et al., 2007) it is assumed that in the absence of the disease, the healthy host area increases logistically to an asymptotic value of H_{max}. In our basic model as well as in the model of Waggoner (1986), the production of new

healthy area in the disease situation is driven by the actual area $H + Y$, in other models (Jeger, 1986; Madden et al., 2007) only by the healthy area. Our modification 1 allows also cases in-between by assigning different growth rates for the healthy and diseased leaf category. In the models of Jeger (1986) and Waggoner (1986), the production of new tissue is density regulated by the actual host area $H + Y$, in the models of Madden et al. (2007) by the healthy area H only. In our model, host growth is density regulated by the total host area formed $H + Y + D$ which is limited by H_{max}. Thus our main assumption in the disease situation is that the dynamics of total host area formed is the same like that without the disease so that in essence, the powdery mildew epidemic does not affect the total biomass production. This is in accordance to experimental results of Chelal and Hau (2012). This characteristic also guarantees that the total amount of leaf area formed cannot increase without bound, a behavior that the other models (Jeger, 1986; Waggoner, 1986; Madden et al., 2007) show.

For the dynamics of the diseased area, two epidemic phases were differentiated. During the initial disease cycle, it is assumed that the progress of diseased area increases linearly reflecting the strong effect of the artificial inoculation but later the epidemic progresses with an ordinary logistic pattern. A uniform logistic rate for the total epidemic turned out to be inadequate.

The model describes the transition from the healthy to the diseased and finally to the defoliated area. Therefore one expects on a long run, when the production of healthy area is halted and the diseased area is defoliated, that the healthy and the diseased areas will go down to 0 and the defoliated area will include all leaf area formed. In fact the model predicts this behavior for experiments B and C, but not for experiment A. In this experiment with the highest defoliation rate, the diseased area is quickly thinned out so that a certain amount of healthy area remains and will not become diseased. For instance, after an extended simulation time of 180 days, 10% of the total leaf area formed in experiment A remains healthy.

The observed temporal disease pattern expressed as the proportion of diseased leaf area varied among the three experiments. In experiment A, the disease progress curve declined in the later stages of the epidemic, which is also reflected in the simulated curve. Ordinarily, it is not possible for a disease progress curve to decline when the amount of host tissue remains constant. However, according to Hau (1990), a disease progress curve can diminish due to instances of a changing host either by (i) an increase of susceptible tissue through refoliation or growth flushes of the host, referred to as a dilution effect, or (ii) by the loss of the diseased tissue through defoliation, termed as a thinning-out effect. The latter case seems to be important in experiment A because the defoliation rate is quite high (0.335 per day) so that the simulated disease progress curve will approach 0. In experiment B, both the observed and the simulated disease progress curves increase and the simulated curve finally reaches a level close to 1. In experiment C, however, the observed disease progress curve increases initially up to day 32, but decreases thereafter. This behavior is not well reflected in the simulated curve which increases in the observation interval and will finally level off close to 1.

Interestingly, the model results in small differences in the total leaf area formed between the diseased and non-diseased situation. In the latter, the leaf area approaches H_{max} while under disease pressure the total production given by $H + Y + D$ is leveling off at a slightly lower value i.e. reaching only a proportion of 0.9683 (experiment C) to 0.9812 (experiment B) of H_{max} on day 60. Even when the simulation time is extended to 180 days, the proportion remains between 0.9817 (experiment C) to 0.9977 (experiment A).

As stated already, the smaller potting containers used in experiment A compared to B and C implied that there was a limitation in the amount of rooting space and in the substrate available for adequate root growth thus retarding development and decreasing plant vigor (NeSmith and Duval, 1998). Consequently, this could have predisposed the plants to infection by powdery mildew and which may in turn explain why we had a higher disease and defoliation rate in experiment A than B and C.

Disease-induced defoliation is one of the important features of the tomato-powdery mildew pathosystem that the modeling work in this paper sought to incorporate. According to Allorent and Savary (2005), the consequences of defoliation include: (i) a reduction of inoculum present within the canopy through loss of diseased leaves, (ii) changes in the crop microclimate rendering it less favorable for disease progress, (iii) a reduction of crop growth hence limiting the amount of host tissue available for infection, and (iv) limited maximum disease severity.

The correlation between defoliation and disease severity (proportion of diseased leaf area) is an important feature of many pathosystems. Willocquet et al. (2004) reported a strong correlation between defoliation and disease severity of angular leaf spot (caused *Phaeoisariopsis griseola*) of common bean, with relatively low severity already causing a substantial defoliation. Accordingly, a disease threshold was defined in the present model such that defoliation is triggered once this threshold is reached. Furthermore, the underlying hypothesis was adopted that the only factor acting on the rate of defoliation of diseased area is the disease severity of leaves (Allorent and Savary, 2005).

Results of the modification 1 differ among the three experiments. In experiments A and B, the factor f_{red} can be assumed to be 0, so that the production of new healthy leaf area is proportional to $H + Y$. In experiment C, however, the goodness-or-fit is better when f_{red} is taken as 1 meaning that only healthy area H is contributing to newly formed tissue. In the latter case one can conclude, based on equation 8, that powdery mildew epidemics lowered the rate of host growth of diseased plants relative to healthy plants which is in accordance to earlier work by Chelal and Hau (2012).

Since defoliation could lead to loss of diseased leaves including diseased and healthy sites within the same leaf (Allorent and Savary, 2005), this aspect was examined in the modification 2 by partitioning total defoliation (D) into defoliated-diseased area D_Y and defoliated-healthy area D_H. However, estimates of the additional rate parameter r_{DH} were not

significantly different from 0, thus leading to the conclusion that powdery mildew mainly results in defoliation of only diseased areas.

In the modification 3, a variable disease rate due to changing environmental conditions was introduced. However, there were no major differences in simulations of either host area or disease severity under the assumption of a constant or a variable disease rate due to changing temperature and relative humidity conditions. Arguably, *Oidium neolycopersici* has wide ranges of temperature and relative humidity over which its spores can germinate. Douglas (2003) reported disease development within temperatures in the range of 10 to 35°C and RH levels >50%, whereas Jacob et al. (2008) observed conidial germination at RH ≥33%. Therefore, considering that the temperature and RH conditions recorded during the experimental period were within the range of 19 to 25°C and 35 to 67%, respectively, it suffices to conclude that these conditions were always within the optimum range for pathogen germination and disease development.

Consequently, this approach provides a platform for the analysis of the dynamic interactions between pathogen, host and environment which collectively contribute to variability in epidemic behavior and the capacity of host development to modify disease progress (Calonnec et al., 2008).

By reviewing past efforts and incorporating new findings, the model developed in this study helps to bridge knowledge gaps that exist and as well act as a basis for developing and implementing sustainable, economic and environmentally acceptable control strategies. However, several opportunities exist for further refinement of this model. The possibility of integrating environmental data with details of the different phases of the disease cycle could be explored by incorporating the three important disease categories, i.e. latent, infectious and post-infectious. It would also be of considerable interest to incorporate the effects of fungicide application on mildew development thus offering a more practical application of this model.

LITERATURE CITED

Agrios, G. N. 2005. Plant Pathology, 5th ed. Elsevier Academic Press, San Diego, CA.

Allorent, D., and Savary, S. 2005. Epidemiological characteristics of angular leaf spot of bean: a systems analysis. Eur. J. Plant Pathol. 113:329-341.

Berger, R. D., Hau, B., Weber, G. E., Bacchi, L. M. A., Bergamin Filho, A., and Amorim, L. 1995. A simulation model to describe epidemics of rust of Phaseolus beans I. Development of the model and sensitivity analysis. Phytopathology 85:715-721.

Blanco, F. F., and Folegatti, M. V. 2005. Estimation of leaf area for greenhouse cucumber by linear measurements under salinity and grafting. Sci. Agric. 62:305-309.

Calonnec, A., Cartolaro, P., Naulin, J. M., Bailey, D., and Langlais, M. 2008. A host–pathogen simulation model: powdery mildew of grapevine. Plant Pathol. 57:493-508.

Chelal, J., and Hau, B. 2012. Temporal dynamics of powdery mildew and its relationship to host growth, defoliation and yield of tomato. Proceedings of the 58th German Plant Protection Conference. 10 to 14th September 2012. Braunschweig, Germany, pp. 105. Available at: http://pub.jki.bund.de/index.php/JKA/article/view/1923/2299. (Accessed: 06 June 2013).

Douglas, S. M. 2003. Powdery mildew of tomato. The Connecticut Agricultural Experimental Station. Available at: http://www.ct.gov/caes/cwp/view.asp?a=3756&q=44-2806&CaesNavPage. (Accessed: 16 May 2013).

Ferrandino, F. J. 2008. Effect of crop growth and canopy filtration on the dynamics of plant disease epidemics spread by aerially dispersed spores. Phytopathology 98:492-503.

Hau, B. 1990. Analytic models of plant disease in a changing environment. Ann. Rev. Phytopathol. 28: 221-245.

Jacob, D., David, R. D., Sztjenberg, A., and Elad, Y. 2008. Conditions for development of powdery mildew of tomato caused by *Oidium neolycopersici*. Phytopathology 98:270-281.

Jeger, M. J. 1986. The potential of analytic compared with simulation approaches to modeling in plant disease epidemiology. Pages 255-281 in: Plant Disease Epidemiology. Population Dynamics and Management. K. J. Leonard and W. E. Fry, eds. MacMillan, New York.

Jones, H., Whipps, J. M., and Gurr, S. J. 2001. The tomato powdery mildew fungus *Oidium neolycopersici*. Mol. Plant Pathol. 2:303-309.

Kranz, J. 2003. Comparative Epidemiology of Plant Diseases. Springer-Verlag, Berlin-Heidelberg, Germany.

Kranz, J., and Jörg, E. 1989. The synecological approach in plant disease epidemiology. Rev. Trop. Plant Pathol. 6:27-38.

Lucas, J. A. 1998. Plant Pathology and Plant Pathogens. Blackwell Science, Bristol.

Madden, L. V., Hughes, G., and van den Bosch, F. 2007. The Study of Plant Disease Epidemics. APS, St. Paul.

Mersha, Z., and Hau, B. 2011. Reciprocal effects of host and disease dynamics in the bean rust pathosystems. J. Plant Dis. Protec. 118:54-62.

Mieslerová, B., Lebeda, A., and Kennedy, R. 2004. Variation in *Oidium neolycopersici* development on host and non-host plant species and their tissue defense responses. Ann. Appl. Biol. 144:237-248.

NeSmith, D. S., and Duval, J. R. 1998. The effect of container size. HortTechnology 8:495-498.

Newton, A. C., Gibson, G., and Cox, D. 1995. Understanding plant disease epidemics through mathematical modelling. Scottish Crop Research Institute Annual Report for 1994:124-127.

Prokopová, J., Mieslerová, B., Hlaváčková, V., Hlavinka, J., Lebeda, A., Nauš, J., and Špundová, M. 2010. Changes in photosynthesis of *Lycopersicon spp.* plants induced by tomato powdery mildew infection in combination with heat shock pre-treatment. Physiol. Mol. Plant Pathol. 74:205-213.

Schwarz, D., and Klaring, H. P. 2001. Allometry to estimate leaf area tomato. J. Plant Nutr. 24:1291-1309.

Van Maanen, A., and Xu, M. 2003. Modelling plant disease epidemics. Eur. J. Plant Pathol. 109:669-682.

Waggoner, P. E. 1986. Progress curves of foliar diseases: Their interpretation and use. Pages 3-37 in: Plant Disease Epidemiology. Population Dynamics and Management. K. J. Leonard and W. E. Fry, eds. MacMillan, New York.

Whipps, J. M., and Budge, S. P. 2000. Effect of humidity on development of tomato powdery mildew (*Oidium lycopersici*) in the glasshouse. Eur. J. Plant Pathol. 106:395-397.

Whipps, J. M., Budge, S. P., and Fenlon, J. S. 1998. Characteristics and host range of tomato powdery mildew. Plant Pathol. 47:36-48.

Willocquet, L., Allorent, D., and Savary, S. 2004. Quantitative analysis of two important epidemiological features in the common bean – *Phaeoisariopsis griseola* pathosystem. Fitopatol. Bras. 29:676-679.

Chapter 3

Modeling the interaction between early blight epidemics and host dynamics of tomato

John Chelal, Ali Al Masri and Bernhard Hau*

Leibniz Universität Hannover

Institut für Gartenbauliche Produktionssysteme, Abteilung Phytomedizin

Herrenhäuser Str. 2, D-30419 Hannover, Germany

*Corresponding author: hau@ipp.uni-hannover.de

ABSTRACT

A model simulating an early blight (*Alternaria solani*) epidemic and the growth dynamics of tomato interacting together is developed. The model is formulated as a set of differential equations for the rate of change in the amount of healthy H, diseased Y and defoliated D area in the disease situation, and healthy H_{DF} and defoliated D_{DF} in the disease-free situation. Model parameters were estimated through fitting the model to experimental data obtained from glasshouse experiments which comprised of tomato plants inoculated with *A. solani* at three inoculation times early (t_{INOC} = 23 days after transplanting (DAT)), intermediate (33 DAT) and late (43 DAT) inoculation time in experiment A and t_{INOC} = 22, 30 and 38 DAT in experiment B. Simulations of the early blight severity and growth of tomato showed a good fit to observed data with $R^2 > 0.995$. The rate parameter for host growth r_H (day^{-1}) was moderately identical in experiment A (0.168, 0.151 and 0.153) whereas in B, r_H increased with increasing inoculation time. Diseased leaf area Y increased linearly during the primary phase of the epidemic reaching between 23 to 58% of the actual leaf area. Defoliation rates r_D (day^{-1}) were 2.5 times higher for late inoculated (older) plants compared to the early inoculated (younger) plants. Except in one case characterized by increasing disease progression, disease progress curves in all other cases decreased progressively finally approached zero in long run. High values of between 141.2 to 367.5 cm² per day were estimated for the initial linear disease rate r_{LIN}. Values of the logistic rate parameter for disease increase r_Y (day^{-1}) were about three-folds higher in the late inoculations (0.380, 0.305 day^{-1}) when compared to the early inoculations (0.151, 0.095 day^{-1}). Based on the good fit of model simulations to observed data and the biological plausibility of parameter estimates, the model can be considered as offering a good description of the dynamic interaction between the early blight epidemic and growth of tomato.

Additional key words: *Alternaria solani, Solanum lycopersicum*, polycyclic, defoliation, senescence

INTRODUCTION

Early blight, caused by *Alternaria solani* (Ellias and Martin) Sorauer is one of the most common and destructive diseases of tomato (*Solanum lycopersicum* L.) in many production areas worldwide, especially in regions with heavy rainfall, high humidity and fairly high temperatures (24° – 29°C) (Sherf and MacNab, 1986; Nash and Gardner, 1988; Pandey et al., 2003; Chaerani and Voorrips, 2006; Chaerani et al., 2007). Epidemics can also occur in semi-arid areas which experience frequent and prolonged night dews (Rotem and Reichert, 1964).

Leaf blight which is commonly referred to as early blight (EB) is the most damaging symptom of this disease (Chaerani et al., 2007; Majid et al., 2008). Other symptoms include collar rot on seedlings, stem lesions and apical fruit rot (Pandey et al., 2003; Chaerani and Voorrips, 2006; Chaerani et al., 2007). The disease begins as small, dark, necrotic lesions on the lower older leaves and then progresses upward to the newly formed leaves as the plant reaches maturity. Enlarging lesions typically have concentric rings that are surrounded by a chlorotic area thus giving a target-like appearance (Sherf and MacNab, 1986; Agrios, 2005).

Due to the necrotrophic nature of the fungus, affected leaves often senesce prematurely and severe epidemics lead to complete defoliation and loss of the tomato plants (Lawrence et al., 2000; Pandey et al., 2003; Chaerani et al., 2007). Moreover, besides reducing the photosynthetic rate and increasing the respiration rate of healthy tissue (Majid et al., 2008), disease-induced defoliation may expose the fruits to sun - scald injury and thus significantly lower the fruit quality (Sherf and MacNab, 1986; Chaerani and Voorrips, 2006; Chaerani et al., 2007). Yield losses in the range of 23 to 78% due to early blight damage have been reported from Australia, Canada, USA, Israel, India, Indonesia, and Nigeria (Basu, 1974b; Datar and Mayee, 1981; Sherf and MacNab, 1986; Vloutoglou and Kalogerakis, 2000; Chaerani and Voorrips, 2006; Chaerani et al., 2007). Datar and Mayee (1981) reported that an early blight severity of 72% could cause a loss in fruit yield of up to 78.5% with each 1% increase in severity reducing yield by 1.36%.

Frequent applications of fungicides from early in the growing season are usually required to achieve adequate control of this disease and avert potential crop damage and subsequent yield loss (Sherf and MacNab, 1986; Vloutoglou and Kalogerakis, 2000; Chaerani and Voorrips, 2006). However, increasing economic and environmental concerns coupled with the rapid development of the disease call for adequate knowledge of the interaction between host, pathogen and weather variables as well as timely application of control measures such as through the use of decision support systems (Sherf and MacNab, 1986; Cook and Yarham, 1998; Pandey et al., 2003; Van Maanen and Xu, 2003; De Wolf and Isard, 2007; Chaerani et al., 2007).

A significant progress has been made in the use of early blight forecasting systems and simulators, for instance, EPIDEM (Waggoner and Horsfall, 1969), FAST (Madden et al., 1975), TOMCAST (Jasinski, 1999), and FODIS-TMEB (Koo, 2002). Majority of these forecast models utilize the daily environmental data (such as maximum and minimum air temperature, hours of leaf wetness, and daily rainfall) to identify periods favourable for early blight development and to advise growers on the appropriate timing of fungicide application (Gleason et al., 1995).

However, in order to gain a better understanding of the disease effects on host growth and yield as well as of the reciprocal effects of host factors on disease progress, the dynamics of host growth and its associated features ought to be incorporated into epidemiological models (Johnson and Teng, 1990; Van Maanen and Xu, 2003). For example, in the case of tomato-early blight pathosystem, effects of the physiological age of the host plant and plant tolerance on epidemic development have been extensively reported (Vloutoglou and Kalogerakis, 2000; Koo, 2002). Other host factors such as natural senescence and disease-induced defoliation of leaves are usually observed in disease assessments yet they are often ignored in modeling or are left unquantified. Further still, due to the relatively simple empirical nature of disease forecast models, difficulties may still occur in utilizing disease forecasts to model disease

progress unless the explicit relationship between disease forecasts and disease occurrences is quantitatively determined (Koo, 2002).

Thus, to enable a better description and understanding of early blight epidemics and its interaction with the growth dynamics of tomato, an improved model coupling host dynamics with temporal disease progress was developed in this study.

MATERIALS AND METHODS

Disease dynamics and host growth data were obtained from two glasshouse experiments conducted at the Institut für Gartenbauliche Produktionssysteme, (Abteilung Phytomedizin) of Leibniz Universität Hannover.

Experimental plants. Seedlings of tomato *cv*. Moneymaker were raised in a nursery for 25 to 30 days after which they were transplanted into 3-litre capacity perforated plastic pots filled with the substrate Frühstorfer Erde (Industrie-Erden Werk, Germany). Neudorff's organic fertilizer Azet $^{®}$ (7-3-10 N, P_2O_5, and K_2O, respectively) was incorporated into the substrate at transplanting at the rate of 10 g.plant^{-1} for experiment A but 25 g.plant^{-1} for experiment B. The plants were then maintained in glasshouse compartments set at 23 ± 3ºC and 21 ± 2 ºC day and night temperatures, respectively. Natural light was supplemented with artificial light (Philips lamps SRG 102/400; 195µmol.sec^{-1}.m^{-2}) to provide a photoperiod of 12 hrs.

Fungal culture. An isolate of *Alternaria solani* was obtained from the Weihenstephan Science Center (Technical University of Munich). To enhance in vitro conidial production, the isolate was propagated on potato dextrose agar (PDA) as a primary medium for ten days. The aerial part of *A. solani* colonies in the primary cultures were then surgically removed using a blade. Agar blocks from the primary cultures were then transferred to the surface of 20 ml S-medium (10 g $CaCO_3$, 10 g Agar, 10 g Saccharose and 500 ml H_2O) in Petri dishes and incubated at 22 °C under alternating 12-hour UV-light and dark conditions. Spores were formed after 24 to 72 hours.

Experimental design. Treatments were arranged in a completely randomized design comprising two levels of inoculation i.e. inoculated (I) and non-inoculated plants (NI) and three inoculation times; early (t_{INOC} = 23 days after transplanting (DAT)), intermediate (33 DAT) and late (43 DAT) inoculation time in experiment A and t_{INOC} = 22, 30 and 38 DAT in experiment B. Following the single-plant approach of Kranz and Jörg (1989), five replicate plants were used at each inoculation time.

Inoculum preparation and inoculation. Conidia of the pathogen were first collected by flooding the conidial plates with distilled water (containing 0.01% of surfactant Tween 20) and gently scraping the media surface with a sterilized spatula. The conidial suspension was then adjusted to 5×10^4 conidia.ml^{-1} (in experiment A) and 4×10^4 conidia.ml^{-1} (in experiment B) using a Fuchs-Rosenthal haemocytometer (Marienfeld GmbH & Co. KG, Germany).

At each of the three inoculation times, plants were artificially inoculated with the conidial suspension until run-off using a hand-held spray bottle. In contrast, non-inoculated plants were sprayed with deionized water. Plants of both treatment groups (I and NI) were then placed under separate polyethylene compartments (0.65 x 0.65 x 1 m) to ensure high relative humidity (>95%) for three consecutive days after which they were separately moved to larger polyethylene compartments (1.1 x 2 x 1.6 m) maintained at 25 ± 3 °C and 85 ± 5% temperature and relative humidity (*RH*), respectively. Sprays of mist (deionized water mixed with Tween 20) were applied frequently to create long wetness duration and thereby promote disease development. Once the initial disease cycle was established, a stand fan was used for 10 minutes, five consecutive days a week to disperse the conidia randomly to the healthy and newly produced leaves.

Host growth and disease analyses. Starting 10 DAT, the length of each leaf of the experimental plants was measured using a metric ruler every four days. Following the approach of Schwarz and Klaring (2001), and Blanco and Folegatti (2005), leaf areas of experimental plants were determined non-destructively by the power function,

$LA=0.1325LL^{2.09}$ ($n = 246$; $R^2 = 0.93$) derived from non-linear regression analysis of the relationship between leaf length (LL) and leaf area (LA) (read from a leaf area meter Model LI – COR – 3100, Lincoln, NE, USA) using the statistical analysis software SigmaPlot12.0 (San Jose, CA, USA). Host growth up to the time of inoculation (t_{INOC}) was calculated as a mean value of 10 plants (5 plants to be inoculated and 5 plants that remain non-inoculated).

Following the onset of early blight symptoms, disease severity of each fully unfolded leaf (~7 leaflets) was visually estimated as proportion of diseased area in relation to the total leaf area. Actual leaf area per plant at any given time was determined from the sum of areas of individual leaves available on the plant. The diseased leaf area of individual leaves was summed up to obtain the total diseased leaf area of a plant. Diseased leaf area was deducted from the actual leaf area to determine healthy leaf area. Once a leaf defoliated, the maximum leaf area recorded prior to defoliation was noted. Loss of leaf area due to defoliation between successive assessments was summed up to compute the cumulative defoliated leaf area. Leaf abscission from non-inoculated plants was attributed to physiological senescence.

Model description

Overview of the model. The system under consideration consists of two major components: tomato as the host plant and early blight as the disease. The fundamental principle of the model is that substantial effects of early blight epidemics on tomato mainly revolve around its effects on the main photosynthetic organ, the leaves, thus leaf area expressed in cm^2 was adopted as the measurement unit for the amount of host area which can be healthy (H_{DF}) and naturally defoliated (D_{DF}) in the disease-free situation, and healthy (H), diseased (Y), and defoliated (D) in the disease situation. In our model, like in those of Jeger (1986) and Waggoner (1986), the diseased area Y is not subdivided into the three categories latent, infectious and post-infectious area. Moreover, implicit in the model is the assumption that the variation of the environmental factors in the greenhouse affect the disease and host only

slightly and therefore constant rates can be assumed. Principal variables and parameters used in the model are listed in Table 1.

TABLE 1. Principal variables and parameters used in the model.

Symbol	Description	Unit
State variables		
	Diseased situation	
H	Healthy leaf area	cm² plant^{-1}
Y	Diseased leaf area	cm² plant^{-1}
D	Defoliated leaf area	cm² plant^{-1}
	Disease-free situation	
H_{DF}	Healthy leaf area	cm² plant^{-1}
D_{DF}	Defoliated leaf area (due to senescence)	cm² plant^{-1}
Derived variable		
y	Disease severity $Y/(H+Y)$	proportion
Parameters		
H_0	Initial host size	cm² plant^{-1}
H_{max}	Maximum leaf area	cm² plant^{-1}
Y_0	Initial diseased area at time $t_{INOC} + IP$	cm² plant^{-1}
r_{LIN}	Linear rate parameter for initial disease increase	cm² day^{-1}
r_Y	Logistic rate parameter for disease increase	day^{-1}
r_H	Logistic rate parameter for host growth	day^{-1}
r_S	Physiological senescence rate	day^{-1}
r_D	Defoliation rate	day^{-1}
Predetermined parameters		
IP	Incubation period (fixed at 2)	days
LP	Latent period (fixed at 7)	days
t_S	Time when physiological senescence starts (fixed at 50)	DAT
y_{DT}	Defoliation threshold (fixed at 0.20)	proportion
t_{DT}	Time when y_{DT} is reached for the first time	DAT
t_{INOC}	Time of inoculation	DAT

Host and disease development. There are three underlying hypotheses to the equations that we used to describe the dynamics of the healthy leaf area (H) as a function of time t:

1. Healthy area is not affected by disease induced defoliation.

2. Natural defoliation due to physiological senescence of H commences after a certain age threshold (t_S) of the host is reached. From non-inoculated plants of experimental data, t_S was set at 50 DAT.

3. At $t = t_S$, the tomato plant has nearly reached its maximum area H_{max} (cm^2) and further growth is stopped.

Thus, the dynamics of healthy leaf area (H) before defoliation starts at t_S is given by the differential equation with initial condition $H(t = 0) = H_0$:

$$\frac{dH}{dt} = r_H \cdot (H + Y) \cdot \left(1 - (H + Y + D)/H_{max}\right) - Rate_{HY} \qquad \text{if } t < t_S \tag{1}$$

The first term on the right hand side describes the increase of the healthy area by newly produced tissue which is essentially proportional to the actual area $H + Y$ and density regulated by the total host area formed $H + Y + D$ (cm^2) which is limited by H_{max} (cm²). The second term $Rate_{HY}$ reflects the rate at which healthy area becomes diseased.

At the start of natural defoliation at t_S, the healthy leaf area has nearly reached its maximum size, and from that time on it can only decrease due to new disease or defoliation. Thus $H(\mathrm{t})$ is then given by the differential equation:

$$\frac{dH}{dt} = -Rate_{HY} - Rate_{HD} \qquad \text{if } t \geq t_S \tag{2}$$

The $Rate_{HD}$ describes the natural defoliation due to physiological senescence and is proportional to the healthy leaf area (H) with proportionality factor r_S such that:

$$Rate_{HD} = r_S \cdot H \qquad \text{if } t \geq t_S \tag{3}$$

The dynamics of the diseased area (Y) is described by the differential equation:

$$\frac{dY}{dt} = Rate_{HY} - Rate_{YD} \tag{4}$$

The first term in the right hand side of equation 4 describes the increase of the diseased area Y by new symptoms. Depending on the observation time in relation to the artificial inoculation with $A.$ $solani$, the $Rate_{HY}$ is described by:

$$Rate_{HY} = \begin{cases} 0 & \text{if } t < t_{INOC} + IP \\ r_{LIN} & \text{if } t_{INOC} + IP \leq t < t_{INOC} + LP + IP \\ r_Y \cdot Y \cdot (1 - Y/(H+Y)) & \text{if } t \geq t_{INOC} + LP + IP \end{cases}$$

The first equation is based on the fact that under favourable environmental conditions, lesions of early blight only become visible after the incubation period IP of 2 to 3 days has ended (Walker, 1957; Jones et al., 1993). For $A.$ $solani$, IP was set to 2 days. In the second equation of $Rate_{HY}$, the effect of the artificial inoculation is given based on the hypothesis that under a strong inoculum pressure the visible early blight epidemic would linearly proceed within an early phase ($t_{INOC} + IP \leq t < t_{INOC} + LP + IP$) with a disease rate r_{LIN} (cm² day^{-1}), starting from $Y(t = t_{INOC} + IP) = Y_0$. For early blight of tomato, the latent period LP (the time from infection to sporulation) was measured as approximately seven days (Walker, 1957; Jones et al., 1993). Thus, the linear phase ends after the incubation period of the secondary disease cycle elapses i.e. $LP + IP = 9$ days after inoculation.

Later on ($t \geq t_{INOC} + LP + IP$) the epidemic follows the ordinary pattern of a polycyclic disease given by a logistic differential equation with disease rate r_Y (day^{-1}) and variable capacity $H+Y$ (cm^2). As the inoculation times t_{INOC} varied (23, 33 and 43 DAT in experiment A, and 22, 30 and 38 DAT in experiment B), also the plant ages at t_{INOC} differed among the three cohorts.

The second term in equation 4 reflects the defoliation due to the disease. Defoliation is triggered once a certain level of disease severity on a whole plant basis is reached. This defoliation threshold for y (y_{DT}) per plant was determined as 0.20 from experimental data. The

time when this threshold is reached for the first time is named t_{DT}. After t_{DT}, the rate of

defoliated leaf area $Rate_{YD}$ due to the disease is proportional to diseased leaf area (Y) with

proportionality factor r_D such that:

$$Rate_{YD} = \begin{cases} 0 & \text{if } t < t_{DT} \\ r_D \cdot Y & \text{if } t \geq t_{DT} \end{cases} \tag{5}$$

The third compartment D comprises the defoliation due to senescence as well as due to the

disease and is therefore described by:

$$\frac{dD}{dt} = \begin{cases} 0 & \text{if } t < t_{DT} \text{ and } t < t_S \\ r_D \cdot Y & \text{if } t \geq t_{DT} \text{ and } t < t_S \\ r_D \cdot Y + r_S \cdot H & \text{if } t \geq t_{DT} \text{ and } t \geq t_S \\ r_S \cdot H & \text{if } t < t_{DT} \text{ and } t \geq t_S \end{cases} \tag{6}$$

In the absence of the disease ($Y = 0$), only the healthy and the defoliated compartment

describe the host dynamics. In order to differentiate these two compartments in the disease-

free situation from that with disease, they are marked with an index DF. Then the following

simpler equations result for host dynamics in the disease-free situation from the above

equations:

$$\frac{dH_{DF}}{dt} = \begin{cases} r_H \cdot H_{DF} \cdot (1 - H_{DF}/H_{max}) & \text{if } t < t_S \\ -r_S \cdot H_{DF} & \text{if } t \geq t_S \end{cases} \tag{7}$$

$$\frac{dD_{DF}}{dt} = \begin{cases} 0 & \text{if } t < t_S \\ r_S \cdot H_{DF} & \text{if } t \geq t_S \end{cases} \tag{8}$$

Therefore, in the disease-free situation, the healthy host area which is then equivalent to the

total host area will increase initially ($t < t_S$) according to the logistic growth function with a

maximum capacity H_{max} (cm^2), a rate r_H (day^{-1}) and initial value $H_{DF}(t = 0) = H_0$. Later ($t \geq t_S$)

it declines exponentially as the plant senesces and natural defoliation occurs with a rate r_S

(day^{-1}). The rate of senescence r_S is assumed to be identical in both diseased and disease-free

situations, an approach consistent with the models of Savary et al. (1997) and Barnwal et al. (2013).

Model evaluation and statistics. The model was built using ModelMaker version 4.0. (Oxford, UK) using the Runge-Kutta 4th order integration algorithm. Parameters were optimized using the Marquardt method by fitting the differential equations 1, 2, 4 and 6 in the disease situation and equations 7 and 8 in the disease-free situation to the data of each sub-experiment differing in the inoculation time. Specifically for each data set, the host growth rate r_H, the rate of natural defoliation r_S and the maximum host area H_{max} were estimated in disease and disease-free situations simultaneously.

The goodness-of-fit of the model was analyzed by examining the weighted sum of squares of the residual, coefficient of determination r^2 as well as the biological plausibility of parameter estimates. The goodness-of-fit statistics were generated by procedures inbuilt in the software package.

RESULTS

The dynamics of the simulated host leaf area, divided in healthy H, diseased Y, and defoliated D area in the disease situation, and healthy H_{DF} and defoliated D_{DF} in the disease-free situation (Figure 1 and 2) each indicate that the model offered a reasonably good description of the dynamic interaction between the early blight epidemic and growth of tomato. Estimates of parameter values and coefficients of determination obtained from model fitting to experimental data are presented in Table 2. R^2 values of 0.9969, 0.9957 and 0.9990 were computed for early (t_{INOC} = 23 DAT), intermediate (33 DAT) and late (43 DAT) inoculation time of experiment A respectively, whereas 0.9962, 0.9963 and 0.9974 were computed for the three inoculation times (22, 30 and 38 DAT) of experiment B, respectively, thus giving further indication of a good fit of the model to the observations.

Figure 1. Progress curves of healthy (H_{DF}) and naturally defoliated (D_{DF}) leaf area in the disease-free situation, and healthy (H), diseased (Y), and defoliated (D) leaf area of tomato as influenced by early blight (*Alternaria solani*) epidemics inoculated at t_{INOC} = 23 DAT (a), 33 DAT (b), and 43 DAT (c) in experiment A.
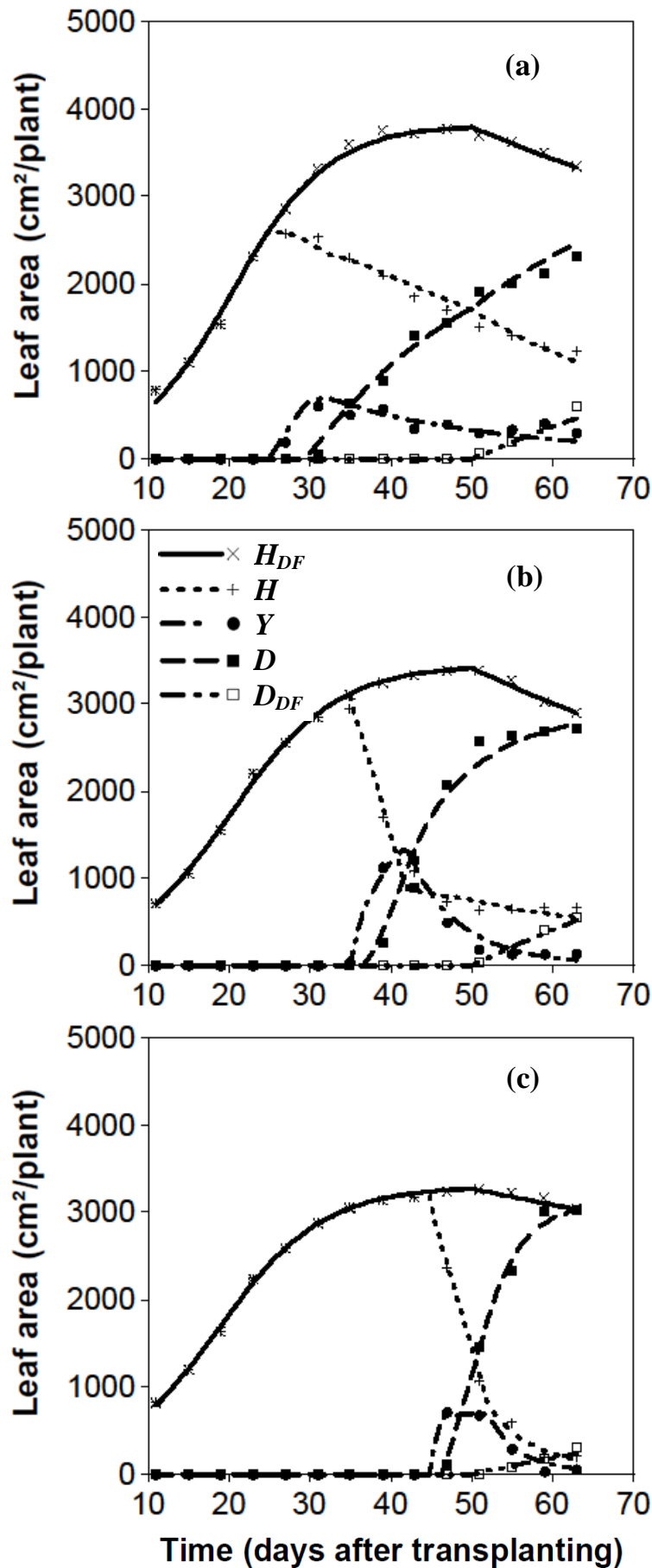
Figure 2. Progress curves of healthy (H_{DF}) and naturally defoliated (D_{DF}) leaf area in the disease-free situation, and healthy (H), diseased (Y), and defoliated (D) leaf area of tomato as influenced by early blight (*Alternaria solani*) epidemics inoculated at t_{INOC} = 22 DAT (a), 30 DAT (b), and 38 DAT (c) in experiment B.
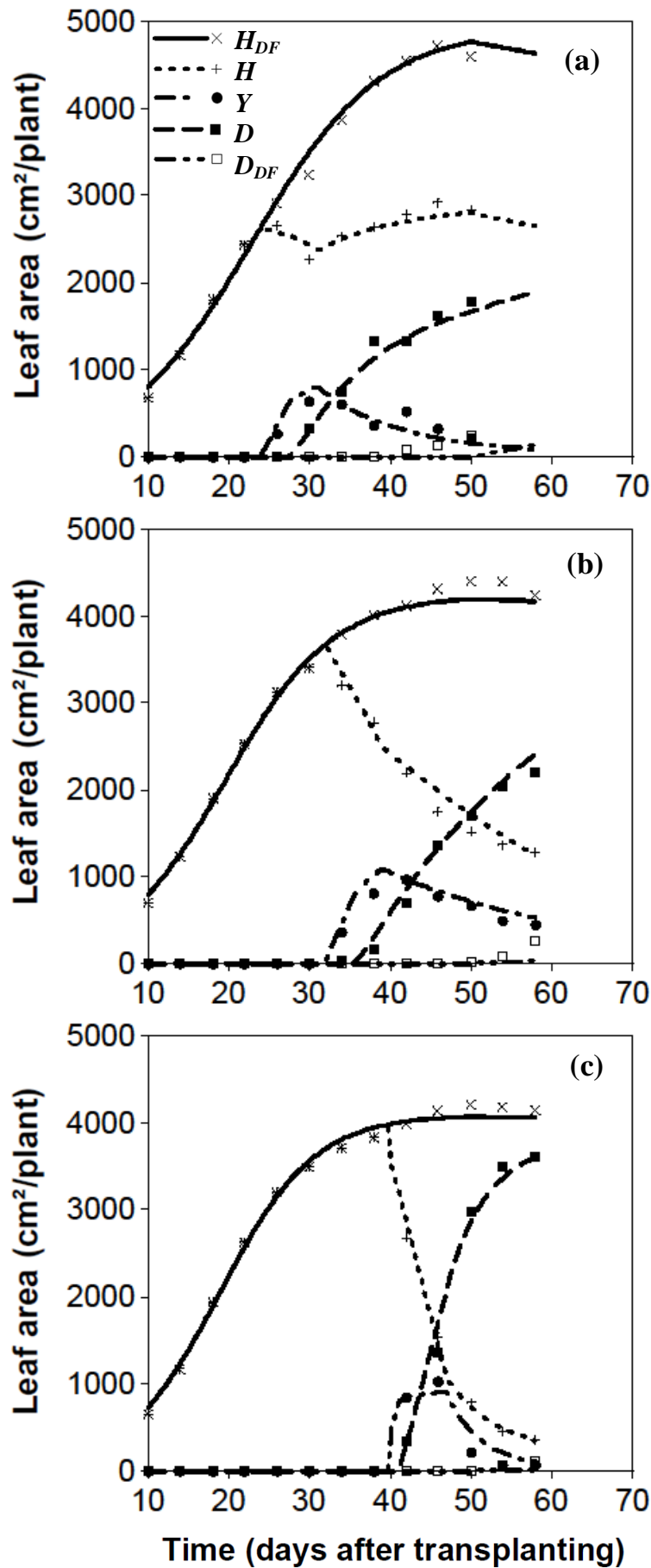
Host growth. In the disease-free situation, healthy leaf area H_{DF} increases progressively but does not attain its maximum area at H_{max} due to onset of natural defoliation at $t \geq t_S$. In essence H_{DF} (cm^2) in both experiments reaches only proportions that range from between 0.9680 to 0.9951 of H_{max} after which it declines gradually. Natural defoliation D_{DF} was much more pronounced in experiment A (Figure 1) than in B (Figure 2) and it would be proportionately 9.4% of the cumulative total leaf area in experiment A compared to only 3.8% in B at 60 DAT.

In the presence of early blight and irrespective of the time of inoculation with *A. solani*, healthy leaf area of the host is considerably reduced in relation to that of the healthy control. With the exception of plants inoculated at 22 DAT in experiment B (Figure 2a), healthy leaf area in both experiments declined progressively with increase in diseased area after $t \geq t_{INOC} + IP$ and accelerated loss of diseased tissues through disease-induced defoliation after $t \geq t_{DT}$ (Figure 1a, b, c and 2b, c). Diseased leaf area Y increased rapidly during the linear phase of the epidemic to approximately 23, 58 and 42% of the actual leaf area (early, intermediate and late inoculation of experiment A) and 25, 30 and 45% (inoculations of experiment B) (Figure 1 and 2). Henceforth, as diseased leaves abscise, the proportion of diseased leaf area steadily decreases and finally approaches zero (not shown).

Comparing the development of disease-induced defoliation D across the three inoculation times (Figure 1 and 2), clearly shows that the progress curves strongly differ in the rate at which diseased area is defoliated. As the inoculation time and thus the age of plants at inoculation increase, also the percentage of defoliation increases. For instance, 20 days after inoculation (DAI), the percentage of defoliated leaf area in relation to the total leaf area produced was 35.4, 72.7 and 93.0% in experiment A (Figure 1) and 31.4, 42.5 and 88.8% in experiment B for the early, intermediate and late inoculations, respectively (Figure 2).

From the estimates of the maximum amount of leaf area produced H_{max}, two observations can be established. Firstly, plants in experiment B achieved higher estimates of H_{max} than in

experiment A (Table 2). This is related mainly to the variation in the amount of substrate fertilizer supplied to the plants, i.e. 10 g.plant^{-1} in experiment A compared to 25 g.plant^{-1} in B, thus resulting in more vigorous plant growth in experiment B. Secondly, in both experiments, the estimated H_{max} generally decreased with increasing plant age at inoculation time. This is probably due to the fact that plants (both inoculated and non-inoculated) were successively transferred from the greenhouse into the polythene cages in the order of early, intermediate and then late inoculation time. The longer period of growth in the warmer condition inside the polythene cages (2 to 4°C higher) relative to the ambient condition in the greenhouse resulted in higher leaf area production.

The rate parameter for host growth r_H (day^{-1}) was moderately identical in experiment A (0.168, 0.151 and 0.153 for t_{INOC} = 23, 33, and 43 DAT, respectively) whereas an increasing trend of r_H in relation to the plant age at inoculation time is discernible in experiment B (0.127, 0.152 and 0.172 for early, intermediate and late inoculation, respectively) (Table 2).

In relation to the estimates of the rate of disease-induced defoliation, r_D (day^{-1}), a notable increase from 0.165 when inoculated at 23 DAT, to 0.192 at 33 DAT and 0.465 at 43 DAT, was detected in experiment A (Table 2). However, this trend does not hold for experiment B where estimates of r_D were 0.171, 0.134 and 0.401 per day for t_{INOC} = 22, 30 and 38 DAT, respectively. Nonetheless, a comparison of the estimated r_D of plants inoculated early (t_{INOC} = 23, 22 DAT) to those inoculated late (t_{INOC} = 43, 38 DAT), presents a strikingly sharp contrast considering that the defoliation rate increases by more than two-folds in the late inoculations. Estimates of the rate of physiological senescence r_S (day^{-1}) were considerably higher in experiment A than B (Table 2). Estimates of r_S were closely identical in experiment A (0.010, 0.013 and 0.006 day^{-1}). In experiment B, the parameter r_S (day^{-1}) was estimated as 0.004, 0.001 and 0.0004 for t_{INOC} = 22, 30, and 38 DAT, respectively, but these estimates were not significantly different from 0 at 5% probability.

TABLE 2. Estimated parameter values and coefficients of determination (R^2) of the model (equations 1, 2, 4 and 6 in the disease situation and equations 7 and 8 in the disease-free situation) simulating epidemics of early blight (*Alternaria solani*) on tomato and the dynamics of host growth of tomato plants with and without inoculation of *A. solani* (see Table 1 for explanation of acronyms).

Experiment	Inoc. time[1]	Estimated parameter values								R^2
		H_0	r_H	r_S	H_{max}	Y_0	r_{LIN}	r_Y	r_D	
A	23	651.7	0.168	0.010	3815.0	0.002	141.2	0.151	0.165	0.9969
		(30.9)[2]	(0.006)	(0.001)	(29.9)	(0.186)	(5.9)	(0.010)	(0.009)	
	33	695.3	0.151	0.013	3447.8	73.557	337.4	0.060	0.192	0.9957
		(36.4)	(0.007)	(0.001)	(35.9)	(53.752)	(11.3)	(0.016)	(0.009)	
	43	784.7	0.153	0.006	3293.5	192.932	322.3	0.380	0.465	0.9990
		(19.4)	(0.004)	(0.001)	(16.1)	(40.381)	(8.2)	(0.027)	(0.019)	
B	22	798.6	0.127	0.004	4919.1	0.014	175.4	0.095	0.171	0.9962
		(38.7)	(0.006)	(0.340)	(88.1)	(67.187)	(12.0)	(0.020)	(0.015)	
	30	786.0	0.152	0.001	4239.7	16.959	215.7	0.135	0.134	0.9963
		(39.1)	(0.006)	(0.002)	(42.3)	(77.551)	(14.3)	(0.010)	(0.007)	
	38	721.0	0.172	0.0004	4088.0	401.430	367.5	0.305	0.401	0.9974
		(35.2)	(0.006)	(0.002)	(32.7)	(80.456)	(15.6)	(0.036)	(0.025)	

[1]Time of inoculation in days after transplanting

[2]Standard errors of the parameter estimates are given in parentheses

Disease progress. Simulations of the progress curves of early blight severity are presented in figure 3 and 4. Graphical examination of the observed and simulated values showed a reasonably good fit of the model to the data for both experiments.

Comparing plants inoculated at identical times in the two experiments, for instance Figure 3a and 4a, the pattern of the simulated progress curves strongly differed in the intermediate inoculations in contrast to the early and late inoculations in which the curves are moderately similar. The early blight epidemics strongly increased after the appearance of lesions and reached the defoliation threshold ($y_{DT} = 0.2$) already during the primary phase of the epidemic

($t_{INOC} + IP \leq t < t_{INOC} + LP + IP$). With the exception of the intermediate inoculation ($t_{INOC} =$ 30 DAT) of experiment B (Figure 4b), disease progress curves in the logistic phase decreased progressively with continued defoliation of diseased leaves (Figure 3 and 4a, c) and finally approached zero in long run (not shown). The simulated epidemic curve of plants inoculated 30 DAT during experiment B was characterized by increasing disease progression (Figure 4b) which eventually levels off at its maximum capacity, in this case 1 (not shown).

On a proportionate scale, the maximum disease severity achieved during the primary phase of the early blight epidemic in both experiments was closely identical for early (0.23 and 0.24) and late (0.46 and 0.45) inoculations, in contrast to the intermediate inoculations which were considerably distinct (0.58 and 0.30 in experiment A and B, respectively).

From the estimates of Y_0 it is discernible that as the inoculation time and thus the size and age of plants at inoculation increase, the initial diseased area Y_0 (cm² plant^{-1}) also increases (Table 2). Overall, the highest and lowest values of Y_0 were estimated for the late and early inoculations, respectively. However, other than for the late inoculations, estimates of Y_0 were not significantly different from 0 in all other cases.

For the initial linear disease rate r_{LIN}, high values of 141.2, 337.4 and 322.3 cm² per day were estimated for the early, intermediate and late inoculation of experiment A, respectively, while 175.4, 215.7 and 367.5 cm² per day were estimated for the inoculations of experiment B (Table 2). With the exception of the intermediate inoculation ($t_{INOC} =$ 33 DAT) of experiment A, the estimated logistic rate parameter for disease increase r_Y (day^{-1}) notably increases with increase in time and also the plant age at inoculation (Table 2). Values of r_Y were roughly three-folds higher in the late inoculation times (0.380, 0.305 day^{-1}) when compared to the early inoculations (0.151, 0.095 day^{-1}).

Figure 3. Progress curves of early blight (*Alternaria solani*) severity on tomato inoculated at t_{INOC} = 23 DAT (a), 33 DAT (b), and 43 DAT (c) in experiment A.
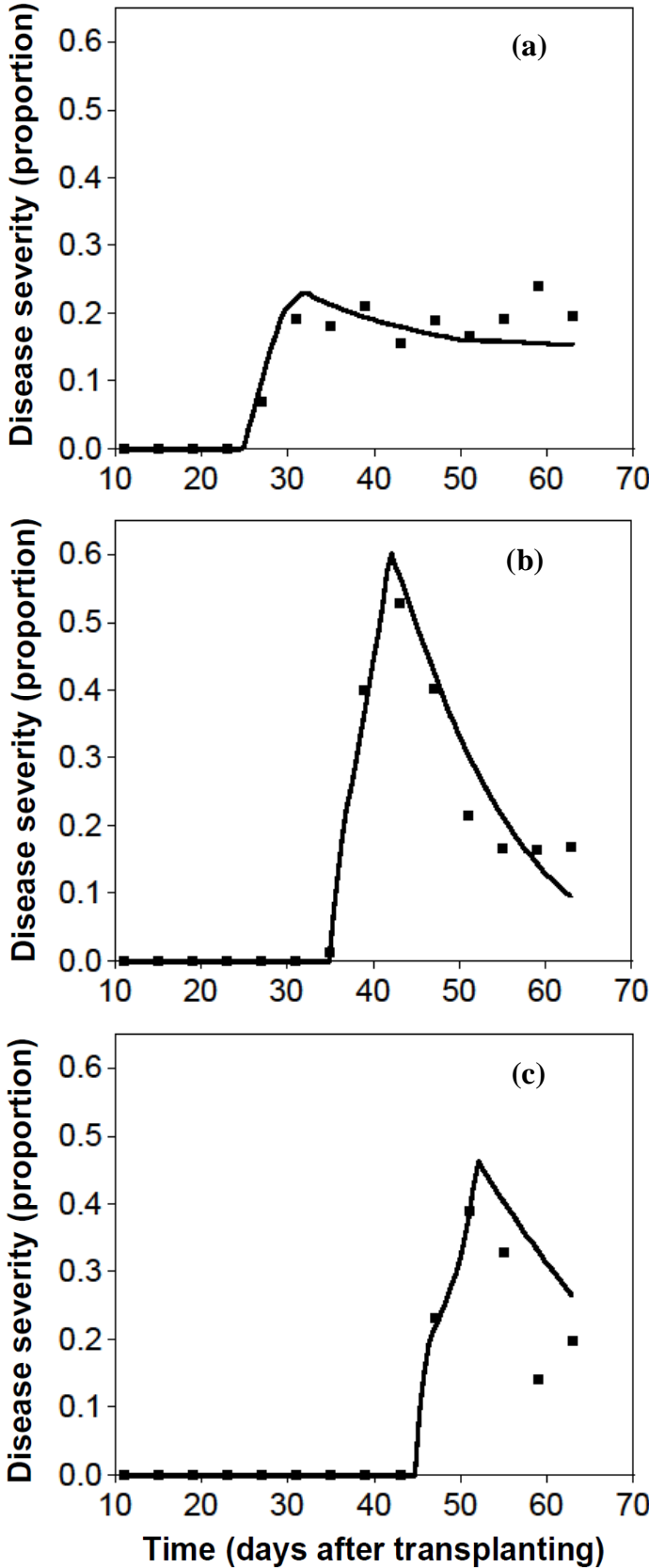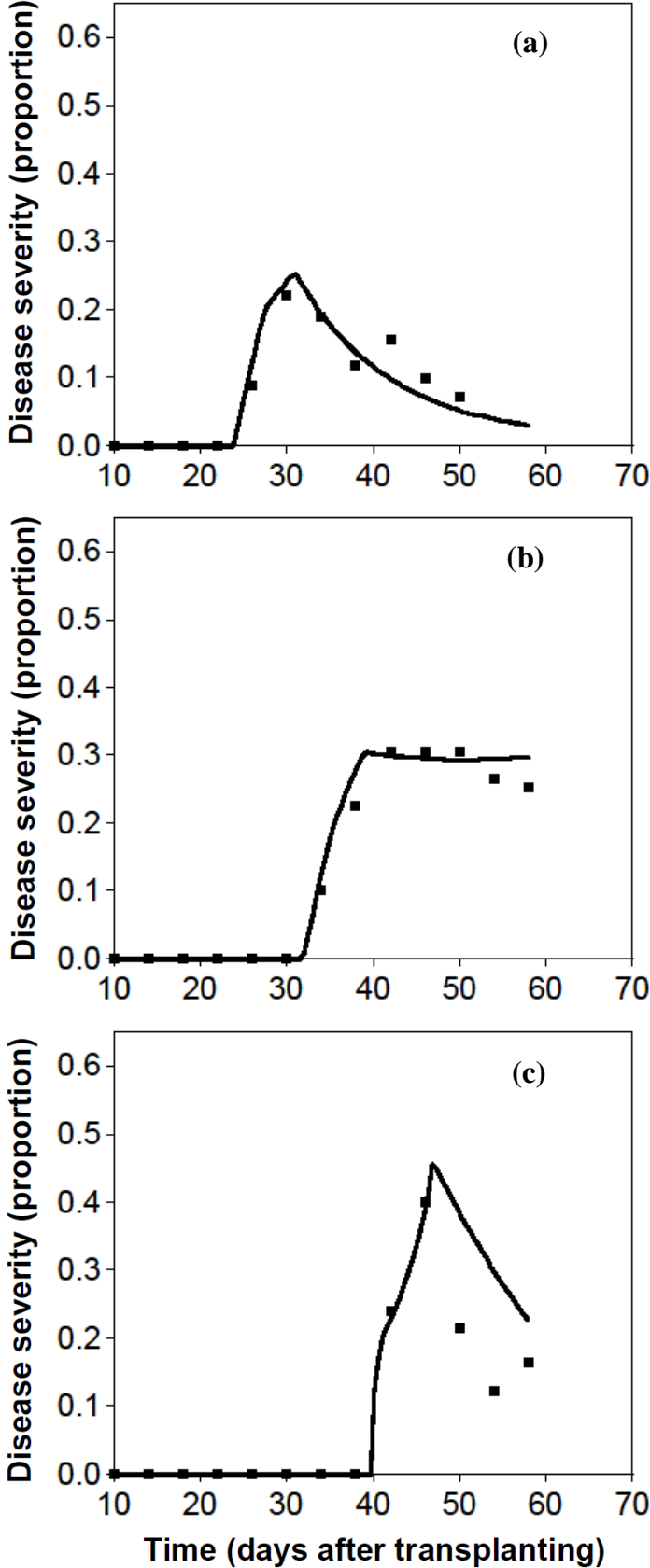
Figure 4. Progress curves of early blight (*Alternaria solani*) severity on tomato inoculated at $t_{INOC} = 22$ DAT (a), 30 DAT (b), and 38 DAT (c) in experiment B.

A dynamic correlation seemingly exists between the rate of disease increase r_Y and the rate of defoliation r_D (Table 2) which to a great extent influences the behaviour of the disease progress curves (Figure 3 and 4). For instance, if the defoliation rate is much higher than the increase of diseased area i.e. $r_D > r_Y$, the disease severity decreases rapidly (Figure 3b, c and 4a, c) and finally approaches zero. On the other hand, if the diseased area increases at a faster rate than the rate of defoliation i.e. $r_D < r_Y$, the disease severity progressively increases (Figure 4b) and finally reaches its maximum capacity.

Besides defoliation of diseased leaf area, the production of new healthy leaf area also contributed to the decline in the disease severity. This was specifically relevant when the inoculation took place early and host growth still continues substantially. As shown in Figure 2a, the total host area is nearly 65% of its maximum area at the time when defoliation begins. Thus, the host is still increasing and consequently '*dilutes*' the proportion of disease severity. Moreover, host growth in this case proceeded a higher rate ($r_H = 0.127$) than the disease was progressing ($r_Y = 0.095$).

DISCUSSION

The objective of the experimental and modeling work presented in this study was to develop a simple but comprehensive model coupling the dynamic interaction of tomato leaf area growth and disease progression of early blight. In this approach which is similar to that adopted among others by Rossi et al. (1997) and Calonnec et al. (2008), state variables for the host and disease, i.e. healthy, diseased, and defoliated leaf areas are described by differential equations with biological parameters for the growth rates and the initial conditions.

Leaf area was adopted as the measurement unit for host growth and disease progress because the major damaging symptoms of *A. solani* are manifested through blighted foliage and premature defoliation of the plant (Lawrence et al., 2000; Pandey et al., 2003; Chaerani et al., 2007; Majid et al., 2008). Moreover, host colonization by the fungus leads to decreased photosynthetic rates and increased respiration in apparently healthy tissues (Rotem, 1994).

The model developed in this study differs from those reported by other workers in three respects. Firstly, unlike the models of Jeger (1986) and Waggoner (1986) where the increase over time in the total amount of leaf area formed as well as the total defoliated leaf area is unlimited, in our model, the production of new tissue is density regulated by the total host area formed $(H + Y + D)$ which is in turn limited by its maximum capacity H_{max} (cm²).

Secondly, the development of the early blight epidemic is modelled in such a way as to feature two distinct phases: an initial disease phase characterized by a linear increase in diseased area and a later disease phase during which the polycyclic epidemic progresses with the ordinary logistic pattern. The distinctiveness between these two phases of the epidemic becomes even more apparent from the high estimates of the disease rate (r_{LIN}) for the primary disease phase. Therefore, the use of a uniform rate for the entire epidemic (Nelson and Campbell, 1993; Godoy, 2003; Pandey et al., 2003; Ojiambo and Scherm, 2005; Mersha and

Hau, 2008) would in our case lead to an erroneous conclusion about the nature of the epidemic progress.

Instead of the linear equation, other alternatives such as the exponential and Gompertz functions were explored to describe the epidemic behavior during the early phase (data not shown). However, based on the goodness-of-fit statistics of the models as well as the general congruence of the simulated and observed data, the linear equation was deemed as giving a better description of the initial epidemic progress.

Thirdly, these studies highlight quantitatively the contribution of defoliation in determining the course of the early blight epidemic on tomato. Other than its consequences on disease measurements, defoliation could significantly change the microclimate within the crop canopy, reduce the available healthy tissue for infection (when disease-induced defoliation also affects the healthy area), and lower the amount of inoculum present within the canopy, all of which have an important bearing on the epidemic progress (Aust and Hoyningen-Huene, 1986; Nelson and Campbell, 1993; Pandey et al., 2003; Willocquet et al., 2004; Allorent et al., 2005). Accordingly, concerted efforts have been made to correct or account for host plant defoliation in various pathosystems (Waggoner, 1986; Waggoner and Berger, 1987; Thal and Campbell, 1988; Johnson and Teng, 1990; Nelson, and Campbell, 1993; Allorent et al., 2005; Allorent and Savary, 2005).

There are two important assumptions in the approach that we used to model defoliation in this work. One is that the only factor acting on the rate of defoliation of diseased area is the disease severity of leaves in such a way that defoliation is triggered once a certain level of disease severity on a whole plant basis (y_{DT}) is reached (Allorent and Savary, 2005). However, unlike the model of Allorent and Savary (2005), in which the contribution of natural leaf senescence in an infected plant is assumed to be negligible compared to disease-induced defoliation, we have in our model included natural defoliation due to physiological

senescence of healthy leaf area under the hypothesis that it commences after a certain age threshold ($t = t_S$) of the host plant is reached.

With a few exceptions, simulations of the early blight severity in the current study appeared to increase rapidly during the primary phase of the epidemic but henceforth declined progressively and finally approached zero as the diseased leaves are rapidly removed by defoliation. These observations differ with reports from Pandey et al. (2003) who observed a bimodal disease progress curve occasioned by the emergence of new healthy leaves after the first cycle of infection.

The physiological age of the host plant at disease onset may considerably affect the development and progress of an epidemic (Mersha and Hau, 2011). In particular, the effects of increased susceptibility to infection with increasing host age in the tomato-early blight pathosystem have been extensively reported (Rotem, 1994; Vloutoglou and Kalogerakis, 2000; Koo, 2002; Pandey et al., 2003; Chaerani and Voorrips, 2006). Pandey et al. (2003) reported a percentage disease index of 54.7% on 35-day-old tomato plants in contrast to 85% on 50-day-old plants of the same variety. These findings collaborate with the simulation results in the present work especially when the early inoculated (younger) plants ($t_{INOC} = 23$ or 22 DAT) are compared with the late inoculated (older) plants ($t_{INOC} = 43$ or 38 DAT). Overall, the proportion of defoliated leaf area increased as the age of plants at inoculation time increased with the defoliation rates being approximately two and half times higher in late inoculations than in the early inoculations. Likewise, estimates of the disease rate r_Y (per day) were approximately two to three times higher in late inoculated plants than those inoculated early.

Based on simulation results of this study, we can conclusively say that the degree of host susceptibility to infection with *A. solani* increases with the age of the tomato plant. Several hypotheses have been advanced to explain the physiological mechanism behind this apparent age-conditioned susceptibility to infection (Rotem, 1994; Chaerani and Voorrips, 2006). Low

sugar content in older leaves and plants as a result of the late-season translocation of sugars to the ripening fruits (Rotem, 1994) has been suggested as the reason behind the increased susceptibility of physiologically older plants to early blight infection. Additionally, the three glycoalkaloids (solanine, chaconine, and solanidine), whose concentrations in tomato and potato leaves tend to decrease as plants mature have been shown to potentially inhibit growth of *A. solani* in vitro (Sinden et al., 1972).

This observation in the tomato-early blight pathosystem is in striking contrast to reports from other host-disease interactions. For example, the common bean (*Phaseolus vulgaris*) and soybean (*Glycine max*) are reported to be susceptible to bean rust (*Uromyces appendiculatus*) and soybean rust (*Phakopsora pachyrhizi*), respectively, during the juvenile period only but become increasingly resistant as the plants age (Melching et al., 1988; Mersha and Hau, 2011). Moreover, adult plant resistance has been widely reported for powdery mildew *(Erysiphe* spp.) and rust *(Puccinia* spp.) diseases of wheat *(Triticum aestivum* L.) (Bennett, 1981; Pretorius et al., 1988; Denissen, 1993; Ma and Singh, 1996). Thus, a better understanding of this age-dependent relationship of infection with host susceptibility is crucial to the refinement of disease management strategies.

Several improvements can be made to the model developed in this work to achieve a better description of the dynamics of the interacting early blight epidemic and the growth of tomato. For instance, the model can be extended to examine the behavior of the host and disease system under the assumption that rate of disease progress is changing with time depending on the conditions of the environment (particularly temperature and leaf wetness duration). Additionally, the effect of fungicide application on epidemic progress is also another important component that can be included in the model.

LITERATURE CITED

Agrios GN (2005) Plant Pathology, 5th ed., Elsevier Academic Press, San Diego, CA.

Allorent D and Savary S (2005) Epidemiological characteristics of angular leaf spot of bean: a systems analysis. European Journal of Plant Pathology 113: 329–341.

Allorent D, Willocquet L, Sartorato A and Savary S (2005) Quantifying and modelling the mobilisation of inoculum from diseased leaves and infected defoliated tissues in epidemics of angular leaf spot of bean. European Journal of Plant Pathology 113: 377–394.

Aust HJ Hoyningen-Huene JV (1986) Microclimate in relation to epidemics of powdery mildew. Annual Review of Phytopathology 24: 491–510.

Barnwal MK, Kotasthane A, Magculia N, Mukherjee PK, Savary S, Sharma AK, Singh HB, Singh US, Sparks AH, Variar M and Zaidi N (2013) A review on crop losses, epidemiology and disease management of rice brown spot to identify research priorities and knowledge gaps. European Journal of Plant Pathology 136: 443–457.

Basu PK (1974) Measuring early blight, its progress and influence on fruit losses in nine tomato cultivars. Canadian Plant Disease Survey 54: 45–51.

Bennett FG (1981) The expression of resistance to powdery mildew infection in winter wheat cultivars. II. Adult plant resistance. Annals of Applied Biology 98: 305–317.

Blanco FF and Folegatti MV (2005) Estimation of leaf area for greenhouse cucumber by linear measurements under salinity and grafting. Scientia Agricola 62: 305–309.

Calonnec A, Cartolaro P, Naulin JM, Bailey D and Langlais M (2008) A host–pathogen simulation model: powdery mildew of grapevine. Plant Pathololology 57: 493–508.

Chaerani R and Voorrips RE (2006) Tomato early blight (*Alternaria solani*): the pathogen, genetics, and breeding for resistance. Journal of General Plant Pathology 72: 335–347.

Chaerani R, Groenwold R, Stam P and Voorrips RE (2007) Assessment of early blight (*Alternaria solani*) resistance in tomato using a drop inoculation method. Journal of General Plant Pathology 73: 96–103.

Chaerani R, Smulders MJM, van der Linden CG, Vosman B, Stam P and Voorrips RE (2007) QTL identification for early blight resistance (*Alternaria solani*) in a *Solanum lycopersicum* × *S. arcanum* cross. Theoretical and Applied Genetics 114: 439–450.

Cook RJ and Yarham DJ (1998) Epidemiology in sustainable systems. In: Jones DG (ed.) The Epidemiology of Plant Diseases (pp 260–277), Kluwer Academic Publishers, Dordrecht, The Netherlands.

Datar VV and Mayee CD (1981) Assessment of losses in tomato yield due to early blight. Indian Phytopathology 34: 191–195.

Denissen CJM (1993) Components of adult plant resistance to leaf rust in wheat. Euphytica 70: 131–40.

Gleason ML, Ricker MD, MacNab AA, East DA, Pitblado RE and Latin RX (1995) Disease-warning systems for processing tomatoes in Eastern North America: Are we there yet? Plant Disease 79: 113–121.

Godoy CV, Amorim L, Bergamin Filho A, Silva HP, Silva WJ and Berger RD (2003) Temporal progress of southern rust in maize under different environmental conditions. Fitopatologia Brasileira 28: 273–278.

Jasinski J (1999) TOMCAST for Ohio, Indiana and Michigan. http://www2.ag.ohiostate. edu/~vegnet/tomcats/tomfrm.htm

Jeger MJ (1986) The potential of analytic compared with simulation approaches to modeling in plant disease epidemiology. In: Leonard KJ and Fry WE (eds) Plant Disease Epidemiology. Population Dynamics and Management (pp 255–281), MacMillan, New York.

Johnson KB and Teng PS (1990) Coupling a disease progress model for early blight to a model of potato growth. Phytopathology 80: 416–425.

Jones JP (1991) Early blight. In: Jones JB, Jones JP, Stall RE and Zitter TA (eds) Compendium of Tomato Diseases (pp 13–14), APS Press, St Paul, Minnesota.

Koo J (2002) Modeling the impacts of climate variability on tomato disease management and production. Unpublished MS thesis, University of Florida, USA. Available at http://etd.fcla.edu/UF/UFE1000136/koo_j.pdf.

Kranz J and Jörg E (1989) The synecological approach in plant disease epidemiology. Review of Tropical Plant Pathology 6: 27–38.

Lawrence CB, Singh NP, Qiu J, Gardener RG and Tuzun S (2000) Constitutive hydrolytic enzymes are associated with polygenic resistance of tomato to *Alternaria* solani and may function as elicitor release mechanism. Physiological and Molecular Plant Pathology 57: 211–220.

Ma H and Singh RP (1996) Expression of adult resistance to stripe rust at different growth stages of wheat. Plant Disease 80: 375–379.

Madden L, Pennypacker SP, MacNab AA (1978) FAST, a forecast system for *Alternaria solani* on tomato. Phytopathology 68: 1354–8.

Majid RF, Heather LM and Hamid A (2008) Genetics, genomics and breeding of late blight and early blight resistance in tomato. Critical Reviews in Plant Sciences 27: 75–107.

Melching JS, Dowler WM, Koogle DL and Royer MH (1988) Effect of plant and leaf age on susceptibility of soybean to soybean rust. Canadian Journal of Plant Pathology 10: 30–35.

Mersha Z and Hau B (2011) Reciprocal effects of host and disease dynamics in the bean rust pathosystems. Journal of Plant Diseases and Protection 118: 54–62.

Nash AF and Gardner RG (1988b) Tomato early blight resistance in a breeding line derived from *Lycopersicon hirsutum* PI 126445. Plant Disease 72: 206–209.

Nelson SC and Campbell CL (1993) Disease progress, defoliation and spatial pattern in a multiple-pathogen disease complex on white clover. Phytopathology 83: 419–429.

Ojiambo PS and Scherm H (2005) Temporal progress of Septoria leaf spot on rabbiteye blueberry (*Vaccinium ashei*). Plant Disease 89: 1090–1096.

Pandey KK, Pandey PK, Kallo G, Banerjee MK (2003) Resistance to early blight of tomato with respect to various parameters of disease epidemics. Journal of General Plant Pathology 69: 364–371.

Pretorius ZA, Rijkenberg FHJ and Wilcoxson RD (1988) Effects of growth stage, leaf position and temperature on adult plant resistance of wheat infected by *Puccinia reconditat* sp. *tritici.* Plant Pathology 37: 36–44.

Rossi V, Racca P, Giosuè S, Pancaldi D and Alberti I (1997) A simulation model for the development of brown rust epidemics in winter wheat. European Journal of Plant Pathology 103: 453–65.

Rotem J (1994) The Genus *Alternaria* Biology, Epidemiology, and Pathogenicity, APS press, St Paul, Minnesota.

Rotem J and Reichert I (1964) Dew—a principal moisture factor enabling early blight epidemics in a semiarid region of Israel. Plant Disease Report 48: 211–215

Savary S, Willocquet L and Teng PS (1997) Modelling sheath blight epidemics on rice tillers. Agricultural Systems 55: 359–384.

Schwarz D and Klaring HP (2001) Allometry to estimate leaf area tomato. Journal of Plant Nutrition 24: 1291–1309.

Sherf AF and MacNab AA (1986) Vegetable Diseases and their Control, Wiley, New York.

Sinden SL, Goth RW and O'brien MJ (1972) Effect of potato alkaloids on the growth of *Alternaria solani* and their possible role as resistance factors in potatoes. Phytopathology 63: 303–307.

Thal WM and Campbell CL (1988) Analysis of progress of alfalfa leaf spot epidemics. Phytopathology 78: 389–395.

Van Maanen A and Xu M (2003) Modelling plant disease epidemics. European Journal of Plant Pathology 109: 669–682.

Vloutoglou I and Kalogerakis SN (2000) Effects of inoculum concentration, wetness duration and plant age on development of early blight (*Alternaria solani*) and on shedding of leaves in tomato plants. Plant Pathology 49: 339–345.

Waggoner PE (1986) Progress curves of foliar diseases: Their interpretation and use. In: Leonard KJ and Fry WE (eds) Plant Disease Epidemiology. Population Dynamics and Management (pp 3–37), MacMillan, New York.

Waggoner PE and Berger RD (1987) Defoliation, disease, and growth. Phytopathology 77: 393–98.

Waggoner PE and Horsfall JG (1969) EPIDEM: A simulator of plant disease written for a computer. Bulletin Connecticut Agricultural Experiment Station No. 698.

Walker JC (1957) Plant Pathology, McGraw-Hill, New York.

Willocquet L, Allorent D and Savary S (2004) Quantitative analysis of two important epidemiological features in the common bean – *Phaeoisariopsis griseola* pathosystem. Fitopatologia Brasileira 29: 676–679.

Chapter 4

Modeling the interaction between bean rust epidemics and host dynamics of common bean

John Chelal[1], Zelalem Mersha[2] and Bernhard Hau[1]*

[1]Leibniz Universität Hannover

Institut für Gartenbauliche Produktionssysteme, Abteilung Phytomedizin

Herrenhäuser Str. 2, D-30419 Hannover, Germany

[2]College of Agricultural and Natural Sciences,

Lincoln University Cooperative Extension,

Jefferson City, MO 65101, USA

*Corresponding author: hau@ipp.uni-hannover.de

ABSTRACT

In this study, a model simulating an interaction between bean rust epidemics and host growth dynamics of common bean is developed. The model is formulated as a set of differential equations for the rate of change in the amount of healthy H, diseased Y, and defoliated D leaf area in the disease situation, and healthy H_{DF} and defoliated D_{DF} leaf area in the disease-free situation. Host and disease parameters were estimated through fitting the model to experimental data obtained from greenhouse and controlled climate chamber experiments. The two main assumptions of the current model are that a) the total leaf area formed is limited in both the diseased and disease-free situations, and b) maximum host area formed is significantly reduced in the diseased compared to the disease-free situation. Simulations of disease severity and bean growth showed a good fit to the observed data ($R^2 > 0.993$). In the diseased situation, the total production given by $H + Y + D$ levels off at a much lower value, i.e. reaching only proportions of 0.5901 to 0.7668 of H_{max}. The rate parameter for host growth r_H was closely identical (0.200, 0.192 and 0.183 per day) in the three experiments. High values of between 9.1 to 70.4 cm² per day were estimated for the initial linear disease rate r_{LIN} due to the strong inoculum pressure within the early cycle of the bean rust epidemic. Estimates of logistic rate parameter for disease increase r_Y were within the range of 0.062 and 0.089 per day. The model showed that host production is only proportional to the healthy area H and not to the actual area $H + Y$. There was good fit between simulated and observed data as well as the biological relevance of the estimated parameter values. Hence, the model can be considered to satisfactorily describe the dynamic interaction between the bean rust epidemic and growth of common bean.

Additional key words: *Uromyces appendiculatus, Phaseolus vulgaris,* leaf area, senescence, defoliation.

INTRODUCTION

Bean rust, caused by *Uromyces appendiculatus* (Pers.: Pers.) Unger, is an economically important and destructive disease of the common bean (*Phaseolus vulgaris* L.) (Lopes, 1999; Jesus Junior et al., 2001; Liebenberg et al., 2006; Liebenberg and Pretorius, 2010). It is a disease of worldwide occurrence and has been reported from most common bean production areas of the world, especially in the humid tropical and subtropical areas (Lindgren et al., 1995; Souza et al., 2013) where cool, moderately humid to humid conditions and long dew periods are prevalent (Stavely, 2005; Liebenberg and Pretorius, 2010). Periodic severe bean rust epidemics have also been observed in humid temperate regions (Stavely and Pastor-Corrales, 1989; Lindgren et al., 1995; Souza et al., 2008).

The most commonly observed symptoms of *U. appendiculatus* are the rust-colored pustules on both the adaxial and abaxial leaf surfaces, often surrounded by a chlorotic halo. Initial symptoms appear as minute, whitish and slightly raised spots on the leaf surface in about 5-6 days (Stavely, 2005). Severely diseased leaves usually curl upwards, dry up and defoliate prematurely (Jesus Junior et al., 2001; Mersha and Hau, 2008; Liebenberg and Pretorius, 2010; Mersha and Hau, 2011; Schwartz et al., 2011).

Yield losses due to rust diseases are primarily the result of a significant growth depression, accelerated defoliation and substantial reduction in the total amount of leaf area produced by the bean plant (Liebenberg and Pretorius, 2010; Mersha and Hau, 2011), which, according to Mersha and Hau (2008), can be as high as 46% on a susceptible cultivar. Yield losses caused by bean rust epidemics can be extremely high, even approaching 100% in the absence of adequate control measures (Habtu & Zadoks, 1994). The extent of yield reduction due to bean rust depends on the degree of susceptibility of bean cultivars, climatic conditions favoring epidemic development, and earliness of the infection (Berger et al., 1995; Lopes, 1999).

Lindgren et al. (1995) estimated a yield loss of approximately 19 kg/ha for every 1% increase in bean rust severity.

Fundamentally, the development of successful disease control strategies as well as accurate estimation of future crop losses depends on the understanding of the epidemiological variables that govern the dynamic interactions between the host and the pathogen systems (Newton et al., 1995; Bergamin Filho et al., 1997; Lopes and Berger, 2001; Xu, 2006; Pangga et al., 2011). Since the pioneering work of Van der Plank (1963), there has been significant interest in developing models which incorporate the dynamics of host growth and epidemics of a disease (Boote et al., 1983; Jeger, 1986; Waggoner, 1986; Hau, 1990; Madden et al., 2007; Ferrandino, 2008; Calonnec et al., 2008). These modeling approaches led not only to a better understanding of how diseases affect their hosts but also gave insight on the reciprocal effects of host factors on epidemic development (Boote et al., 1983; Pangga et al., 2011).

For the bean rust pathosystem and particularly with regard to empirical quantification of host-disease interactions, the contributions of Mersha and Hau (2008; 2011) are to our knowledge some of the most notable. Moreover, Berger et al. (1995) developed and validated (Amorim et al., 1995) FERRUGEM, a simulation model of bean rust epidemics based on infections of *U. appendiculatus* that occurred on daily cohorts of bean leaves. However, what was not included in their model was the acceleration of defoliation due to disease and the contribution of total lesion (the entire chlorotic area including the pustule and surrounding halo) to disease progress.

Hau (1990) drew attention to the epidemiological consequences of a changing host either by an increase of susceptible tissue through growth flushes of the host or by the loss of the diseased tissue through defoliation. Moreover, disease-induced defoliation, besides being an important injury component leading to yield loss, may also strongly influence the course of an epidemic by reducing the amount of inoculum present within the canopy, changing the

canopy microclimate and limiting host growth (Allorent and Savary, 2005; Allorent et al., 2005).

Amongst others, Waggoner (1986), Jeger (1986) and Madden et al. (2007) have incorporated the negative effect of defoliation and disease on host growth in their models. However, a major drawback to these models is the inherent characteristic that total leaf area formed as well as total leaf area defoliated in the disease situation will increase over time without any limitation.

In this paper, we describe the details of an improved dynamic model coupling host growth of the common bean with temporal progress of the rust disease so as to provide a framework within which the dynamic interactions between disease and host are examined.

MATERIALS AND METHODS

Experimental data. Data for bean rust epidemics and host dynamics of common bean were obtained from a greenhouse experiment conducted in October 2003 (experiment 1) and repeated twice in controlled climate chambers experiments in January 2004 (experiment 2) and April 2004 (experiment 3) at the Institut für Gartenbauliche Produktionssysteme, (Abteilung Phytomedizin) of Leibniz Universität Hannover. A brief description of the experiments is outlined in this paper. A detailed description has already been presented by Mersha and Hau (2008). The single-plant approach of Kranz and Jörg (1989) was adopted in which each treatment, i.e. inoculated with *U. appendiculatus* (I) or non-inoculated (NI), comprised of six (experiment 1) or five (experiment 2 and 3) times replicated plants.

Bean plants of the susceptible and determinate cultivar 'Dufrix' were artificially inoculated with a *U. appendiculatus* suspension of 1 x 10^5 spores mL^{-1} at 21, 22 and 25 DAS in experiment 1, 2 and 3, respectively. In contrast, non-inoculated plants were sprayed with deionized water. To enhance the bean rust epidemics after the initial inoculation, night relative humidity levels in the climate chambers were raised from 65% to 95% for 3

consecutive nights per week for 3 weeks. Other than these times, plants were maintained at 24 ºC and 20 ºC day and night temperatures, respectively, 65% relative humidity and a photoperiod of 13 h.

From the experimental data, the following information (on a plant basis) was used as model data: actual total lesion proportion, actual and total leaf area (cm²), and total loss of leaf area (due to leaf shriveling + defoliation). Total loss of leaf area is herein referred to as defoliated leaf area. Defoliation from non-inoculated plants was attributed to physiological leaf senescence. The diseased leaf area was obtained from the estimated proportion of total lesion area and the calculated leaf area. Healthy leaf area was determined by deducting diseased leaf area from the actual leaf area.

Model description

Overview of the model. The model presented here is based on the theoretical and experimental knowledge of the dynamic interaction between epidemics of the bean rust and growth of the common bean. The model is formulated as a system of differential equations that describe the dynamics of healthy (H), diseased (Y) and defoliated (D) leaf area of an inoculated and hence diseased plant, and healthy (H_{DF}), and defoliated (D_{DF}) leaf area of non-inoculated and hence a disease-free situation. Diseased leaf area Y, like in the models of Jeger (1986) and Waggoner (1986), is not subdivided into latent (pre-infectious), infectious, and removed (post-infectious) categories. In this, we differ from models by, among others, Segarra et al. (2001), Madden et al. (2007), and Burie et al. (2012).

It is well known that the development and severity of bean rust are highly influenced by environmental variables (particularly temperature, humidity and leaf wetness duration) and host factors such as leaf age, nutrition and cultivar resistance (Imhoff et al., 1981; Mendes and Bergamin, 1989; French et al., 1993; Berger et al., 1995; Lopes, 1999; Stavely, 2005; Liebenberg and Pretorius, 2010). There is also the effect of changing environmental

conditions on host growth which would also require the input of information related to the agronomy of the host (Hau, 1990). However, for the sake of model simplicity, we do not take these effects into account because the first experiment was conducted in semi-controlled conditions in a greenhouse and the last two experiments were conducted in controlled climate chambers. Principal variables and parameters used in the model are listed in Table 1.

TABLE 1. Principal variables and parameters used in the model.

Symbol	Description	Unit
State variables		
	Diseased situation	
H	Healthy leaf area	cm² plant^{-1}
Y	Diseased leaf area	cm² plant^{-1}
D	Defoliated leaf area	cm² plant^{-1}
	Disease-free situation	
H_{DF}	Healthy leaf area	cm² plant^{-1}
D_{DF}	Defoliated leaf area (due to senescence)	cm² plant^{-1}
Derived variable		
y	Disease severity $Y/(H+Y)$	proportion
Parameters		
H_0	Initial host size	cm² plant^{-1}
H_{max}	Maximum leaf area	cm² plant^{-1}
Y_0	Initial diseased area at time $t_{INOC} + IP$	cm² plant^{-1}
r_{LIN}	Linear rate parameter for initial disease increase	cm² day^{-1}
r_Y	Logistic rate parameter for disease increase	day^{-1}
r_H	Logistic rate parameter for host growth	day^{-1}
r_S	Physiological senescence rate	day^{-1}
r_D	Defoliation rate	day^{-1}
f_{Hred}	Factor of the disease effect on maximum leaf area	–
f_{red}	Factor of the disease effect on host production	–
Predetermined parameters		
t_S	Time when defoliation due to senescence as well as due to the disease starts (fixed at 34)	DAS
IP	Incubation period (fixed at 5)	days
LP	Latent period (fixed at 7)	days
t_{INOC}	Time of inoculation	DAS

Basic Model

Host growth and bean rust development under disease inoculation. For bean rust epidemics, it is known (Mersha and Hau, 2008; 2011) that the disease substantially affects host growth by reducing total leaf area produced, relative to the healthy plants. Also, natural defoliation due to a physiological aging (senescence) of healthy plants begins at a certain age threshold (t_S) of the host. From non-inoculated plants of experimental data, t_S was set at 34 days after sowing (DAS). Thus, the dynamics of healthy leaf area (H) is given by the differential equation with initial condition $H(t = 0) = H_0$:

$$\frac{dH}{dt} = \begin{cases} r_H \cdot (H+Y) \cdot \left(1 - \dfrac{H+Y+D}{H_{max} \cdot (1 - f_{Hred} \cdot Y/(H+Y))}\right) - Rate_{HY} - Rate_{HD} & \text{if } t < t_{maxH} \\ -Rate_{HY} - Rate_{HD} & \text{if } t \geq t_{maxH} \end{cases} \tag{1}$$

In the first equation of H(t), the first term on the right hand side describes the increase in H over time as a function of the actual area $H + Y$ and density regulated by the total leaf area formed $H + Y + D$ (cm^2) which is limited by the maximum leaf area $H_{max} \cdot (1 - f_{Hred} \cdot Y/(H + Y))$. The factor $f_{Hred} > 0$ represents the reducing effect of disease on the maximum leaf area produced. The maximum leaf area is not constant but decreases with increasing disease severity $y = Y/(H + Y)$. When the condition $H + Y + D = H_{max} \cdot (1 - f_{Hred} \cdot Y/(H + Y))$ is achieved, healthy leaf area in the diseased case has already reached its maximum size, further growth is halted and H can only decrease due to new disease or defoliation (for $t \geq t_S$). The time when this condition is reached for the first time is named t_{maxH}.

The second term on the right hand side, $Rate_{HY}$ reflects the rate at which healthy area becomes diseased. Depending on the observation time in relation to the time t_{INOC} when artificial inoculation with *U. appendiculatus* occurred, the $Rate_{HY}$ is described by:

$$Rate_{HY} = \begin{cases} 0 & \text{if } t < t_{INOC} + IP \\ r_{LIN} & \text{if } t_{INOC} + IP \leq t < t_{INOC} + LP + IP \\ r_Y \cdot Y \cdot (1 - Y/(H+Y)) & \text{if } t \geq t_{INOC} + LP + IP \end{cases} \tag{2}$$

The first equation is based on the fact that symptoms of the disease caused by the artificial inoculation at t_{INOC} are only visible after the incubation period IP has ended, i.e. the time between the pathogen's entry and the appearance of symptoms. For bean rust, IP was set to 5 days since it is known (Stavely, 2005; Schwartz et al., 2011) that spores of *U. appendiculatus* germinate and develop within the host tissue to form small whitish spots in 5-6 days.

Under optimum conditions, the latent period LP (the time from host penetration to sporulation) was estimated for bean rust as approximately 7 days (Berger et al., 1995). During the initial phase of the disease, i.e. before the symptoms of the secondary disease cycle appear at $LP + IP$ days after inoculation, the disease increases linearly with constant disease rate r_{LIN} (cm² day^{-1}), starting from $Y(t = t_{INOC} + IP) = Y_0$. Later on ($t \geq t_{INOC} + LP + IP$), the rust epidemic would follow the ordinary pattern of a polycyclic disease given by a logistic differential equation, the change being proportional to the existing diseased area Y and the healthy leaf proportion $1 - Y/(H + Y)$ with a proportionality factor r_Y (day^{-1}). Inoculation times (t_{INOC}) were 21, 22 and 25 DAS in experiment 1, 2 and 3, respectively.

The third term on the right hand side of equation 1 $Rate_{HD}$, reflects the natural defoliation of healthy area due to physiological senescence and is proportional to the healthy leaf area (H) with a proportionality factor r_S such that:

$$Rate_{HD} = \begin{cases} 0 & \text{if } t < t_S \\ r_S \cdot H & \text{if } t \geq t_S \end{cases} \tag{3}$$

For the diseased leaf area $Y(t)$, the following differential equation can be established:

$$\frac{dY}{dt} = Rate_{HY} - Rate_{YD} \tag{4}$$

The first term on the right hand side describes the rate at which healthy area becomes diseased (equation 2), while the second term $Rate_{YD}$, reflects the defoliation due to the disease. In the model, it is assumed that defoliation due to disease starts at the same time when natural defoliation due to physiological senescence begins (at $t = t_S$). This hypothesis was

collaborated by experimental data (Mersha and Hau 2008). After t_S, the rate of defoliation of diseased area $Rate_{YD}$ is proportional to diseased leaf area (Y) with the proportionality factor r_D such that:

$$Rate_{YD} = \begin{cases} 0 & \text{if } t < t_S \\ r_D \cdot Y & \text{if } t \geq t_S \end{cases} \quad (5)$$

From equation 3 and 5, the defoliated leaf area (D) compartment which comprises the defoliation of healthy area due to senescence and defoliation due to the disease can be described as:

$$\frac{dD}{dt} = \begin{cases} 0 & \text{if } t < t_S \\ r_S \cdot H + r_D \cdot Y & \text{if } t \geq t_S \end{cases} \quad (6)$$

Disease-free situation. In the absence of disease ($Y = 0$), the dynamics of the host which is now described by only the healthy and defoliated compartments is given by:

$$\frac{dH_{DF}}{dt} = r_H \cdot H_{DF} \cdot \left(1 - \frac{H_{DF} + D_{DF}}{H_{max}}\right) - \frac{dD_{DF}}{dt} \quad (7)$$

$$\frac{dD_{DF}}{dt} = \begin{cases} 0 & \text{if } t < t_S \\ r_S \cdot H_{DF} & \text{if } t \geq t_S \end{cases} \quad (8)$$

The index DF in this paper refers to disease-free situation. The first term on the right hand side of equation 7 describes the logistic increase of the healthy host area which is equivalent to the total host area (for $t < t_S$), while the second term reflects the natural defoliation due to physiological senescence. The production of new tissue is density regulated by the total host leaf area formed $H_{DF} + D_{DF}$ (cm^2) which is limited by H_{max} (cm²). Natural defoliation of host area in disease free situation D_{DF} (equation 8) increases in proportion to H_{DF} with a proportionality factor r_S. In this model, like in those of Savary et al. (1997) and Barnwal et al. (2013), the rate of natural defoliation r_S is assumed to be identical in both diseased and disease-free situations.

Modified model: Negative effect of the disease on host production

According to equation 1 (basic model), the negative effect of the disease on the host is reflected through the reduction in the maximum leaf area produced. Moreover, the increase in healthy leaf area is essentially proportional to the actual host area $H + Y$. As a modification, it could be assumed that the disease also affects the production of new healthy area such that the increase is now only proportional to the healthy area H like in the model of Jeger (1986). Thus, equation 1 can be replaced by:

$$\frac{dH}{dt} = \begin{cases} r_H \cdot H \cdot \left(1 - \dfrac{H + Y + D}{H_{max} \cdot \left(1 - f_{Hred} \cdot Y/(H + Y)\right)}\right) - Rate_{HY} - Rate_{HD} & \text{if } t < t_{maxH} \\ -Rate_{HY} - Rate_{HD} & \text{if } t \geq t_{maxH} \end{cases} \qquad (9)$$

Furthermore, other possibilities exist through which bean rust disease negatively affects host production. For instance, diseased area may contribute to host production but less than the healthy area or the extreme case where the disease has a strong negative effect beyond the visible diseased area (visual lesions) so that the surrounding healthy leaf area is also negatively affected (Bastiaan, 1991; Bassanezi et al., 2001). This feature can be examined by the following differential equations for host growth:

$$\frac{dH}{dt} = \begin{cases} Rate_{HH} - Rate_{HY} - Rate_{HD} & \text{if } t < t_{maxH} \\ -Rate_{HY} - Rate_{HD} & \text{if } t \geq t_{maxH} \end{cases} \qquad (10)$$

Where $Rate_{HH} = \left(r_H \cdot H + r_H \cdot (1 - f_{red}) \cdot Y\right) \cdot \left(1 - \dfrac{H + Y + D}{H_{max} \cdot \left(1 - f_{Hred} \cdot Y/(H + Y)\right)}\right)$

The factor f_{red} represents the reducing effect of disease on host healthy leaf area production. Equations 1 and 9 are special cases of equation 10 when $f_{red} = 0.0$ and 1.0 respectively.

Model evaluation and statistics

All models were built using ModelMaker version 4.0. (Oxford, UK) using the Runge-Kutta 4th order integration algorithm. Parameters were optimized using the Marquardt method by fitting the differential equations 1, 4, 6, 7 and 8 (basic model) and equations 4, 6, 7, 8 and 9 or 10 (modified model) to the data of the disease-free and diseased situation. Specifically, the host growth rate r_H, the rate of natural defoliation r_S and the maximum host area H_{max} were estimated in disease and disease-free situations simultaneously.

The goodness-of-fit of the models was analyzed by examining the weighted sum of squares of the residual, coefficient of determination R^2 as well as the biological plausibility of parameter estimates. In particular, the variance ratio or F-Value which takes into account not only the goodness of fit but also the number of parameters in the model was used to verify whether the modified model (with additional parameters) gave a significantly better fit to the data when compared to the basic model. The higher the F-Value the less likely it is that the model explained the variation by chance (ModelMaker 4.0. Oxford, UK). The goodness-of-fit statistics were generated by default procedures in the software package.

RESULTS

Basic Model

Simulations of healthy H, diseased Y and defoliated D leaf areas in the disease situation, and healthy H_{DF} and naturally defoliated D_{DF} leaf areas in the disease-free situation were considerably consistent with experimental observations as shown in figure 1. The model thus offered a satisfactory description of the dynamic interaction between the bean rust epidemic and host growth. In all the three experiments, leaf areas changed dynamically depending on host growth, influence of the disease epidemics, and defoliation (natural defoliation or defoliation due to disease).

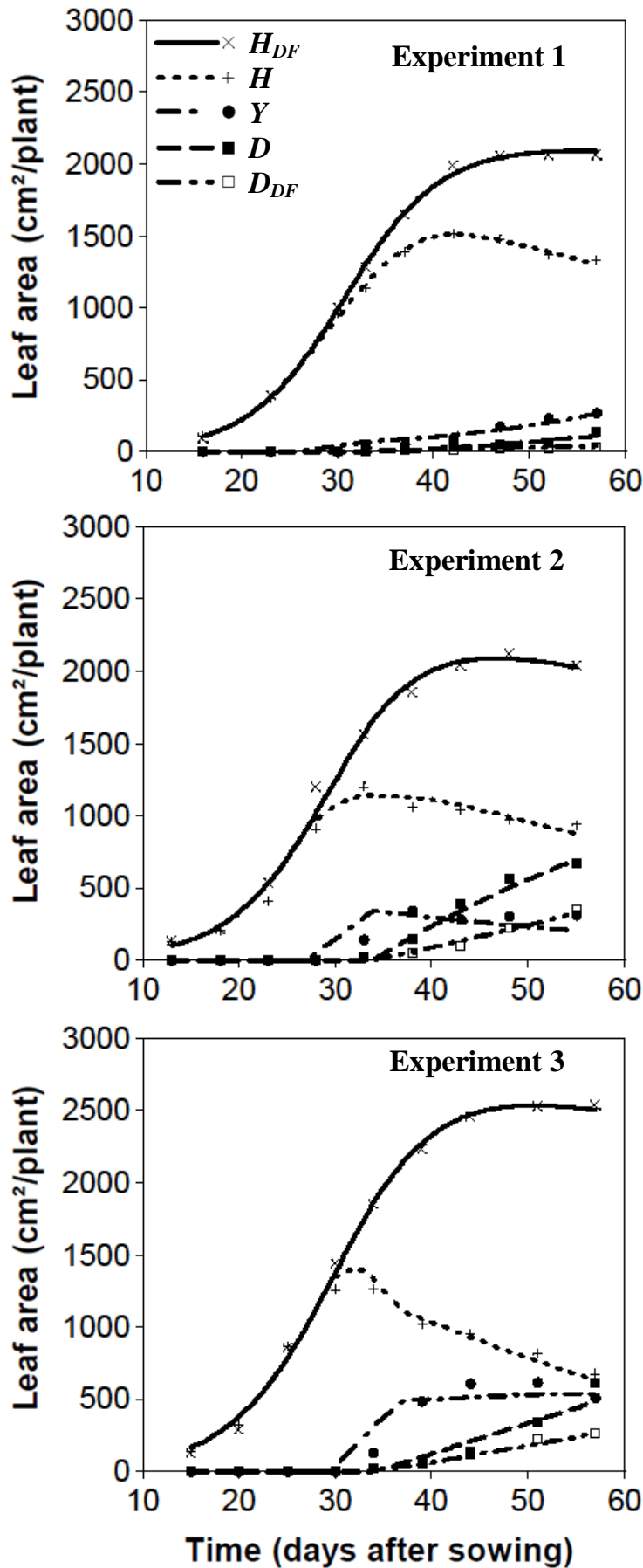**Figure 1.** Progress curves of healthy (H_{DF}) and naturally defoliated (D_{DF}) leaf area in the disease-free situation, and healthy (H), diseased (Y), and defoliated (D) leaf area of bean (*Phaseolus vulgaris*) as influenced by bean rust (*Uromyces appendiculatus*) epidemics during experiments 1, 2, and 3, observed (dots) and simulated (lines) with the **basic model** (equations 1, 4, 6, 7 and 8).

Estimates of parameter values and coefficients of determination obtained from model fitting to experimental data are presented in Table 2. High R^2 values of 0.9993, 0.9933 and 0.9952 computed for experiment 1, 2 and 3, respectively, showed a reasonably good fit of the model to the observations.

Host growth. In the disease-free situation, healthy leaf area H_{DF} increased progressively but does not attain its maximum area at H_{max} (cm^2) due to natural defoliation at $t \geq t_S$. In fact H_{DF} (cm^2) reaches only a proportion of 0.9775 (experiment 1), 0.8810 (experiment 2) and 0.9086 (experiment 3) of H_{max} on day 57, 47 and 50 after sowing, respectively, after which H_{DF} decreases gradually as a consequence of natural defoliation D_{DF}. However, this decline is hardly noticeable from the curves (Figure 1) especially in experiment 1 where the decline is only discernible much later ($t \geq 62$ DAS) due to the relatively low level of natural defoliation (figure not shown). Simulations of D_{DF} showed that it was much more pronounced in the controlled climate chambers (experiments 2 and 3) than in the greenhouse (experiment 1) accounting for 14.9 and 9.4 % of the total host production in experiment 2 and 3 compared to only 1.2% in experiment 1 at 57 DAS (Figure 1).

In the disease situation, there was a clear divergence of healthy area relative to the disease-free situation generally a few days after inoculation (6 to 9 days) and onwards (Figure 1). Healthy leaf area declined progressively in experiments 2 and 3 with increase in diseased area after $t \geq t_{INOC} + IP$ and accelerated loss of diseased tissues through disease-induced defoliation after $t \geq t_S$ in contrast to experiment 1 where healthy area continues to increase and attains a proportion of 0.9086 of its total production given by $H + Y + D$ at 42 DAS beyond which it gradually decreases. Simulated host area defoliated due to disease (D) was clearly low in experiment 1 in comparison to experiments 2 and 3 which showed substantial effects of the disease through defoliation (Figure 1).

The estimates of the maximum amount of leaf area produced H_{max}, were moderately identical in all the three experiments (Table 2). The parameter f_{Hred} (the reducing effect of disease on the maximum leaf area produced) was estimated as 2.862, 1.250 and 2.238 in experiment 1, 2 and 3, respectively. From the significance of the f_{Hred} values, it is apparent that the bean rust epidemics significantly lowered the H_{max} of diseased plants when compared to the disease-free situation. Infact, in the diseased situation, the total production given by $H + Y + D$ levels off at a much lower value, i.e. reaching only a proportion of 0.7668 (experiment 1), 0.7493 (experiment 2) to 0.5901 (experiment 3) of H_{max} on day 57 after sowing. Even when the simulation time is extended to 100 DAS, the proportion slightly increases to 0.7634 for only experiment 2 while the rest remain the same as before.

TABLE 2. Estimated parameter values and coefficients of determination (R^2) of the **basic model** (equations 1, 4, 6, 7 and 8) simulating epidemics of bean rust (*Uromyces appendiculatus*) on bean (*Phaseolus vulgaris*) and the dynamics of host growth of bean plants with and without inoculation of *U. appendiculatus* (see Table 1 for explanation of acronyms).

Expt[a]	Estimated parameter values									F	R^2
	H_0	r_H	r_S	f_{Hred}	H_{max}	Y_0	r_{LIN}	r_Y	r_D		
1	104.9	0.200	0.0008	2.862	2144.0	0.6	9.1	0.089	0.024	7711.2	0.9993
	(6.3)[b]	(0.005)	(0.0003)	(0.325)	(17.7)	(16.8)	(2.9)	(0.008)	(0.006)		
2	94.9	0.192	0.0076	1.250	2370.7	0.1	48.9	0.088	0.095	837.5	0.9933
	(13.3)	(0.010)	(0.0009)	(0.176)	(54.5)	(44.3)	(8.6)	(0.012)	(0.011)		
3	163.1	0.183	0.0047	2.238	2786.7	29.7	70.4	0.062	0.033	1163.7	0.9952
	(16.5)	(0.008)	(0.0007)	(0.511)	(53.9)	(37.3)	(8.2)	(0.009)	(0.004)		

[a]Experiment

[b]Standard errors of the parameter estimates are given in parentheses

The rate parameter for host growth r_H was closely identical (0.200, 0.192 and 0.183 per day) in the three experiments. Estimates of the rate of natural defoliation due to physiological senescence r_S were also within close range (0.0076 and 0.0047 per day) for experiments 2 and

3 (controlled climate chamber experimnents), but which were six to ten times higher than that of the greenhouse experiment 1 (Table 2). Estimates of the rate of disease-induced defoliation, r_D were moderately identical, 0.024 and 0.033 per day in experiment 1 and 3 in comparison to 0.095 per day in experiment 2.

Disease dynamics. Simulations of the temporal progression of bean rust severity measured in terms of actual lesion proportion are presented in figure 2 for all the experiments. In experiments 1 and 3 where $r_Y > r_D$ (Table 2), the simulated disease progress curves increase monotonously towards their maximum capacity of 1 in contrast to experiment 2 with the condition $r_D > r_Y$ where the curve subsequently decreases gradually after reaching a maximum at $y = 0.23$ (Figure 2).

Estimates of the initial diseased area Y_0 (cm² plant^{-1}) were in all experiments not significantly different from 0. For the initial disease rate r_{LIN}, high values of 9.1, 48.9, and 70.4 cm² per day were estimated for experiment 1, 2 and 3, respectively, due to the strong inoculum pressure within the early cycle of the bean rust epidemic ($t_{INOC} + IP \leq t < t_{INOC} + LP + IP$). Considering that the amount of host area at inoculation time was lower in experiment 1 ($t_{INOC} = 21$ DAS), than in 2 and 3 ($t_{INOC} = 22$ and 25 DAS) coupled together with the less severe bean rust epidemic during experiment 1, it is not unexpected that the rate r_{LIN} was also much lower compared to the two other experiments. The estimated logistic rate parameter for disease increase r_Y was closely identical (0.089 and 0.088 day^{-1}) in experiment 1 and 2 when compared to 0.062 day^{-1} in experiment 3.
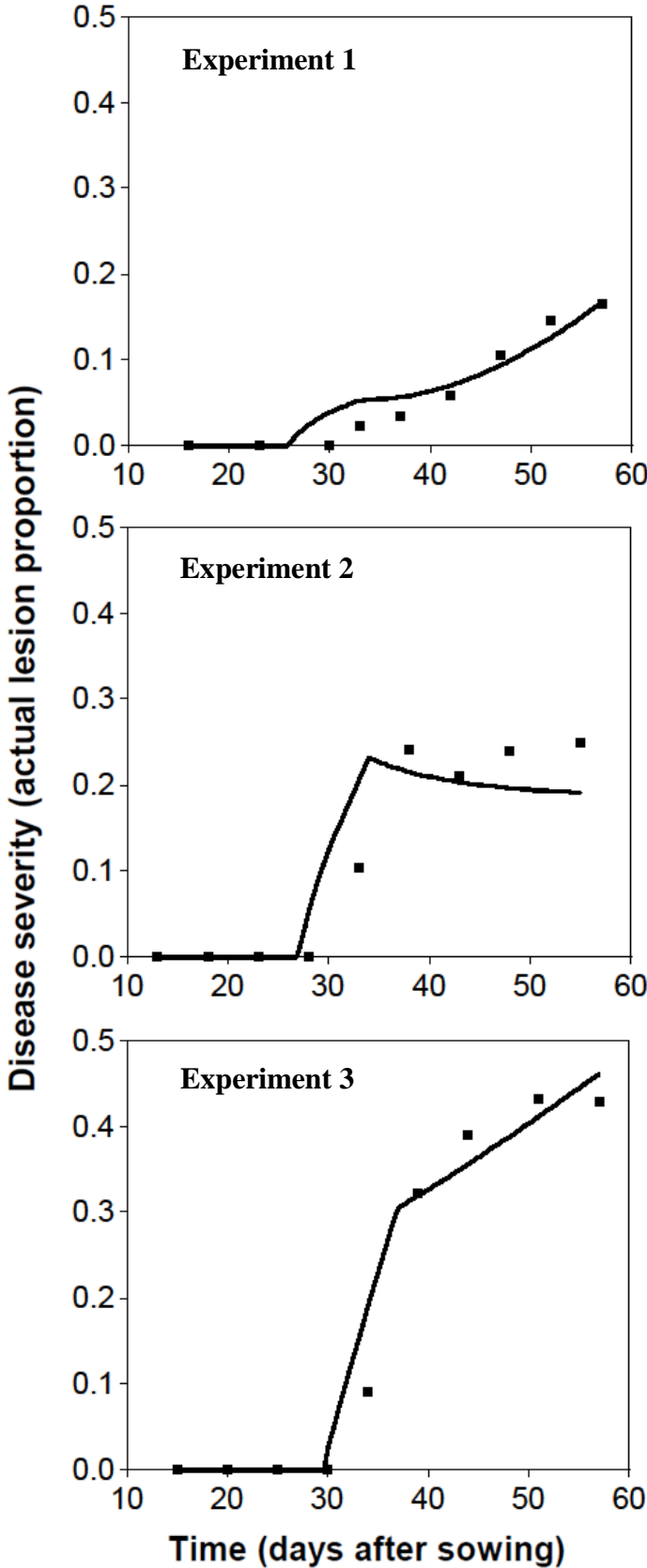
Figure 2. Progress curves of bean rust (*Uromyces appendiculatus*) severity on bean (*Phaseolus vulgaris*) during experiments 1, 2 and 3, observed (dots) and simulated (lines) with the **basic model** (equations 1, 4, 6, 7 and 8).

Modified model

In the modified model (equations 4, 6, 7, 8 and 9) it was at first assumed that host production is only proportional to the healthy area H and not to $H + Y$ (basic model). Except for slight changes especially in f_{Hred} and r_Y, the estimated parameter values (Table 3) are closely identical to those of the basic model (Table 2). Also, there were hardly any visible differences in the dynamics of the different leaf areas as well as the disease progress curves compared to those of the basic model (Figure 1) and are therefore not shown. The goodness of fit, expressed in R^2, was only slightly higher than in the basic model for experiment 2 (Table 3). Moreover, the F-values calculated for this modified model (8267.3, 858.1 and 1167.0 for experiments 1, 2 and 3, respectively) were comparatively higher than those of the basic model (7711.2, 837.5 and 1163.7). This implies that this modified model gives a significantly better fit to the experimental data than the basic model.

TABLE 3. Estimated parameter values and coefficients of determination (R^2) of the **modified model** (equations 4, 6, 7, 8 and 9) simulating epidemics of bean rust (*Uromyces appendiculatus*) on bean (*Phaseolus vulgaris*) and the dynamics of host growth of bean plants with and without inoculation of *U. appendiculatus*. The hypothesis of the modification is that host production of new healthy area is proportional to the healthy area only (see Table 1 for explanation of acronyms).

Expt[a]	Estimated parameter values									F	R^2
	H_0	r_H	r_S	f_{Hred}	H_{max}	Y_0	r_{LIN}	r_Y	r_D		
1	104.4 (6.1)[b]	0.201 (0.004)	0.0008 (0.0003)	2.765 (0.312)	2142.3 (17.1)	0.5 (13.9)	8.8 (2.7)	0.092 (0.008)	0.024 (0.005)	8267.3	0.9993
2	94.8 (13.2)	0.192 (0.010)	0.0076 (0.0009)	1.097 (0.180)	2367.0 (53.7)	0.1 (41.7)	47.3 (8.3)	0.095 (0.012)	0.094 (0.011)	858.1	0.9935
3	164.0 (16.4)	0.182 (0.008)	0.0047 (0.0007)	1.901 (0.439)	2789.9 (54.2)	35.0 (36.8)	70.4 (8.3)	0.062 (0.009)	0.033 (0.004)	1167.0	0.9952

[a]Experiment

[b]Standard errors of the parameter estimates are given in parentheses

When the equation 1 for $H(t)$ in the basic model is replaced by equation 10 (with a variable factor f_{red} for the reducing effect of disease on the host production), the parameter estimates of f_{Hred} are lower than in the basic model in the three experiments (Table 4), while changes in the other parameters vary within the experiments. The estimated values of f_{red} were closely identical, 3.3 and 3.6 in experiment 1 and 2 , respectively, in comparison to 2.8 in experiment 3 that is however not significantly different from 0.

TABLE 4. Estimated parameter values and coefficients of determination (R^2) of the **modified model** (equations 4, 6, 7, 8 and 10) simulating epidemics of bean rust (*Uromyces appendiculatus*) on bean (*Phaseolus vulgaris*) and the dynamics of host growth of bean plants with and without inoculation of *U. appendiculatus* . The hypothesis of the modification is that bean rust has a strong negative effect on host production beyond the diseased area (see Table 1 for explanation of acronyms).

Expt[a]	Estimated parameter values										F	R^2
	H_0	r_H	r_S	f_{red}	f_{Hred}	H_{max}	Y_0	r_{LIN}	r_Y	r_D		
1	104.1 (6.0)[b]	0.203 (0.004)	0.0008 (0.0003)	3.3 (2.2)	2.7 (0.4)	2137.2 (16.5)	0.002 (7.0)	7.5 (1.2)	0.103 (0.011)	0.027 (0.006)	7707.2	0.9994
2	93.5 (12.7)	0.194 (0.010)	0.0077 (0.0011)	3.6 (1.7)	0.1 (2.6)	2366.6 (51.8)	0.022 (34.2)	38.9 (7.5)	0.117 (0.026)	0.099 (0.010)	818.1	0.9941
3	164.7 (16.5)	0.182 (0.008)	0.0047 (0.0007)	2.8 (4.4)	1.3 (1.7)	2792.8 (54.4)	34.743 (38.7)	70.8 (8.3)	0.062 (0.009)	0.033 (0.004)	1038.1	0.9953

[a]Experiment

[b]Standard errors of the parameter estimates are given in parentheses

Due to the additional parameter, the goodness of fit, expressed in R^2, was higher than in the basic model and modified model (using equation 9) for all the experiments (Table 4). However, the F-values calculated for this modification (7707.3, 818.1 and 1038.1 for experiments 1, 2 and 3) were lower than those of the basic model (Table 2) in all the three experiments. Consequently, it was concluded that this modification with an additional

variable factor f_{red} for the reducing effect of disease on the host production (equation 10) does not give a significantly better fit to the experimental data when compared to the basic model. Moreover, graphical examinations of the observed and simulated curves describing the dynamics of the different leaf areas as well as the disease progress curves showed hardly any visible differences when compared to those of the basic model (Figure 1) and are therefore not shown.

DISCUSSION

In this work, an improved model for the interaction of rust epidemics (caused by *Uromyces appendiculatus*) and bean growth dynamics was developed. The model allowed changes over time in the healthy, diseased (rust affected) and defoliated leaf areas of a diseased plant to be simulated and compared to that of a disease-free situation. In this modeling approach like in the models of Savary et al. (1997) and Calonnec et al. (2008), host and disease dynamics were described by a system of differential equations and to some extent were analogous to the H-L-I-R (Healthy-Latent-Infectious-Removed) approach followed in the epidemic models of Segarra et al. (2001) and Madden et al. (2007).

The unit adopted for the host and disease dynamics is the leaf area expressed in cm^2. The relative importance of leaf area and more specifically healthy leaf area duration (HAD) or healthy leaf area absorption (HAA) as a major determinant of crop growth and predictor of yeild has been highlighted among others by Waggoner and Berger (1987), Bergamin Filho et al. (1997) and Lopes and Berger (2001). Furthermore, as an obligate biotrophic fungus, *U. appendiculatus* cannot live independently of its host but it entirely depends upon availability of a susceptible host tissue for continued infection and disease development (Liebenberg and Pretorius, 2010).

In the absence of disease, the healthy host area and the total host area are equivalent like in the models of Madden et al. (2007), and will increase initially according to the logistic

growth function with a maximum capacity H_{max}. In this, our model differs from the model of Berger et al. (1995) in which host production is considered in terms of daily increment in leaf cohorts described by a modified Weibull function. Also, the contribution of natural defoliation due to leaf senescence is often neglected in modeling or is assumed to be negligible compared to disease-induced defoliation like in the model of Allorent and Savary (2005). However, it is evident from the simulations of healthy leaf area H_{DF} in our model that as a consequence of natural defoliation D_{DF}, the healthy host may only reach proportions ranging from as low as 0.8810 to 0.9775 of its H_{max}.

One of the advantages of the model developed in this study over other existing models is that the total leaf area formed as well as the defoliated leaf area (in both disease-free and diseased situations) do not increase continuously without any limitation like in the models of Jeger (1986), Waggoner (1986) and Madden et al. (2007). The production of new healthy area is density regulated by the total host area formed ($H_{DF} + D_{DF}$) in the disease-free situation and ($H + Y + D$) in the diseased case and which are also limited by their respective maximum capacities, i.e. H_{max} (disease-free) and $H_{max} \cdot (1 - f_{Hred} \cdot Y/(H + Y))$ in the presence of disease.

The main assumption in the disease situation is that the rust epidemic affects host production in such a way that the dynamics of maximum host area formed is significantly reduced in a disease situation compared to the disease-free situation. The significance of this negative disease effect on the host's maximum capacity was confirmed by the significance of the factor f_{Hred} for the reducing effect of disease on the maximum leaf area produced with estimated values ranging from 1.25 to 2.86. Moreover, the total host production in the diseased situation (given by $H + Y + D$) could only attain proportions that ranged from 0.5901 to 0.7668 of H_{max} at 57 DAS. This implies that the bean rust epidemics reduced the maximum host area by between 23 to 40%. Thus, the simulation results of this study are in agreement with that of Mersha and Hau (2011) where maximum host area of bean plants artificially inoculated with *U. appendiculatus* was reduced by up to 38%. In contrast, the epidemics of

powdery mildew (*Oidium neolycopersici*) and early blight (*Alternaria solani*) on tomato do not affect the total biomass production (Chelal and Hau, 2012; Al Masri, 2012) such that the dynamics of total host area formed can be assumed to be identical without and with the disease.

It is known that some foliar diseases such as *Cercospora arachidicola* on peanut (*Arachis hypogaea* L.) and *Colletotrichum lindemuthianum* (Sacc. and Magn.) on common bean affect plant growth by inducing or accelerating defoliation of leaves (Ketring and Melouk, 1982; Boote et al., 1983; Pastor-Corrales and Tu, 1989; Mohammed, 2013). Specifically for bean rust, it has been shown that severe infection causes leaves to turn chlorotic, dry up and fall prematurely (Duniway and Durbin, 1971; Mersha and Hau, 2008; Liebenberg and Pretorius, 2010; Schwartz et al., 2011). From the results of r_D and r_S, it is apparent that defoliation in the presence of rust could be enhanced by more than 7 times compared to the disease-free case.

While in the basic model like in the model of Waggoner (1986), the production of new healthy area in the disease situation is proportional to the actual area $H + Y$, in the modified model (using equation 9) it was assumed that only the healthy area H give rise to new host area. Jeger (1986) and Madden et al. (2007) have used a similar approach in their models. With this modification of the basic model, the goodness-or-fit and the calculated the F-values were higher than in the basic model implying that only healthy area contributes to newly formed leaf area. A similar effect was simulated in some instances for powdery mildew (*Oidium neolycopersici* Kiss.) on tomato (Chelal and Hau, unpublished).

Given that diseased area may contribute to host production but less than the healthy area or negatively affect the surrounding healthy leaf area, this effect was examined as a further modification of the basic model with a variable factor f_{red} (equation 10) for the reducing effect of disease on the host production. The f_{red} values of 3.3, 3.6 and 2.8 that were obtained indicate that the bean rust disease may affect the production of the remaining healthy area. The goodness-of-fit was better than in the basic and modified model (equation 9). However,

the calculated F-values for this modified model were lower than in the basic and modified model (equation 9).

The virtual lesion concept as proposed by Bastiaans (1991) has been extensively used to account for the disease effects on the photosynthetic activity of the apparently healthy leaf area around the visual lesion (i.e. leaf area with visible disease symptoms), where photosynthesis is considered to be zero (Rabbinge et al., 1985; Jesus Junior, 2001; Lopes and Berger, 2001; Robert et al., 2004). The relationship between disease severity and photosynthesis is described by the parameter, β whose value indicate whether the disease effect is lower ($\beta < 1$), equal to ($\beta = 1$), or higher ($\beta > 1$) than that accounted for by the visual lesion. For bean rust (*U. appendiculatus*), contrasting β values have been obtained with Lopes and Berger (2001) determining β values near to 1 which meant minimal effect of the disease on the surrounding healthy leaf area while Jesus Junior (2001) reported a $\beta = 2$.

In conclusion, information obtained from the model developed in this study could be used to bridge some of the knowledge gaps that exist concerning the dynamics of the bean rust epidemic and its impact on bean growth as well act as a basis for the development and implementation of integrated disease management strategies. For instance, breeding programs can benefit from knowledge gained from the dynamics of defoliation and its effects on the epidemic progress (Allorent and Savary, 2005). High defoliation rates of diseased area would perhaps prevent inoculum build up within the plant canopy. Of course, striking a balance between duration of healthy area, disease progress and yield components would be essential to the success of such a strategy.

LITERATURE CITED

Allorent D and Savary S (2005) Epidemiological characteristics of angular leaf spot of bean: a systems analysis. European Journal of Plant Pathology 113: 329-341.

Allorent D, Willocquet L, Sartorato A and Savary S (2005) Quantifying and modelling the mobilisation of inoculum from diseased leaves and infected defoliated tissues in epidemics of angular leaf spot of bean. European Journal of Plant Pathology 113: 377-394.

Al Masri A (2012) Epidemiological investigations on the interactions between early blight (*Alternaria solani*) progression and host dynamics of tomato (*Solanum lycopersicum* L.). MSc. Thesis. Leibniz Universität Hannover, Germany.

Amorim L, Berger RD, Bergamin Filho A, Hau B, Weber GE, Bacchi LMA, Vale FXR, Silva MB (1995) A simulation model to describe epidemics of rust of *Phaseolus* beans. II. Validation. Phytopathology 85: 722-727.

Barnwal MK, Kotasthane A, Magculia N, Mukherjee PK, Savary S, Sharma AK, Singh HB, Singh US, Sparks AH, Variar M and Zaidi N (2013) A review on crop losses, epidemiology and disease management of rice brown spot to identify research priorities and knowledge gaps. European Journal of Plant Pathology 136: 443-457.

Bassanezi BR, Amorim L, Bergamin Filho A, Hau B, Berger RD (2001) Accounting for photosynthetic efficiency of bean leaves with rust, angular leaf spot and anthracnose to assess crop damage. Plant Pathology 50: 443-52.

Bastiaans L (1991) Ratio between virtual and visual lesion size as a measure to describe reduction in leaf photosynthesis of rice due to leaf blast. Phytopathology 81: 611–615

Bergamin Filho A, Carneiro SMTPG, Godoy CV, Amorim L, Berger RD, and Hau B (1997) Angular leaf spot of *Phaseolus* beans: Relationships between disease, healthy leaf area, and yield. Phytopathology 87: 506-515.

Berger RD, Hau B, Weber GE, Bacchi LMA, Bergamin Filho A, and Amorim L (1995) A simulation model to describe epidemics of rust of *Phaseolus* beans. I: Development of the model and sensitivity analysis. Phytopathology 85: 715-721.

Boote KJ, Jones JW, Mishoe JW and Berger RD (1983) Coupling pests to crop growth simulators to predict yield reductions. Phytopathology 73: 1581-1587.

Burie JB, Calonnec A, Langlais M and Mammeri Y (2012) Modeling the spread of a pathogen over a spatially heterogeneous growing crop. Paper presented at the 2012 IEEE 4th International Symposium on Plant Growth Modeling, Simulation, Visualization and Applications (PMA), Shanghai, China.

Calonnec A, Cartolaro P, Naulin JM, Bailey D, Langlais M (2008) A host–pathogen simulation model: powdery mildew of grapevine. Plant Patholology 57: 493-508.

Chelal J and Hau B (2012) Temporal dynamics of powdery mildew and its relationship to host growth, defoliation and yield of tomato. Proceedings of the 58th German Plant Protection Conference. 10 to 14th September 2012. Braunschweig, Germany, pp. 105. Available at: http://pub.jki.bund.de/index.php/JKA/article/view/1923/2299.

Duniway JM and Durbin RD (1971) Some effects of *Uromyces phaseoli* on the transpiration rate and stomatal response of bean leaves. Phytopathology 61:114-119.

Ferrandino FJ (2008) Effect of crop growth and canopy filtration on the dynamics of plant disease epidemics spread by aerially dispersed spores. Phytopathology 98: 492-503.

French RC, Nester SE and Stavely JR (1993) Stimulation of germination of teliospores of *Uromyces appendiculatus* by volatile aroma compounds. Journal of Agricultural and Food Chemistry 41: 1743-1747.

Godoy CV, Carneiro SMTBG, Iamauti MT, Amorim L, Berger RD, Bergamin Filho A (1997) Diagrammatic scales for bean diseases: development and validation. Zeitschrift für Pflanzenkrankheiten und Pflanzenschutz 104: 336-45.

Habtu A and Zadoks JC (1994) Crop growth, disease and yield components of rusted *Phaseolus* beans in Ethiopia. Journal of Phytopathology 143: 391-401.

Hau B (1990) Analytic models of plant disease in a changing environment. Annual Review of Phytopathology 28: 221-245.

Imhoff MW, Main CE and Leonard KJ (1981) Effect of temperature, dew period and age of leaves, spores and source pustules on germination of bean rust urediospores. Phytopathology 71: 577-583.

Jeger MJ (1986) The potential of analytic compared with simulation approaches to modeling in plant disease epidemiology. In: Leonard KJ and Fry WE (eds) Plant Disease Epidemiology. Population Dynamics and Management (pp 255-281), MacMillan, New York.

Jesus Junior WC, Vale FXR, Coelho RR, Hau B, Zambolim L, Costa LC and Bergamin Filho A (2001) Effects of angular leaf spot and rust on yield loss of *Phaseolus vulgaris*. Phytopathology 91: 1045-1053

Kranz J and Jörg E (1989) The synecological approach in plant disease epidemiology. Review of Tropical Plant Pathology 6: 27-38.

Liebenberg MM and Pretorius ZA (2010) Common Bean Rust: Pathology and Control. Horticultural Reviews 37: 1-99.

Liebenberg MM, Mienie CMS and Pretorius AZ (2006) The occurrence of rust resistance gene *Ur-13* in common bean cultivars and lines. Euphytica 150: 365-386.

Lindgren DT, Escridge KM, Steadman JR, Schaaf DM (1995) A model for dry bean yield loss due to rust. HortTechnology 5: 35-37.

Lopes DB (1999) Photosynthetic Competence of Bean Leaves with Rust and Anthracnose. Gainesville, University of Florida, PhD thesis.

Lopes DB and Berger RD (2001) The effects of rust and anthracnose on the photosynthetic competence of diseased bean leaves. Phytopathology 91: 212-220.

Madden LV, Hughes G, and van den Bosch F (2007) The Study of Plant Disease Epidemics. APS, St. Paul.

Mendes BMJ and Bergamin Filho A (1989) Influence of temperature, wetness duration, and leaf type on the quantification of monocyclic parameters of bean rust. Journal of Phytopathology 126: 183-189.

Mersha Z and Hau B (2008) Effects of bean rust (*Uromyces appendiculatus*) epidemics on host dynamics of common bean (*Phaseolus vulgaris*). Plant Pathology 57: 674-686.

Mersha Z and Hau B (2011) Reciprocal effects of host and disease dynamics in the bean rust pathosystems. Journal of Plant Diseases and Protection 118: 54-62.

Mohammed A (2013) An Overview of Distribution, Biology and the Management of Common Bean Anthracnose. Journal of Plant Pathology and Microbiology 4: 193 doi:10.4172/2157-7471.1000193

Newton AC, Gibson G, and Cox D (1995) Understanding plant disease epidemics through mathematical modelling. Scottish Crop Research Institute Annual Report for 1994: 124-127.

Panggaa IB, Hananb J and Chakrabortyc S (2011) Pathogen dynamics in a crop canopy and their evolution under changing climate. Plant Pathology 60: 70-81.

Pastor-Corrales MA and Tu JC (1989) Anthracnose In: Schwartz HF and Pastor-Corrales MA (eds.) Bean Production Problems in the Tropics (pp. 77-104), Centro Internacional de Agricultura Tropical Press, Cali Colombia.

Rabbinge, R., Jorritsma, I. T. M. and Schans, J. 1985. Damage components of powdery mildew in winter wheat. Netherlands Journal of Plant Pathology 91: 235-247.

Robert C, Bancal MO, Nicolas P, Lannou C, Ney B (2004) Analysis and modelling effects of leaf rust and *Septoria tritici* blotch on wheat growth. Journal of Experimental Botany 55: 1079-1094.

Savary S, Willocquet L and Teng PS (1997) Modelling sheath blight epidemics on rice tillers. Agricultural Systems 55: 359-384.

Schwartz HF, Steadman JR and Harveson RM (2011) Rust of Dry Beans. Fort Collins, CO, USA: Colorado State University: Cooperative Extension Fact Sheet No. 2.936 Available: http://www.ext.colostate.edu.

Segarra J, Jeger MJ and van den Bosch F (2001) Epidemic dynamics and patterns of plant diseases. Phytopathology 91: 1001-1010.

Souza TLPO, Alzate-Marin AL, Faleiro FG, Barros EG (2008) Pathosystem common bean– *Uromyces appendiculatus*: host resistance, pathogen specialization, and breeding for rust resistance. Pest Technology 2: 56-69.

Souza TLPO, Faleiro FG, Dessaune SN, Paula-Junior TJ, Moreira MA and Barros EG (2013) Breeding for common bean (*Phaseolus vulgaris* L.) rust resistance in Brazil. Tropical Plant Pathology 38: 361-374 .

Stavely JR (2005) Rust. In: Schwartz HF, Steadman JR, Hall R and Forster RL (eds.) Compendium of Bean Diseases (pp 38-39) 2nd edition, APS Press, St. Paul.

Stavely JR and Pastor-Corrales MA (1989) Rust. In: Schwartz HF and Pastor-Corrales MA (eds.) Bean Production Problems in the Tropics (pp. 159-194) Centro Internacional de Agricultura Tropical Press, Cali Colombia.

Van der Plank JE (1963) Plant Diseases: Epidemics and Control. Academic Press, New York.

Waggoner PE (1986) Progress curves of foliar diseases: Their interpretation and use. In: Leonard KJ and Fry WE (eds) Plant Disease Epidemiology. Population Dynamics and Management (pp 3-37), MacMillan, New York.

Xu X (2006) Modelling and interpreting disease progress in time. In: Cooke BM, Gareth Jones D and Kaye B (eds.) The Epidemiology of Plant Diseases (pp. 215-238) 2nd edition, Springer, Dordrecht, The Netherlands.

GENERAL DISCUSSION

It is reasonable to expect that a disease that lowers the photosynthetic area of plants often translates to smaller growth and yield of these plants (Agrios, 2005). Foliar plant diseases in particular reduce leaf photosynthetic activity by either decreasing photosynthetically active radiation intercepted on the plant surface through the necrotic lesions themselves or by reducing the green (healthy) leaf area of plants through leaf tissue destruction and defoliation (Boote et al., 1983; Waggoner and Berger, 1987; Robert et al., 2004; Robert et al., 2006).

Conversely, during the course of an epidemic, the host is rarely static but comprises growth of new tissue and/or loss of old tissue as a result of natural senescence or disease-induced defoliation. The changing size and characteristics of a growing host have substantial implications on epidemic progression (Ferrandino, 2008), for instance a decreasing disease progress curve resulting from either an increase in susceptible tissue (dilution effect) or by the loss of diseased tissue through defoliation (thinning-out effect). Also, it should be considered that the amount of host tissue available influences the probability of spores landing on the host plant (Hau, 1990; Calonnec et al., 2008).

In the absence of disease, the assumption is usually taken for most annual crops that the total host area and the healthy area are identical, which increase according to a logistic growth equation asymptotically approaching a maximum leaf area (Hau 1990; Madden et al., 2007; Ferrandino, 2008). Towards the end of the growing season, natural defoliation may occur as senescent leaves abcisse from the plant canopy (Ferrandino, 2008). However, in a disease situation, the dynamics of the host are usually affected either by the reduction in host growth or by the accelerated rate of leaf area loss through leaf senescence and defoliation (Waggoner, 1986; Jeger, 1986; Agrios, 2005). A classical example is the *Cercospora spp.* on peanut (*Arachis hypogae* L.) which induces and accelerates the senescence and abscission of leaves (Boote et al., 1980). Based on the aforementioned remarks, it is evident that empirical

130

quantification of the damaging effects of diseases on crop growth and the reciprocal effects of host growth on disease epidemics represent an important step towards characterizing potential damage and the coupling of these effects to crop growth simulators (Lopes, 1999).

Therefore, the first part of this study sought to address several aspects of the pathosystem tomato-powdery mildew in an effort to fill critical gaps in knowledge particularly on the disease effects on leaf area production, defoliation, healthy leaf area duration and yield. It is notable that despite its widespread distribution and potential impact on tomato production (Jones et al., 2001), little quantitative information has been reported for powdery mildew (*Oidium neolycopersici* Kiss.) and its effects on the host's growth dynamics.

From this study, it is apparent that in the absence of disease intervention measures, powdery mildew is capable of reaching disease severities higher than 0.53 (proportion) on a plant basis. Likewise, the final disease severity assessed on individual leaves can be as high as 0.79 and which is undoubtedly much higher than those observed in other pathosystems (Kranz, 1977). It was shown that fungicide application significantly reduced the severity of powdery mildew by two- to four fold when compared to the non-sprayed situation.

Noteworthy also were instances when the actual disease severity on a whole plant basis declined between successive assessments as a result of new healthy leaf production and/or defoliation of diseased leaves. This result also highlight one of the limitations of commonly used simple growth models (Gompertz and logistic models) which despite having a widespread application in describing temporal disease progress, ignore important aspects of plant disease epidemics such as host growth and defoliation (Campbell and Madden, 1990).

Analyses of host dynamics in terms of total leaf area showed that powdery mildew did not change the final amount of the cumulative total leaf area. However, hastened shriveling and defoliation of diseased leaves as a result of the powdery mildew epidemics significantly reduced the actual leaf area of inoculated plants especially those without fungicide

application. Similarly, the duration of healthy leaf area and yield of tomato plants were significantly reduced when inoculated with powdery mildew.

Other than providing key information that would help fill critical knowledge gaps regarding the epidemics of powdery mildew, more importantly, this information also formed the basis for the development of models coupling the dynamic interaction of tomato leaf area growth and disease progression of powdery mildew which was focused on in the subsequent chapter.

As mentioned already one of the main goals of the present study was to develop models that combine the growth dynamics of the host plant with the development of the disease epidemic in order to provide a framework within which the interactions between disease and host dynamics are described. This has been shown here for the pathosystems tomato-powdery mildew, tomato-early blight and common bean-rust. Like in the model of Kosman and Levy (1994), model development was motivated by (i) the need for biological realism of model variables and parameters, (ii) a high similarity between observed and simulated host and disease dynamics, and (iii) model simplicity.

In our models, three time periods were differentiated for the increase of the diseased area Y by new symptoms. Initially, during the incubation period IP the symptoms caused by the artificial inoculation at t_{INOC} are not visible ($t_{INOC} = 0$ for the powdery mildew model). Subsequently, it is assumed that under the strong inoculum pressure of the inoculation, the visible epidemic after the end of the incubation period increases linearly within an early phase with disease rate r_{LIN} (cm^2 day^{-1}). The linear phase is assumed to end before the symptoms of the second cycle that starts after the latent period LP appear at $LP + IP$. Later on ($t \geq t_{INOC} + LP + IP$) the epidemic follows the ordinary pattern of a polycyclic disease given by a logistic differential equation with disease rate r_Y (day^{-1}) and variable capacity $H+Y$ (cm^2). For this latter phase, a system of differential equations that describe the change of healthy H, diseased Y and defoliated leaf area D in the disease situation can be formulated as follows:

$$\frac{dH}{dt} = r_H \cdot (H+Y) \cdot \left(1 - \frac{H+Y+D}{H_{max} \cdot (1 - f_{Hred} \cdot Y/(H+Y))}\right) - r_Y \cdot Y \cdot (1 - Y/(H+Y)) - r_S \cdot H \quad (1)$$

$$\frac{dY}{dt} = r_Y \cdot Y \cdot (1 - Y/(H+Y)) - r_D \cdot Y \quad\quad (2)$$

$$\frac{dD}{dt} = r_D \cdot Y + r_S \cdot H \quad\quad (3)$$

Where r_S, r_D and r_H measured per day are the physiological senescence rate, defoliation rate, and logistic rate parameter for host growth, respectively. H_{max} represents the maximum leaf area (cm²) while the factor $f_{Hred} > 0$ represents the reducing effect of disease on the maximum leaf area produced.

By setting the conditions and defining the thresholds that are distict for each of the studied pathosytems, we can develop models that describe a wide range of foliar disease pathosystems. For instance, when the parameter $f_{Hred} = 0$ and $r_S = 0$ (since natural defoliation was not observed) in equation 1 and 3 above, the resulting set of differential equations are identical to the basic model of the tomato-powdery mildew pathosystem (chapter 1). In this case, it is assumed that only diseased area is defoliated and that defoliation is triggered once a certain level of disease severity y on a whole plant basis is reached. This defoliation threshold for y (y_{DT}) per plant was determined as 0.34 from experimental data. The time when this threshold is reached for the first time is termed t_{DT}.

For the tomato-early blight pathosystem (chapter 3), natural defoliation due to physiological senescence is considered to commence after an age threshold (t_S) of the host is reached. t_S was set at 50 days after transplanting. For $t \geq t_S$, the host has nearly reached its maximum area H_{max}, further growth is halted, and healthy leaf area from that time onwards can only decrease due to new disease or natural defoliation (for $t \geq t_S$). In this case also, like in the tomato-powdery mildew pathosystem, defoliation is triggered when the defoliation threshold for y (y_{DT}) per plant (determined as 0.20 from experimental data) is reached.

For the common bean-rust pathosystem (chapter 4), it was considered that natural defoliation of healthy area begins at t_S. From non-inoculated plants of experimental data, t_S was set at 34 days after sowing. Moreover, the disease substantially reduces the total amount of leaf area produced relative to the healthy plants. When the condition $H + Y + D = H_{max} \cdot (1 - f_{Hred} \cdot Y/(H + Y))$ is achieved, healthy leaf area in the diseased situation has already reached its maximum size, further growth is stopped and H can only decrease due to new disease or defoliation (for $t \geq t_S$). The time when this condition is reached for the first time is named t_{maxH}.

Generally, simulations of the different leaf areas, i.e. healthy, diseased and defoliated area were consistent with experimental observations, an indication that the models offered a satisfactory description of the dynamic interactions between the disease and host growth.

The models developed in this study had several advantages over other existing models. Key among them is that unlike the models of Jeger (1986), Waggoner (1986) and Madden et al. (2007) where in the disease situation the total leaf area formed as well as the total defoliated leaf area increase over time without bound, in our models, host production of new tissue is density regulated by the total host area formed which is in turn limited by its maximum capacity. Also, important mechanisms of the host-disease interactions that determine the progress of the epidemic were included. In particular, the contribution of defoliation due to disease and physiological senescence, the influence of changing environmental conditions on the disease rate, the negative effect of the disease on host production as well as the acceleration of leaf senescence due to disease were examined and quantified. Specifically for the pathosystem tomato-early blight, simulated results from our models highlighted the aspect of increased susceptibility to infection with increasing host age at disease onset. This represents an important step towards achieving a better understanding of this foliar disease of tomato.

Host plant defoliation is one of the important features that we sought to incorporate into the models developed in this study. Some of the reported consequences of disease-induced defoliation include: (i) direct effects on disease assessments, (ii) reduction in the amount of healthy tissue for infection (when healthy area is also defoliated), (iii) reduction of inoculum present within the canopy through loss of diseased leaves, (iv) microclimatic changes within the crop canopy, and (v) limited maximum disease severity (Aust and Hoyningen-Huene, 1986; Nelson and Campbell, 1993; Pandey et al., 2003; Allorent and Savary, 2005; Allorent et al., 2005).

We have successfuly demonstrated especially for tomato-early blight and powdery mildew that when the defoliation rate is much higher than the increase of diseased area, the disease severity can only increase up to a certain maximum but afterwards decreases steadily and finally approaches zero. Nelson and Campell (1993) observed in the white clover leaf spot pathosystem that defoliation accounted largely for the maintenance of relatively low levels of disease severity and incidence during leaf spot epidemics. Moreover, under high defoliation rates, the diseased area is rapidly removed so that in principle a certain amount of healthy area remains which is not diseased. It was also established for powdery mildew that defoliation of healthy area does not contribute significantly to total defoliated area so that only diseased area is essentially defoliated.

From a comparative approach, we have demonstrated that due to the bean rust epidemics, maximum host area produced is significantly reduced (by between 23 to 40%) in a disease situation compared to the disease-free situation. In contrast, the epidemics of powdery mildew and early blight on tomato showed small differences in the maximum host area formed between the diseased and non-diseased situation such that the dynamics of total host area formed can be assumed to be identical without and with the disease.

Secondly, we can conclude for the bean rust pathosystem that the production of new healthy area in the disease situation is proportional only to the healthy area (H). On the contrary, for

the pathosystem tomato-early blight and in two of three experiments of tomato-powdery mildew, host production of new healthy leaf area is proportional to the actual area ($H + Y$). This behavior for tomato-powdery mildew is not unexpected since it has been shown (Lucas, 1998; Prokopová et al., 2010) that the overall photosynthetic activity of leaves infected by powdery mildew fungi is impaired only minimally during the initial stages of infection. Progressive loss in the overall photosynthetic activity is usually noticeable in the later stages of infection as leaves senesce. For early blight blight, however, such a behavior was rather unexpected especially since host colonization is accompanied by the secretion alternaric acid, a toxin which destroys host cells and enables the pathogen to derive nutrients from the host (Langsdorf et al., 1991). The necrotic lesions which are symptomatic of early blight are considered to be photosynthetically useless (Lopes, 1999).

By examining the three foliar plant pathogens that were in focus in this study and their effects on host dynamics, it is obvious that we cannot place each one of them under solely one category in the grouping of Boote et al. (1983). For example, common bean rust could be considered as not only a leaf senescence accelerator but also as an assimilate sapper and photosynthetic rate reducer.

In conclusion, the knowledge gained from this study together with other information from ecological and epidemiological studies of these three economically important diseases are an essential requirement to the development and implementation of integrated disease management strategies (Bergamin Filho et al., 1997). It also follows that future research aiming to increase knowledge of the interactions between host and disease dynamics must focus on a holistic approach (Campbell and Madden, 1990; Kranz, 2003) rather than studies that are directed at pathogen development alone (Van Maanen & Xu, 2003).

LITERATURE CITED

Agrios GN (2005) Plant Pathology, 5th ed., Elsevier Academic Press, San Diego, CA.

Alfano JR and Collmer A (1996) Bacterial Pathogens in Plants: Life up against the Wall. Plant Cell. 88 :1683–1698.

Allorent D and Savary S (2005) Epidemiological characteristics of angular leaf spot of bean: a systems analysis. European Journal of Plant Pathology 113: 329–341.

Allorent D, Willocquet L, Sartorato A and Savary S (2005) Quantifying and modelling the mobilisation of inoculum from diseased leaves and infected defoliated tissues in epidemics of angular leaf spot of bean. European Journal of Plant Pathology 113: 377–394.

Arie T, Takahashi H, Kodama M and Teraoka T (2007) Tomato as a model plant for plant-pathogen interactions. Plant Biotechnology 24: 135–147.

Aust HJ and Hoyningen-Huene JV (1986) Microclimate in relation to epidemics of powdery mildew. Annual Review of Phytopathology 24: 491–510.

Bailey DJ and Gilligan CA (2004) Modeling and analysis of disease induced host growth in the epidemiology of take-all. Phytopathology 94: 535–540.

Barnwal MK, Kotasthane A, Magculia N, Mukherjee PK, Savary S, Sharma AK, Singh HB, Singh US, Sparks AH, Variar M and Zaidi N (2013) A review on crop losses, epidemiology and disease management of rice brown spot to identify research priorities and knowledge gaps. European Journal of Plant Pathology 136: 443–457.

Bastiaans L (1991) Ratio between virtual and visual lesion size as a measure to describe reduction in leaf photosynthesis of rice due to leaf blast. Phytopathology 81: 611–615.

Bergamin Filho A, Carneiro SMTPG, Godoy CV, Amorim L, Berger RD and Hau B (1997) Angular leaf spot of *Phaseolus* beans: Relationships between disease, healthy leaf area, and yield. Phytopathology 87: 506–515.

Literature cited

Berger RD and Jones JW (1985) A general model for disease progress with functions for variable latency and lesion expansion on growing plants. Phytopathology 75: 792–797.

Boote KJ, Jones JW, Mishoe JW and Berger RD (1983) Coupling pests to crop growth simulators to predict yield reductions. Phytopathology 73: 1581–87.

Calonnec A, Cartolaro P, Naulin JM, Bailey D and Langlais M (2008) A host-pathogen simulation model: powdery mildew of grapevine. Plant Pathology 57:493–508.

Campbell CL (1998) Disease progress in time: Modelling and data analysis. In: Gareth Jones D (ed) The Epidemiology of Plant Diseases (pp 181–206), Kluwer Academic Publishers, Dordrecht, The Netherlands.

Campbell CL and Madden LV (1990) Introduction to Plant Disease Epidemiology. Wiley, New York.

Chaerani R and Voorrips RE (2006) Tomato early blight (*Alternaria solani*): the pathogen, genetics, and breeding for resistance. Journal of General Plant Pathology 72: 335–347.

Chakraborty S and Newton AC (2011) Climate change, plant diseases and food security: an overview. Plant Pathology 60: 2–14.

De Wolf ED and Isard SA (2007) Disease cycle approach to plant disease prediction. Annual Review of Phytopathology 45: 203–220.

Deadman LM (2006) Epidemiological consequences of plant disease resistance. In: Cooke BM, Gareth Jones D and Kaye B (eds.) The Epidemiology of Plant Diseases (pp 139–146) 2nd edition, Springer, Dordrecht, The Netherlands.

Ferrandino FJ (2008) Effect of crop growth and canopy filtration on the dynamics of plant disease epidemics spread by aerially dispersed spores. Phytopathology 98: 492–503.

Fry WE, Apple AE and Bruhn JA (1983) Evaluation of potato blight forecasts modified to incorporate host resistance and fungicide weathering. Phytopathology 73: 1054–1059.

Glazebrook J (2005) Contrasting mechanisms of defense against biotrophic and necrotrophic pathogens. Annual Review of Phytopathology 43: 205–27

Literature cited

Hau B (1990) Analytic models of plant disease in a changing environment. Annual Review of Phytopathology 28: 221–245.

Jeger MJ (1986) The potential of analytic compared with simulation approaches to modeling in plant disease epidemiology. In: Leonard KJ and Fry WE (eds) Plant Disease Epidemiology. Population Dynamics and Management (pp 255–281), MacMillan, New York.

Jesus Junior WC, Vale FXR, Coelho RR, Hau B, Zambolim L, Costa LC and Bergamin Filho A (2001) Effects of angular leaf spot and rust on yield loss of *Phaseolus vulgaris*. Phytopathology 91: 1045–1053

Johnson KB (1987) Defoliation, disease, and growth: a reply. Phytopathology 77: 1495–1497.

Jones H, Whipps JM and Gurr SJ (2001) The tomato powdery mildew fungus *Oidium neolycopersici*. Molecular Plant Pathology 2: 303–309.

Jones JB, Jones PJ, Stall RE and Zitter TA (1991) Compendium of Tomato Diseases. APS Press, St. Paul, USA.

Kosman E and Levy Y (1994) Fungal foliar plant pathogen epidemics: Modelling and qualitative analysis. Plant Pathology 44: 328–337.

Kranz J (1977) A study on maximum severity in plant diseases. in: Travaux dédiés à G. Viennot-Bourgin (pp 169-173), Société Francaise de Phytopathologie, Paris.

Kranz J (2003) Comparative Epidemiology of Plant Diseases. Springer-Verlag, Berlin, Germany.

Kushalappa AC and Ludwig A (1982) Calculation of apparent infection rate in plant diseases: development of a method to correct for host growth. Phytopathology 72: 1373–1377.

Laluk K and Mengiste T (2010) Necrotroph attacks on plants: wanton destruction or covert extortion? Arabidopsis Book 8: e0136, doi/10.1199/tab.0136.

Literature cited

Langsdorf G, Furuichi N, Doke N and Nishimura S (1991) Investigations on *Alternaria solani* infections: detection of alternaric acid and susceptibility-inducing factor in the spore germination fluid of *A. solani*. Journal of Phytopathology 128: 271–282.

Liebenberg MM and Pretorius ZA (2010) Common Bean Rust: Pathology and Control. Horticultural Reviews 37: 1–99.

Lopes DB (1999) Photosynthetic Competence of Bean Leaves with Rust and Anthracnose. Gainesville, University of Florida, PhD thesis.

Lucas JA (1998) Plant Pathology and Plant Pathogens. Blackwell Science, Bristol.

Madden LV, Hughes G and van den Bosch F (2007) The Study of Plant Disease Epidemics. APS, St. Paul.

Medina-Ruíz CA, Mercado-Luna IA, Soto-Zarazúa GM, Torres-Pacheco I and Rico-García E (2011) Mathematical modeling on tomato plants: A review. African Journal of Agricultural Research 6: 6745–6749.

Mersha Z and Hau B (2008) Effects of bean rust (*Uromyces appendiculatus*) epidemics on host dynamics of common bean (*Phaseolus vulgaris*). Plant Pathology 57: 674–686.

Michaels TE (2005) The Bean Plant. In: Schwartz HF, Steadman JR, Hall R and Forster RL (eds.) Compendium of bean diseases (pp 1–5) 2nd edition, APS Press, St. Paul.

Nelson SC and Campbell CL (1993) Disease progress, defoliation and spatial pattern in a multiple-pathogen disease complex on white clover. Phytopathology 83: 419–429.

Oliver RP and Ipcho SVS (2004) Arabidopsis pathology breathes new life into the necrotrophs-vs.-biotrophs classification of fungal pathogens. Molecular Plant Pathology 5: 347–352.

Pandey KK, Pandey PK, Kallo G and Banerjee MK (2003) Resistance to early blight of tomato with respect to various parameters of disease epidemics. Journal of General Plant Pathology 69: 364–371.

Panggaa IB, Hananb J and Chakrabortyc S (2011) Pathogen dynamics in a crop canopy and their evolution under changing climate. Plant Pathology 60: 70-81.

Prokopová J, Mieslerová B, Hlaváčková V, Hlavinka J, Lebeda A, Nauš J and Špundová M (2010) Changes in photosynthesis of *Lycopersicon spp.* plants induced by tomato powdery mildew infection in combination with heat shock pre-treatment. Physiological and Molecular Plant Pathology 74: 205–213.

Robert C, Bancal MO, Lannou C and Ney B (2006) Quantification of the effects of *Septoria tritici* blotch on wheat leaf gas exchange with respect to lesion age, leaf number, and leaf nitrogen status. Journal of Experimental Botany 57: 225–234.

Robert C, Bancal MO, Nicolas P, Lannou C and Ney B (2004) Analysis and modelling effects of leaf rust and *Septoria tritici* blotch on wheat growth. Journal of Experimental Botany 55: 1079–1094.

Rossi V, Giosuè S and Caffi T (2010) Modelling plant diseases for decision making in crop protection. In: Oerke EC, Gerhards R, Menz G and Sikora RA (eds.) Precision crop protection—The challenge and use of heterogeneity (pp. 241–258), Springer, Dordrecht, The Netherlands.

Schulze-Lefert P and Panstruga R (2003) Establishment of biotrophy by parasitic fungi and reprogramming of host cells for disease resistance. Annual Review of Phytopathology 41: 641–667.

Schwartz HF, Steadman JR and Harveson RM (2011) Rust of Dry Beans. Fort Collins, CO, USA: Colorado State University: Cooperative Extension Fact Sheet No. 2.936 Available: http://www.ext.colostate.edu.

Singh VP, Zargar GH and Fazili MA (1986) Growth of foliage of pigeon pea (*Cajanus cajan* [L.] [millsp.] and disease progress of Alternaria blight. Phytopathology 115: 147–151.

Souza TLPO, Faleiro FG, Dessaune SN, Paula-Junior TJ, Moreira MA and Barros EG (2013) Breeding for common bean (*Phaseolus vulgaris* L.) rust resistance in Brazil. Tropical Plant Pathology 38: 61–374.

Stavely JR (2005) Rust. In: Schwartz HF, Steadman JR, Hall R and Forster RL (eds.) Compendium of Bean Diseases (pp 38-39) 2nd edition, APS Press, St. Paul.

Stone JK (2001) Necrotroph. In: Maloy OC, Murray TD (eds) Encyclopedia of Plant Pathology (pp 676–677), Wiley, New York.

Strange RN and Scott PR (2005) Plant disease: a threat to global food security. Annual Review of Phytopathology 43: 83–116.

Talbot NJ (2010) Living the Sweet Life: How Does a Plant Pathogenic Fungus Acquire Sugar from Plants? PLoS Biol 8: e1000308, doi:10.1371/journal.pbio.1000308.

Van der Plank JE (1963) Plant Diseases: Epidemics and Control. Academic Press, New York.

Van Maanen A and Xu M (2003) Modelling plant disease epidemics. European Journal of Plant Pathology 109: 669–682.

Waggoner PE (1986) Progress curves of foliar diseases: Their interpretation and use. In: Leonard KJ and Fry WE (eds) Plant Disease Epidemiology. Population Dynamics and Management (pp 3–37), MacMillan, New York.

Waggoner PE and Berger RD (1987) Defoliation, disease, and growth. Phytopathology 77: 393–98.

Wener ZH (2000) Importance of Tomato. Available at: http://www.agrisupportonline.com.

Whipps JM, Budge SP and Fenlon, JS (1998) Characteristics and host range of tomato powdery mildew. Plant Pathology 47: 36–48.

Xu X (2006) Modelling and interpreting disease progress in time. In: Cooke BM, Gareth Jones D and Kaye B (eds.) The Epidemiology of Plant Diseases (pp. 215-238) 2nd Edition, Springer, Dordrecht, The Netherlands.

Zadoks JC and Schein RD (1979) Epidemiology and Plant Disease Management. Oxford University Press, New York.

ACKNOWLEDGEMENTS

This work would not have been completed without the help of several people to whom I wish to express my sincere appreciation. My utmost gratitude goes to my advisor, Prof. Dr. Bernhard Hau for his constant guidance, invaluable advice and relentless support throughout the study period.

I would like to thank to Ms. Natalie Röder and Ms. Seraphine Hermann for their assistance while I was conducting the experiments. The timely input of Dr. Gebauer with the abstract translation is highly appreciated. I also express my appreciation to my fellow PhD students and friends at HIBC for their moral support and encouragements.

I am deeply indebted to my lovely wife Lilian Sing'oei. She has been a vital support through her continued patience, encouragement and understanding. Finally, I thank God for 'of Him and through Him and to Him are all things'.

CURRICULUM VITAE

Personal Data

Name: John Koech Chelal

Date of Birth: 29.03.1984

Place of Birth: Keiyo, Kenya

Citizenship: Kenyan

Marital Status: Married

E-mail: chelaljohn@yahoo.com

EDUCATION BACKGROUND

2010 – 2014   PhD Student, Leibniz Universität Hannover, Germany

Thesis- Modeling the interactions between host dynamics and epidemics of foliar diseases in three plant pathosystems

2008 – 2010   Master of Science International horticulture (M.Sc), Specialization in Phytopathology and Entomology

Leibniz Universität Hannover, Germany

Thesis- Interactions between powdery mildew (*Oidium neolycopersici*) epidemics and the host dynamics of tomato

2000 – 2004   Bachelor of Science in Horticulture (B.Sc)

Jomo Kenyatta University of Agriculture and Technology, Kenya

Thesis- Effects of deflowering and harvesting frequency on the growth and yield of *Crotalaria brevidens*

1998 – 2001   Kenya Certificate of Secondary Education (K.C.S.E)

Nakuru high school, Kenya

PUBLICATIONS IN REFEREED JOURNALS (FROM THIS THESIS)

1. Chelal J. and Hau B. (2014) Temporal dynamics of powdery mildew and its effects on the host dynamics of tomato (*To be Submitted*)

2. Chelal J. and Hau B. (2014) Modeling the interaction between powdery mildew epidemics and host dynamics of tomato (*To be Submitted*)

3. Chelal J., Al Masri A. and Hau B. (2014) Modeling the interaction between early blight epidemics and host dynamics of tomato (*To be Submitted*)

4. Chelal J., Mersha Z. and Hau B. (2014) Modeling the interaction between bean rust epidemics and host dynamics of common bean (*In preparation*).

CONFERENCE CONTRIBUTIONS

1. Chelal J. and Hau B. (2012) Temporal dynamics of powdery mildew and its relationship to host growth, defoliation and yield of tomato. Proceedings of the 58th German Plant Protection Conference. Technical University of Braunschweig, Germany.

2. Chelal J. and Hau B. (2010) Effects of powdery mildew (*Oidium neolycopersici*) epidemics on host dynamics of tomato (*Solanum lycopersicum* L.). TROPENTAG: International Research on Food Security, Natural Resource Management and Rural Development. Proceedings of an international symposium. Zurich, Switzerland.

DECLARATION

I, John Koech Chelal, hereby declare that this dissertation, entitled 'Modeling the interactions between host dynamics and epidemics of foliar diseases in three plant pathosystems' is an original piece of work conducted by myself and has not been submitted for a degree in any other university.

Hannover, 21.03. 2014

Gottfried Wilhem Leibniz Universität Hannover